universität wien

MASTERARBEIT / MASTER'S THESIS

Titel der Masterarbeit

L-carnitine is directly involved in the regulation of transcription factors and their interaction with the CRAT promoter

verfasst von

Lars Zver

angestrebter akademischer Grad

Master of Science (MSc)

Wien, 2017

Studienkennzahl lt. Studienblatt:	A 066 877
Studienrichtung lt. Studienblatt:	Genetik und Entwicklungsbiologie
Betreut von:	Ass.-Prof. Mag. Dr. Reinhold Hofbauer

Acknowledgements

First of all, I want to thank Ass.-Prof. Mag. Dr. Reinhold Hofbauer for giving me the chance to do my master's thesis in his lab. I also want to express my gratitude for everything he taught me, for his moral support and for believing in me.

I also want to thank my family for supporting me through all these years.

Last but not least, I want to thank everyone I have not mentioned who supported me in any way to reach this stage of my life.

Table of contents

1. Introduction 9
   1.1. Carnitine 9
      1.1.1. Sources and homeostasis 9
      1.1.2. Roles of L-carnitine 11
      1.1.3. Primary and secondary carnitine deficiency 11
   1.2. The mTOR pathway 12
   1.3. Hypercholesterolaemia 13
   1.4. Genes 13
      1.4.1. Solute carrier (SLC) superfamily 13
         1.4.1.1. Organic carnitine/cation transporter OCTN1 (SLC22A4) 14
         1.4.1.2. SLC35F2 14
      1.4.2. Rac1 15
      1.4.3. Ras homolog enriched in brain (Rheb) 15
      1.4.4. General control non-derepressible 2 (GCN2) 15
      1.4.5. Peroxisome proliferator-activated receptor gamma coactivator 1α (PGC1α) 16
      1.4.6. Sterol regulatory element-binding protein-1c (SREBP1c) 16
   1.5. Carnitine acetyltransferase (CRAT) 17
      1.5.1. Transcription factors 19
         1.5.1.1. Peroxisome proliferator-activated receptor α (PPARα) 19
         1.5.1.2. Hepatocyte nuclear factor 4α(HNF4α) 19
         1.5.1.3. Retinoic acid receptor and retinoid X receptor (RAR and RXR) 20
         1.5.1.4. Glucocorticoid receptor α(GRα) 20
   1.6. Nutrigenomic factors, influencing the lipid metabolism 21
   1.7. Aim of our work 21
2. Materials and methods 24
   2.1. Cell culture 24
      2.1.1. Propagation of cells 24
      2.1.2. Metabolic conditions for cell cultivation in hyperglycaemic medium 24
      2.1.3. Metabolic conditions for cell cultivation in normoglycaemic medium 26
      2.1.4. Freezing of cells 27
      2.1.5. Thawing of cells 28
   2.2. Testing of new PCR-primers 28
      2.2.1. Primers 28
      2.2.2. Gradient PCR 28
      2.2.3. Gel electrophoresis: 29

2.2.4. Gel elution and DNA isolation 29
2.3. Measuring of gene expression 30
2.3.1. Cell harvesting 30
2.3.2. RNA isolation 31
2.3.3. cDNA synthesis 31
2.3.4. Real-time RT-PCR 32
2.3.5. Statistical analysis 33
2.4. Pinpointing of L-carnitine-regulated pathways 33
2.4.1. Cignal multi-pathway activity assay 33
2.4.2. Luciferase assay 34
2.5. Electrophoretic mobility shift assay and supershift assay 34
2.5.1. Metabolic conditions for cell cultivation 34
2.5.2. List of antibodies 35
2.5.3. Nuclear extract isolation 35
2.5.4. Preparation of spun columns 37
2.5.5. Radioactive labelling of oligonucleotides 38
2.5.6. Cherenkov counting for radioactivity measurement 38
2.5.7. Electrophoretic mobility shift and supershift assays 38
2.5.8. Optimization of electrophoresis conditions 39
3. Results 40
3.1. Simulation of hypercholesterolaemia in the cell culture 40
3.2. Real-time RT-PCR 40
3.2.1. Steady state mRNA levels of cells in a hyperglycaemic medium 40
3.2.1.1. OCTN1 40
3.2.1.2. SLC35F2 43
3.2.1.3. Rac1 46
3.2.1.4. Rheb 49
3.2.1.5. GCN2 52
3.2.1.6. PGC-1α 55
3.2.1.7. SREBP-1 58
3.2.2. Steady state mRNA levels of cells in a normoglycaemic medium 60
3.2.1.1. OCTN1 61
3.2.1.2. SLC35F2 62
3.2.1.3. Rac1 64
3.2.1.4. Rheb 65
3.2.1.5. GCN2 67
3.2.1.6. PGC-1 68

3.2.1.7. SREBP1 70
3.3. Pinpointing of L-carnitine regulated pathways 72
3.3.1. Oestrogen pathway 72
3.3.2. Androgen pathway 73
3.3.3. PPAR pathway 74
3.3.4. Retinoic acid pathway 75
3.3.5. Vitamin D pathway 76
3.3.6. Glucocorticoid pathway 77
3.3.7. Progesterone pathway 78
3.3.8. Retinoid X pathway 79
3.3.9. Liver X pathway 80
3.3.10. Hepatocyte nuclear factor 4 (HNF4) pathway 81
3.4. Electrophoretic mobility shift assays (EMSA) 82
3.4.1. Analysis of the putative hRARRXR binding site 82
3.4.2. Analysis of the putative glucocorticoid α (GR α) binding site 88
3.4.3. Analysis of the putative PPAR binding site 94
3.4.4. Analysis of the putative Hepatocyte Nuclear Factor 4 (HNF4) binding site. 99
3.5. Analysis of the effect of varying concentrations of SDS on the binding of the oligonucleotides to the CrAT promoter 104
3.6. Supershift assay 105
4. Discussion 107
5. References 125

1. Introduction

1.1. Carnitine

L-carnitine (L-3-hydroxy-4-N,N,N-trimethylaminobutyrate – chemical structure: see fig. 1) is an amino acid derivative that can be found in most or all animal species and also in many plants and microorganisms. It is synthesized from the amino acids lysine, which provides the carbon backbone, and methionine, which provides the 4-N-methyl groups of the molecule [1]. L-carnitine is a zwitterion that can be found as a white powder in its pure form and is highly water-soluble. It has major functions in the oxidation of fatty acids and as an acetyl buffer [2].

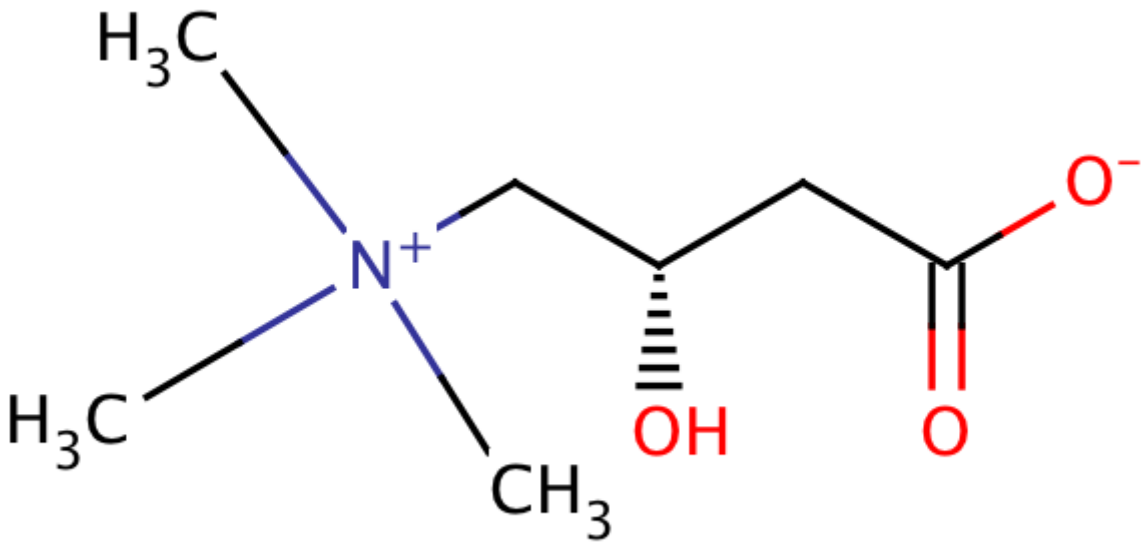

Figure 1: Molecular structure of L-carnitine [3].

1.1.1. Sources and homeostasis

While carnitine, being classified as a “conditionally-essential” amino acid derivative, can be synthesized in mammals, most of it is taken up through food. In mammals, about 25% of carnitine is synthesized endogenously through a multistep process, while about 75% is taken up by nutrition [4]. While most enzymes required for the synthesis of carnitine can be found in heart and skeletal muscles, brain, liver and kidneys, resulting in the synthesis of its precursors, the final step of L-carnitine synthesis can only be carried out in the liver, kidneys and brain [1, 2, 4-6]. In humans, an average of 1 to 2 µmol/kg body weight/day is synthesized endogenously [7, 8]. Biosynthesis of carnitine increases with

age and is less effective in infants than in adults, while preterm neonates are unable to produce sufficient amounts of it and require administration of exogenous carnitine [9].

The most important source of carnitine for humans is nutrition. Animal source foods contain higher amounts of carnitine than plants, with the highest concentrations being in red meat, fish, chicken and dairy products [5, 7].The bioavailability of carnitine for humans ranges from 54-86%, with less of it absorbed from carnitine-rich food [8]. Dietary uptake of carnitine is 6-15 μmol/kg body weight/day when consuming high-carnitine diet and 1-8μmol/kg body weight/day in the case of low-carnitine diet, while the dietary uptake of vegans is less than 1 μmol/kg body weight/day, which is why it must be supplemented artificially. The drawback of carnitine supplements is their low absorption rate, with a bioavailability of only 14-18%/dose [7]. Dietary carnitine is absorbed in the small intestine, but the mechanism is not yet known, while the unabsorbed carnitine is degraded in the large intestine [7, 8].

Another important factor in keeping the carnitine levels in the body constant is the very effective reabsorption in the kidneys. While urine is the main medium through which carnitine gets excreted from the body, under normal conditions 90-98% of the carnitine is reabsorbed in the kidneys through tubular reabsorption. The rest is excreted either in its pure form, degraded into trimethylamine oxide [8] or as acylcarnitine [5, 10]. The rate of carnitine reabsorption depends on its dietary uptake, such as in vegetarians, who excrete less carnitine through their urine than omnivores [8]. Other methods of carnitine excretion are through milk [5] and faeces, though excretion in the latter is less than 2% of total excretion [11].

Distribution of carnitine in the body depends on factors such as tissue type, age and gender. Most of the carnitine in the body is stored in skeletal muscles, liver, brain and kidneys [10], with 95% of it being stored in muscles, even though it is unable to synthesize it on its own [12]. The absorbed and synthetized carnitine is transported to its target via the bloodstream [1, 12]. As carnitine concentrations are much lower in plasma than in tissue, carnitine enters the target cells by active transport with the help of the sodium ion-dependent transporter OCTN2 (SLC22A5) [13], which is also responsible for the reabsorption in the kidneys. While OCTN2 is responsible for transporting carnitine from the bloodstream into the cells, it has a threshold and transport does not increase even if carnitine levels in the plasma are elevated above normal [12].

1.1.2. Roles of L-carnitine

L-carnitine has varying roles in the body. Two of these are its function in the beta-oxidation of fatty acids in the mitochondria and as an acetyl buffer in the preservation of the ratio between coenzyme A (CoA) and acyl-CoA [2]. Fatty acids are activated into acyl-CoA esters after entering the cells, but cannot pass through the inner mitochondrial membrane into the matrix for mitochondrial beta-oxidation in this form. L-carnitine is responsible for helping to transport these esters through the membrane in a process called the “L-carnitine shuttle”, so they can be used as an energy source. The enzyme carnitine palmitoyltransferase I (CPT-I) catalyses the transfer of the acyl residue from the acyl-CoA ester to L-carnitine, resulting in the formation of acylcarnitine. The acylcarnitine molecule passes the inner mitochondrial membrane with the help of the acylcarnitine-carnitine translocase (CACT), which simultaneously transports a molecule of L-carnitine from the matrix into the cytosol for each acylcarnitine molecule. Inside the matrix, the enzyme carnitine palmitoyltransferase II (CPT-II) removes the carnitine from the acylcarnitine and restores the acyl-CoA ester, which is now able to enter beta-oxidation [10]. L-carnitine is also used in peroxisomal beta-oxidation. This reaction is an incomplete oxidation and produces shortened fatty acids, which are transported into the mitochondria with the help of L-carnitine to complete the process [14].

Another important function of L-carnitine is in the CoA homeostasis. L-carnitine is used to bind excess acetyl-CoA that is formed in cases such as after intense exercise, resulting in the formation of acylcarnitine, which prevents the acetylation of free CoA and keeps its levels steady [2, 15]. Excessive acylcarnitine is transported out of the tissue and can be excreted through urine [7].

1.1.3. Primary and secondary carnitine deficiency

The most prominent diseases, connected with carnitine, are primary and secondary carnitine deficiency, with primary carnitine deficiency being a genetic disease, while secondary carnitine deficiency can be genetic or acquired [16].

Primary carnitine deficiency is an autosomal recessive disorder that is caused by a mutation in OCTN2, inhibiting the reabsorption of carnitine in the kidneys, leading to the loss of most of the filtered carnitine, and the transport of carnitine into the cells, which leads to decreased fatty acid oxidation and increased excretion of carnitine through urine. In patients with primary carnitine deficiency, tissue carnitine levels can drop below 10% of normal levels [16, 17]. Primary carnitine deficiency can be either systemic, which results in reduced carnitine levels in both tissue and plasma, and myopathic, where

carnitine levels are reduced only in skeletal muscles [17]. Because it can be caused by a large number of different mutations of OCTN2, its onset can be either perinatal, infantile or adult [18]. The main symptoms of primary carnitine deficiency are progressive cardiomyopathy, hypoketotic hypoglycaemic encephalopathy and skeletal myopathy [19]. Progressive myopathy develops at an older age and is lethal if not treated with carnitine supplementation in time. If discovered, primary carnitine deficiency can be successfully treated with either intravenous or oral supplementation of carnitine [17].

In contrast to primary carnitine deficiency, secondary carnitine deficiency is not necessarily a genetic defect [16, 17]. It is caused by enzymatic defects which lead to impaired fatty acid oxidation in the mitochondria [6], and can be the secondary symptom to some other genetic defects or it can be caused later by various disorders or even drugs [17]. Patients with secondary carnitine deficiency accumulate large amounts of organic acids, which leads to increased urinary excretion of acylcarnitines. It is more common and less dangerous than primary carnitine deficiency, and can be treated with carnitine supplementation, alleviating muscle symptoms, cardiac problems and other symptoms [16].

1.2. The mTOR pathway

Mechanistic target of rapamycin (also known as mammalian target of rapamycin) – mTOR – is a serine/threonine protein kinase, belonging to the phosphatidylinositol 3-kinase-realeted protein kinase family, and is an important regulator of cell growth and nutrient sensing [20], and is the target of rapamycin, an antifungal metabolite of *Streptomyces hygroscopicus*, that blocks proliferation of cells in mammals [21]. mTOR is conserved among eukaryotes and can be found in two complexes: mTOR complex 1 (mTORC1) and mTOR complex 2 (mTORC2), which have a similar structure, but fulfil different tasks and respond differently to rapamycin [22]. Together with GCN2, mTOR represents the major amino acid-sensing signalling pathways in eukaryotes [23].

mTORC1 is responsible for the sensing of amino acids, growth factors, cellular stress and the energy status [24], and manages cell growth according to the presence of these signals [21]. The complex consists of mTOR, mLST8, regulatory associated protein of mTOR (raptor), which is required for almost all of its functions, and some other factors. It is the main target of rapamycin, which has to form a complex with FKBP12 to be active, and directly inhibits the activity of the complex by binding to the mTOR subunit [21, 24]. One of the main activators of mTORC1 are Rag GTPases such as Rheb, which are needed for amino acid sensing. These GTPases are regulated by the tuberous sclerosis

complex 1/2 (TSC1/2). When both amino acids and growth factors are abundant TSC1/2 is inhibited by phosphorylation, keeping Rheb active and preventing the inhibition of mTORC1 [24, 25]. Another regulator of mTORC1 is the energy-sensing kinase 5' adenosine monophosphate-activated protein kinase (AMPK), which is activated under low energy conditions resulting from a lack of nutrients and inhibits mTORC1 by increasing TSC2 activity [24].

The other complex, mTORC2, has a similar structure to mTORC1 and contains both mTOR and mLST8, but contains Raptor-independent companion of mTOR (Rictor) instead of Raptor, which renders it unattackable for the rapamycin/FKBP12 complex, preventing direct inhibition. The task of mTORC2 is the regulation of the actin cytoskeleton and the phosphorylation of some substrates [20, 24].

1.3. Hypercholesterolaemia

Hypercholesterolaemia is a lipid disorder, characterised by increased levels of serum cholesterol, which can lead to atherosclerosis. The disorder is caused by the mutation of the low-density lipoprotein (LDL) receptor encoding gene on chromosome 19, inhibiting the uptake of LDL from the tissue fluid into the cells, causing the increase of cholesterol levels in the serum up to twofold compared to normal values. Normal serum concentrations for adults are below 7.5 mmol/L[26], while those in patients with hypercholesterolaemia can reach 15 mmol/L or even above 30 mmol/L. Hypercholesterolaemia can be medically managed with the help of statins, but these drugs can only lower LDL levels and not completely cure the disorder [26].

1.4. Genes

1.4.1. Solute carrier (SLC) superfamily

The solute carrier (SLC) superfamily consist of 55 families and at least 362 members, coding for membrane bound proteins, which can act as passive transporters, symporters, or antiporters. Members of the SLC superfamily transport a wide range of organic and inorganic endogenous substrates, but drugs or environmental toxins can also use them to get inside or outside the cell. They are present in all or most prokaryotes and eukaryotes, on the cellular or organelle membrane, but they are not present on the nuclear membrane. Because of their functions, they present a good target for medical, pharmacological, or other research [27].

1.4.1.1. Organic carnitine/cation transporter OCTN1 (SLC22A4)

The SLC22 family belongs to the SLC superfamily of transporters. Its members can be divided into two groups: the organic cation transporters (OCT) and the “novel” organic carnitine/cation transporters (OCTN) [28].They can transport different substrates and most are polyspecific, enabling them to transport more than one type of substrate. The main substrates of the SLC22 family members are zwitterions, organic anions, and organic cations, but they can also help in the absorption or excretion of drugs, xenobiotics, or endogenous compounds. They can work either as uniporters, anion exchangers, or sodium/L-carnitine cotransporters. SLC22 transporters can be found in the liver, kidney, and heart, but they also have a homeostatic function in the heart and the brain [29].

The organic carnitine/cation transporter OCTN1 (SLC22A4) is a polyspecific member of the SLC22 family of transporters. It is expressed in immune-related tissues and organs [30], numerous human cancer cell lines, foetal liver [31], kidneys and the trachea [31, 32]. While OCTN1 can transport carnitine, it has a considerably weaker affinity for it than OCTN2, whereas its main substrate has been found to be the antioxidant L-ergothioneine [33]. Various studies have shown that genetic polymorphisms of OCTN1 can be associated with some autoimmune diseases, such as rheumatoid arthritis or type 1 diabetes [34].

1.4.1.2. SLC35F2

The SLC35 family belongs to the SLC superfamily. Its members function as nucleotide sugar transporters and can be found on the membrane of the Golgi apparatus and/or the endoplasmic reticulum, transporting the sugar from the lumen of the cell into the organelles [35, 36].

One member of this family is the understudied transporter SLC35F2. The gene encoding it is located on the long arm of chromosome 11. While it is highly expressed in salivary glands and contributes to construction of the blood-brain barrier in humans, its other functions are not known. Various researches have shown that its expression is elevated in non-small cell lung cancer cells, such as human lung squamous cell tumour tissues, compared to the surrounding healthy cells, indicating a possible role in lung cancer [36, 37]. Winter *et al*. have conducted a research on SLC35F2, indicating it as a possible target for tumour-targeting drugs in cells with SLC35F2 overexpression [38].

1.4.2. Rac1

Rac1 is an insulin-activated Rho family GTPase, with various functions such as GLUT4 translocation in cultured muscle cells, stimulation of glucose uptake and assembly and disassembly of the actin cytoskeleton by activating the p21-activate kinase (PAK) [39, 40]. Rac1 is also important in the development of various types of cancer, such as skin cancer, by controlling proliferation and apoptosis during tumorigenesis [41]. Rac1 has an important function in the release of insulin into the bloodstream. When high blood glucose levels lead to glucose-stimulated insulin secretion (GSIS), Rac1 may help in the trafficking of the intracellular insulin-loaded vesicles, whose contents are released into the bloodstream [42]. Impairment of GSIS results in chronic high glucose levels (hyperglycaemia), which leads to glucose and lipid toxicity (dyslipidaemia) and the subsequent development of Type 2 Diabetes [43]. While cells in Type 2 Diabetes have increased insulin resistance, research has shown that elevated glucose levels can be counteracted by both L-carnitine and acyl-L-carnitine in an insulin-dependent manner [44].

1.4.3. Ras homolog enriched in brain (Rheb)

Rheb is a small GTPase, belonging to the Ras superfamily of GTPases, and an important part of the mTOR signalling pathway. In the cell, it is located on various endomembrane compartments, such as the lysosome, where it acts as a direct activator of mTORC1 [25, 45]. mTORC1 is recruited to the lysosomes in the presence of amino acids by Rag heterodimers, which bind to the Raptor subunit of the complex. Once bound, the complex is activated by GTP-bound Rheb [46]. Rheb is directly regulated by the TSC1/2 complex. When there are not enough amino acids, TSC1/2 is un-phosphorylated and it lowers the concentration of GTP-bound Rheb, thus inhibiting mTORC1 activity [47]. Another inhibitor of mTORC1 is the Rheb binding protein glyceraldehyde-3-phosphate dehydrogenase (GAPDH), which binds to Rheb in the presence of low glucose concentrations [45]. Zu *et al.* have shown in their research that Rheb can also act as an oncogene and is overexpressed in different carcinomas [48].

1.4.4. General control non-derepressible 2 (GCN2)

The second major amino acid sensing pathway beside mTOR is GCN2. This eIF2α protein kinase senses amino acids and activates in their absence. Activated GCN2 acts as an inhibitor to mTORC1, but the mechanisms are still unknown. It supresses protein

synthesis and general mRNA translation, while also upregulating the synthesis of amino acids and inducing the translation of mRNAs that stimulate the expression of stress-responsive genes [20, 23]. One of the mechanisms by which GCN2 promotes amino acid synthesis is the upregulation of the amino acid transporter SLC38A2 by upregulating its expression, translation and protein stability, in a process known as adaptive regulation [23].

1.4.5. Peroxisome proliferator-activated receptor gamma coactivator 1α (PGC1α)

PGC1α is a key nuclear cofactor in mitochondrial biogenesis, oxidative metabolism and hepatic gluconeogenesis, and is upregulated by both mTOR and AMPK [25, 49]. Its highest expression levels are in tissues with high metabolic rate, such as skeletal and heart muscle, stimulating genes that are involved in fatty acid oxidation in the latter. Its levels are also diet dependent in some tissues, as there is more PGC1α in the liver during fasting [50]. One of the genes PGC1α stimulates is CPT-I, an important member of fatty acid oxidation. While CPT-I expression is upregulated by the thyroid hormone (T3), Zhang *et al.* (2004) have shown in their research that PGC1α overexpression enhances the stimulation of CPT-I expression by T3 in rat liver [49]. It is also important in mediating the expression of CPT-I during starvation, together with CREB and HNF4 [51].

1.4.6. Sterol regulatory element-binding protein-1c (SREBP1c)

Sterol regulatory element-binding protein-1c (SREBP-1c) is a protein involved in fatty acid synthesis and is a possible target of the AMPK pathway, as AMPK regulates lipid metabolism by promoting beta-oxidation and decreasing fatty acid synthesis, while on the other hand it is upregulated by mTORC1 [25]. SREBP-1 has two isoforms, SREBP-1a and SREBP-1c, with SREBP-1c being expressed in the liver. Deng *et al.* have shown that enzymatic activity of lipid oxidation genes increases at low expression of SREBP-1c in bovine hepatocytes [52]. Overexpression of SREBP-1c leads to lipid metabolism disorders, such as fatty liver disease (or non-alcoholic fatty liver disease in humans) [52, 53].

1.5. Carnitine acetyltransferase (CRAT)

The enzyme carnitine acetyltransferase (CRAT) belongs to the family of carnitine acetyltransferases and is a part of the carnitine system that transfers the acyl groups between CoA and L-carnitine [54]. It is a monomer with 2 domains, which form a tunnel that is required for the transfer of the acyl group. Most of the CRAT activity takes place in the mitochondrial matrix. CRAT activity is also present in peroxisomes and in the endoplasmic reticulum, but there is no activity in the cytoplasm. Both the mitochondrial (597 amino acids) and the peroxisomal (605 amino acids) isoform are encoded by the same gene and are a result of alternative splicing [55]. The highest expression in humans is in the liver and in skeletal muscles [56].

CRAT has several different functions. In the mitochondria, it is responsible for determining the ratio between acetyl-CoA and free L-carnitine and between free CoA and acetyl-L-carnitine [56, 57]. Carnitine acetyltransferases are classified based on their substrate: CRAT catalyses the transfer of short-chain acyls between CoA and L-carnitine, while other members of this family are responsible for the transfer of medium-chain and long-chain acyls [57].Other functions of CRAT include regulation of body glucose tolerance and muscle activity of pyruvate dehydrogenase [58], it possibly plays a role in the excretion of acyl molecules in the form of acylcarnitines [59] and it plays a role in the transition from the G1 to the S phase in the cell cycle [60].

CRAT activity is downregulated in obese people and is possibly inhibited by a lack of carnitine, while its overexpression increases glucose uptake and inhibits fat oxidation in primary human myocytes [58]. Mutations can affect CRAT by either affecting the binding of CoA or L-carnitine, or by affecting its stability or production [59].

As part of our research, a theoretical promoter analysis of the human CRAT promoter was carried out using the bioinformatical web tools PROMO [61, 62] and PATCH [63] to detect possible binding sites for regulating transcription factors (see fig. 2). The promoter sequence was obtained from the Eukaryotic Promoter Database – EPD [64, 65]. Based on this analysis, the analysis of the murine CRAT promoter by Klemens Kienesberger [66] and the results of the Cignal assay, the factors chosen for analysis were RARβ/RARα/RXR, GR-alpha, HNF4A and PPARα/RXRα. A schematic presentation of these binding sites on the human CRAT promoter is given in fig. 3.

SP1 CREB

-499 GGCCGCCCGA ACGTCGGGCG CCGCGACTGC CACGATTGTG CGGGGCGTCA

GR-alpha

-449 AGTTTGGGTT GTGCTCAGCC ATGTTTTTCC GGGACAGTCT CCTGTCCCGG

RAR-β

-399 AGTACCACCT GTCATCTTTG TGGGTGGTAC TGACCCTAAC CCAAGGAATA

RAR-β HNF-3β

-349 TTAGAGGACA TTCCCCGGTC AACATGGTTG TGTTTTCCTA TCACTCTAAG

-299 AGTTAGGCTC AAGGACACCA GACGGAGTTG GAAAGGTGCA CACCACTACC

RAR-beta:RXR-alpha

-249 TCCAACAGCT TAGAAGACAT GTGGGGACAG GGGAGAGACA GCTGGACGGT

RARβ/RARα/RXR cMyc_up

-199GACCTCCTCC TTCCTCCTCC ACAGGTCTCA ATGACTCGCC CTCGGCCCTG

-149 CCCCTCTGTC CCCGCCCGCC GTGGTCCCGC CCCCGACTCG CAGCCAGCCT

-99 ACTGCGACCC GCTACCGGGC GACGCCCCGC CCCTCCGTCC CCGCCCCTCC

-49 TGTCCCTCCT CAAGGAGACT CCGCCCCATC GATGCCCCGT CCCCGCCCCA

cMyc_start PPARα/RXRα

+1 CAGCCAACCT CCCGGGCACC GTTGCCCGCC CGGGGCCCGC TACCGGCCCA

HNF4A/Sp1

+51 GGCCCCGCCT CGCGAGTCCT CCTCCCCGGG TGCCTTCCCG CAGCCCGCTC

Figure 2: Theoretical analysis of the human CRAT promoter, performed with PROMO [61, 62] and PATCH [64, 65].

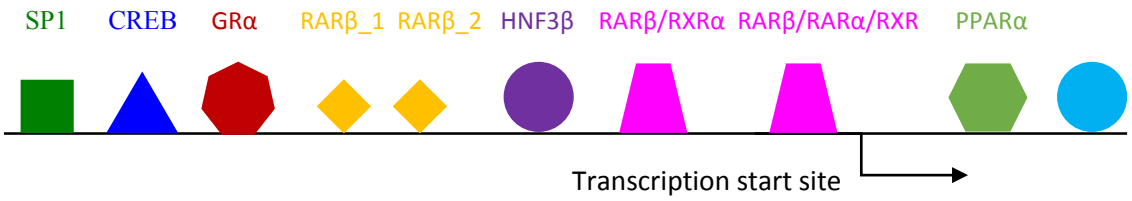

Figure 3: Scheme of the putative transcription factor binding sites on CRAT promoter region based on a theoretical promoter analysis.

1.5.1. *Transcription factors*

*1.5.1.1. Peroxisome proliferator-activated receptor α (*PPARα*)*

Peroxisome proliferator-activated receptors (PPARs) are nuclear hormone receptors, belonging to the steroid receptor superfamily. There are three types of PPARs: α, β/δ and γ, with all three having a modular structure consisting of six domains. They have different functions, ligands and show varying expression levels across tissues. PPARs can be activated by different natural or artificial substances, such as fatty acids, fibrates, hypolipidaemic drugs [67, 68], eicosanoids or others [69], but no PPAR-specific ligands have been discovered so far [68]. In the cells, inactive PPARs are located in the cytosol [69]. Once activated, they are translocated to the nucleus where they form heterodimers with RXRs and regulate gene expression by binding to the PPAR response elements (PPRE) of their target [70]. The general roles of PPARs are regulation of inflammatory signalling and of metabolic pathways [68, 71].

PPARα is expressed in tissues with high metabolic activity, such as liver, heart, kidney and brown fat [67, 68], and is also expressed in human and mouse immune cells [71]. It is involved in the regulation of both the mitochondrial and the peroxisomal beta-oxidation, in inflammatory responses [68, 71, 72] and oxidative stress [72]. PPARα activity is important in lowering lipid levels, as it was shown in rats that its absence causes lipid accumulation in the liver [72]. It is a regulator of CPT-I [72] and downregulates both HNF4 expression and its binding to the HNF4 response elements [73].

1.5.1.2. Hepatocyte nuclear factor 4α(HNF4α)

Hepatocyte nuclear factor 4 (HNF4) is a liver transcription factor, belonging to the nuclear hormone receptor superfamily, and is one of many regulatory elements of gene expression in hepatocytes [74]. It is an important factor in liver development during embryogenesis and the regulation and maintenance of gene expression in hepatocytes in adult livers [74, 75]. It has two forms, HNF4α and HNF4γ [76]. HNF4 binds to DNA as a homodimer [77] and is constitutively active by being bound to a fatty acid molecule or acyl-CoA, but which are not its ligand [78]. Thioesters were shown to be possible ligands, but there are conflicting reports whether they can [79] or cannot [80] bind to HNF4.

The HNF4α isoform, beside the liver, is expressed in the kidneys, pancreatic isles and the intestine. It regulates hepatocytes by activating genes which regulate lipoprotein and lipid metabolism, carbohydrate metabolism [78], triglyceride metabolism, insulin secretion [76] and other functions. HNF4α itself is regulated by fatty acids and acyl-CoA bound in its binding pocket, resulting in effects being dependent on chain length: short

chain acyl-CoAs (chain length 14-16) upregulate its DNA binding, while longer chain acyl-CoAs inhibit it [75]. Defects of HNF4α can lead to various health problems: downregulation can lead to liver disorders such as liver cancer, steatohepatitis and liver fibrosis [75], while mutations can lead to the development of maturity onset diabetes of the young (MODY), a hereditary form of diabetes mellitus[78].

1.5.1.3. Retinoic acid receptor and retinoid X receptor (RAR and RXR)

Retinoic acid receptors (RAR) and retinoid X receptors (RXR) are ligand-activated transcription factors, belonging to the nuclear receptor superfamily. They are activated by retinoic acid isomers: RAR can be activated by both the all-trans and 9-cis retinoic acid isomers, while RXR only reacts to 9-cis retinoic acid [81]. RAR and RXR do not influence gene expression directly, but bind to the promoter and recruit coregulator complexes, which can be either activating or repressing [82]. Both receptors have a dimerization function in their ligand binding domain, and while RAR forms homodimers or heterodimers with RXR before binding to the promoter, RXR can form heterodimers with other nuclear hormone receptors [83]. One such heterodimer is built up between PPARα and RXRβ, which helps regulate peroxisomal beta-oxidation by activating the promoter of the acetyl CoA oxidase [84].

1.5.1.4. Glucocorticoid receptor α(GRα)

The glucocorticoid receptors are part of the nuclear hormone receptor superfamily. There are two isoforms of the glucocorticoid receptor: GRα and GRβ, where GRα mediates all know effects, while GRβ may be responsible for inhibiting GRα [85]. Inactive GRα is located in the cytoplasm, where it is bound to various receptor-associated proteins (RAPs). When glucocorticoids are present, GRα dissociates from the RAPs and forms homodimers. These homodimers can then enter the nucleus, where they affect gene expression by binding to the glucocorticoid responsive element (GRE) region on the promoter of the target gene. While glucocorticoids are the main ligand of GRα, L-carnitine at significantly higher concentrations is also able to activate the receptor [86].

Glucocorticoids have diverse functions in the body, such as in basic and stress homeostasis [86], cell growth and development, or increasing the availability of substrates for mitochondrial oxidation [87], but long-time exposure to increased glucocorticoid concentrations leads to Cushing's syndrome, which has different symptoms, such as bone weakening [87]. L-carnitine is a possible replacement for glucocorticoid treatment, as concentrations in the millimolar range are able to replace

them in the treatment of inflammatory, allergic or autoimmune diseases, without having the deleterious effect on tissues such as bones [86].

1.6. Nutrigenomic factors, influencing the lipid metabolism

While L-carnitine can be addressed to bethe most prominent nutrigenomic factor that helps increasing β-oxidation by transporting fatty acids through the inner mitochondrial membrane into the matrix, thus increasing the availability of substrates, other factors, such as conjugated linoleic acid (CLA) [88], liquorice flavonoid oil [89], retinoic acid [90] or phytol and phytanic acid [91], contributing to lipid metabolism by upregulating the genes involved in β-oxidation or indirectly via upregulation of their activators, such as PPARα.

Conjugated linoleic acid (CLA) is a conjugated fatty acid, mostly found in the meat of ruminant animals, with the highest concentrations found in lamb [92], but is created synthetically from linoleic acid for supplementation purposes [88]. Its most researched function is as an anticarcinogen which is able to inhibit various cancer cell lines [summarized in [88]], but is also able to activate PPARα [93], which influences the energy metabolism by increasing β-oxidation, possibly by increasing CPT activity [94]. Phytanic acid is a phytol derivative that is taken up by humans through nutrition, with the highest concentrations found in milk products, meat and fat of ruminant animals and fish fat [95]. One of the discovered functions of phytanic acid is the upregulation of PPARα [96], an important member of β-oxidation. Later it was discovered that phytol is also able to increase PPARα activity, through which it contributes to lipid metabolism [97]. While CLA and phytanic acid influence β-oxidation through the activation of PPARα, liquorice flavonoid oil, which is extracted from the roots of *Glycyrrhiza glabra*, was shown to upregulate genes, involved in β-oxidation, while inhibiting fatty acid synthesis in mice [98]. While two of the previously mentioned factors help regulate lipid metabolism through the activation of PPARα, retinoic acid (more specifically 9-cis-retinoic acid)activates the retinoid X receptor β (RXRβ), which contributes to peroxisomal β-oxidation by forming heterodimers with PPARα [84].

1.7. Aim of our work

The first aim of our work was to see how genes, involved in the mTOR pathway (Rheb, GCN2, PGC1α and SREBP-1c), Rac1, and previously untested members of the SLC family (SLC22A4 and SLC35F2) show changes in cellular steady state mRNA levels after

supplementation of L-carnitine. Because the impact of varying concentrations of L-carnitine on the expression of specific genes have already been studied by others, we wanted to observe the time-dependent effect of increased L-carnitine levels on the expression of the above described genes in the human hepatic cell line WRL68. For this purpose, cultured cells were grown in a growth medium with artificially reduced carnitine content (dialysed FCS) and supplemented with 40 µM L-carnitine for 4 hours or with 80 µM L-carnitine for 4 hours, 15 hours, 24 hours or 48 hours. Because human cell culture cells in our lab are routinely cultivated in a hyperglycaemic medium containing 4500 mg/l glucose, we repeated the experiments using a normoglycaemic medium with a 1000 mg/l glucose content to see how L-carnitine supplementation affects steady state mRNA levels under these conditions. As an extra step, we also measured how concurrent L-carnitine supplementation and the raising of glucose levels to hyperglycaemic amounts influences expression. Expression of the genes was measured via real-time reverse transcription polymerase chain reaction (real-time RT-PCR).

The second aim was testing how the gene expression changes in cells with raised cholesterol levels and how L-carnitine supplementation influences said steady state mRNA levels. For this purpose, cultured cells were kept in a carnitine-deprived growth medium with 250 µl, 500 µl or 1000 µl Lipids Cholesterol Rich from adult bovine serum (Sigma-Aldrich) added to one set of plates, while for another set of plates an additional 80 µM of L-carnitine was supplemented. All plates were incubated for 24 hours. Steady state mRNA levels were measured via real-time RT-PCR.

The third goal was using the Cignal Finder™ Multi-Pathway Reporter Arrays (Plate Format) (SABiosciences) to test if any of the ten signalling pathways on the plate are regulated by L-carnitine, with the intention to see if any of these signalling pathway members could be later used as additional candidates for the electrophoretic mobility shift analysis.

In the fourth part, we tested which transcription factors contribute to the carnitine-dependent upregulation of the human CRAT promoter. Transcription factors were chosen based on the results of the theoretical promoter analysis, the results of the Cignal assay and on similar transcription factors from the murine CRAT promoter [66]. To reach our goal, the theoretically predicted sequences were used in electrophoretic mobility shift assays (EMSA). In these in vitro tests radioactively marked oligonucleotides are incubated with protein extracts isolated from cells, grown either under normal conditions, or under carnitine deficiency and/or with supplementation of 40 µM or 80 µM L-carnitine for 4 hours. We also tested how varying concentrations of unlabelled (not marked by

radioactivity) acetyl-L-carnitine influences the stability and formation of these promoter factor complexes. Two of the sequences were also used for supershift analysis together with specific antibodies (LXRα/β, PPARγ, PPARβ, PPARα, RXRβ_2, RXRβ_1, RXR$\alpha/\beta/\gamma$, RXRγ, FXR1, FXR2 and RARγ)that could bind to these promoter factors.

2. Materials and methods

2.1. Cell culture

All experiments were performed using the human hepatic cell line WRL68.

2.1.1. Propagation of cells

WRL68 cells were grown in 100 mm petri dishes in 10 ml Dulbecco's Modified Eagle Medium (DMEM) with 4500 mg/l glucose, supplemented with 10% foetal calf serum (FCS), 5 ml penicillin/streptomycin – P/S, 10000 U/ml and 10 mg/ml, respectively – and 5 ml Qmax (Gibco), in an incubator with 100% air humidity at 37°C and 7.5% CO_2. Upon reaching 80-90% confluence, the cultures were split to allow further growth or stored as frozen cells batches (10% DMSO as additive). Splitting was done by removing the medium and washing the cells (3x) with 1x PBS, followed by trypsinization. For this purpose, a few drops of Trypsin/EDTA were added to the attached cells and incubated at 37°C for 2-5 minutes. The detached cells were resuspended in 10 ml full growth medium and split in the desired ratio for further propagation or counted with CASY Cell Counter to seed the desired number of cells for experiments.

2.1.2. Metabolic conditions for cell cultivation in hyperglycaemic medium

The WRL68 cells were grown under following conditions for the light cycler measurements:

- Normal (N): cells were grown in 10 ml DMEM + 10% FCS + P/S + Qmax until they reached 80-90% confluence (2-3 x 10^6 cells); medium was changed once per 2 days.
- Dialysed (D): 1.7-2 x 10^6 cells were grown in 10 ml DMEM + 10% dialysed FCS (dialFCS) + P/S + Qmax for 48h. Medium was changed after 24h.
- 40 µM L-carnitine: 1.7-2 x 10^6 cells were grown in 10 ml DMEM + 10% dialysed FCS (dialFCS) + P/S + Qmax for 24h and subsequently induced with 40 µM L-carnitine for 4h.
- 80 µM L-carnitine – 4h: 1.7-2 x 10^6 cells were grown in 10 ml DMEM + dialysed 10% FCS + P/S + Qmax for 24h and then induced with 80 µM L-carnitine for 4h.

- 80 µM L-carnitine – 15h: 1.7-2 x 10^6 cells were grown in 10 ml DMEM + dialysed 10% FCS + P/S + Qmax for 24h and then induced with 80 µM L-carnitine for 15h.
- 80 µM L-carnitine – 24h: 1.7-2 x 10^6 cells were grown in 10 ml DMEM + dialysed 10% FCS + P/S + Qmax for 24h and then induced with 80 µM L-carnitine for 24h.
- 80 µM L-carnitine – 48h: 1.7-2 x 10^6 cells were grown in 10 ml DMEM + dialysed 10% FCS + P/S + Qmax for 24h and then induced with 80 µM L-carnitine for 24h. The next day, the medium was changed and cells were again induced with 80 µM L-carnitine for 24h.
- 2.5 mg/ml cholesterol: cells were grown in 10 ml DMEM + dialysed 10% FCS + P/S + Qmax for 24h, after which 250 µl of Lipids Cholesterol Rich from adult bovine serum (Sigma-Aldrich) was added and incubated for 24h.
- 5 mg/ml cholesterol: cells were grown in 10 ml DMEM + dialysed 10% FCS + P/S + Qmax for 24h, after which 500 µl of Lipids Cholesterol Rich from adult bovine serum (Sigma-Aldrich) was added and incubated for 24h.
- 10 mg/ml cholesterol: cells were grown in 10 ml DMEM + dialysed 10% FCS + P/S + Qmax for 24h, after which 1000 µl of Lipids Cholesterol Rich from adult bovine serum (Sigma-Aldrich) was added and incubated for 24h.
- 2.5 mg/ml cholesterol + L-carnitine: cells were grown in 10 ml DMEM + dialysed 10% FCS + P/S + Qmax for 24h, after which 250 µl of Lipids Cholesterol Rich from adult bovine serum (Sigma-Aldrich) and incubated for 24h. Cells were then induced with 80 µM L-carnitine for 4 hours.
- 5 mg/ml cholesterol + L-carnitine: cells were grown in 10 ml DMEM + dialysed 10% FCS + P/S + Qmax for 24h, after which 500 µl of Lipids Cholesterol Rich from adult bovine serum (Sigma-Aldrich) and incubated for 24h. Cells were then induced with 80 µM L-carnitine for 4 hours.
- 10 mg/ml cholesterol + L-carnitine: cells were grown in 10 ml DMEM + dialysed 10% FCS + P/S + Qmax for 24h, after which 1000 µl of Lipids Cholesterol Rich from adult bovine serum (Sigma-Aldrich) was added and incubated for 24h. Cells were then induced with 80 µM L-carnitine for 4 hours.

2.1.3. Metabolic conditions for cell cultivation in normoglycaemic medium

The WRL68 cells for the normoglycaemic experiments were all grown in Dulbecco's Modified Eagle Medium (DMEM) with 1000 mg/l glucose under following conditions:

- Normal (N): 7.5 x 10^5 cells were grown in 10 ml DMEM (4500 mg/l glucose) + P/S + Qmax (hyperglycaemic medium) + 10% FCS. After 24 hours, the medium was changed for 10 ml DMEM (1000 mg/l glucose) + P/S + Qmax (normoglycaemic medium) + 10% FCS for 48 hours.
- Dialysed (D): 7.5 x 10^5 cells were grown in 10 ml hyperglycaemic medium + 10% FCS. After 24 hours, the medium was changed for 10 ml normoglycaemic medium + 10% dialysed FCS for 48 hours, with a medium change after 24 hours.
- 40 µM L-carnitine: 7.5 x 10^5 cells were grown in 10 ml hyperglycaemic medium + 10% FCS. After 24 hours, the medium was changed for 10 ml normoglycaemic medium + 10% dialysed FCS for 24 hours, followed by supplementation of 40 µM L-carnitine for 4 hours.
- 40 µM L-carnitine + glucose: 7.5 x 10^5 cells were grown in 10 ml hyperglycaemic medium + 10% FCS. After 24 hours, the medium was changed for 10 ml normoglycaemic medium + 10% dialysed FCS for 24 hours, followed by supplementation of 40 µM L-carnitine and raising of glucose levels to 4500 mg/l for 4 hours.
- 4h 80 µM L-carnitine: 7.5 x 10^5 cells were grown in 10 ml hyperglycaemic medium + 10% FCS. After 24 hours, the medium was changed for 10 ml normoglycaemic medium + 10% dialysed FCS for 24 hours, followed by supplementation of 80 µM L-carnitine for 4 hours.
- 4h 80 µM L-carnitine + glucose: 7.5 x 10^5 cells were grown in 10 ml hyperglycaemic medium + 10% FCS. After 24 hours, the medium was changed for 10 ml normoglycaemic medium + 10% dialysed FCS for 24 hours, followed by supplementation of 80 µM L-carnitine and raising of glucose levels to 4500 mg/l for 4 hours.
- 15h 80 µM L-carnitine: 3.75 x 10^5 cells were grown in 10 ml hyperglycaemic medium + 10% FCS. After 24 hours, the medium was changed for 10 ml normoglycaemic medium + 10% dialysed FCS for 24 hours, followed by a medium change and supplementation of 80 µM L-carnitine for 15 hours.

- 15h 80 µM L-carnitine + glucose: 3.75 x 10^5 cells were grown in 10 ml hyperglycaemic medium + 10% FCS. After 24 hours, the medium was changed for 10 ml normoglycaemic medium + 10% dialysed FCS for 24 hours, followed by a medium change and supplementation of 80 µM L-carnitine and raising of glucose levels to 4500 mg/l for 15 hours.
- 24h 80 µM L-carnitine: 3.75 x 10^5 cells were grown in 10 ml hyperglycaemic medium + 10% FCS. After 24 hours, the medium was changed for 10 ml normoglycaemic medium + 10% dialysed FCS for 24 hours, followed by a medium change and supplementation of 80 µM L-carnitine for 24 hours.
- 24h 80 µM L-carnitine + glucose: 3.75 x 10^5 cells were grown in 10 ml hyperglycaemic medium + 10% FCS. After 24 hours, the medium was changed for 10 ml normoglycaemic medium + 10% dialysed FCS for 24 hours, followed by a medium change and supplementation of 80 µM L-carnitine and raising of glucose levels to 4500 mg/l for 24 hours.
- 48h 80 µM L-carnitine: 3.75 x 10^5 cells were grown in 10 ml hyperglycaemic medium + 10% FCS. After 24 hours, the medium was changed for 10 ml normoglycaemicmedium + 10% dialysed FCS for 24 hours, followed by a medium change and supplementation of 80 µM L-carnitine for 48 hours, with a medium change and new supplementation after 24 hours.
- 48h 80 µM L-carnitine + glucose: 3.75 x 10^5 cells were grown in 10 ml hyperglycaemic medium + 10% FCS. After 24 hours, the medium was changed for 10 ml normoglycaemic medium + 10% dialysed FCS for 24 hours, followed by a medium change and supplementation of 80 µM L-carnitine and raising of glucose levels to 4500 mg/l for 48 hours, with a medium change and new supplementation after 24 hours.

2.1.4. Freezing of cells

When cells were intended to be stored and /or later propagation they were grown to 90% confluence. For this purpose, they were washed 3x with 1x PBS and treated with Trypsin-EDTA in order to detach them. After a few minutes of incubation at 37°C the cells were resuspended in 1.5 ml DMEM + 10% FCS + P/S + Qmax and transferred to a cryotube and incubated on ice for 5 minutes. After this incubation 10% (v/v) of DMSO was added to the suspensionand incubation on ice was continued for additional 15 minutes, followed by freezing at -80°C.

2.1.5. Thawing of cells

Frozen cells were slowly thawed and then resuspended in 10 ml warm full growth medium by pipetting them on a 100 mm cell culture plate.

2.2. Testing of new PCR-primers

2.2.1. Primers

EIF2AK4

Sense: 5’ GAC TTC AGA CCT CCC TTG CC 3’

Antisense: 3’ AGC TGT ACA GAA ATA GCA CAG ACA 5’

PGC-1α

Sense: 5’ CTG GTT GCC TGC ATG AGT GT 3’

Antisense: 3’ ACT TGA GTC CAC CCA GAA AGC 5’

Rac1

Sense: 5’ TGA TGC AGG CCA TCA AGT GT 3’

Antisense: 3’ AGA ACA CAT CTG TTT GCG GAT 5’

Rheb

Sense: 5’ CGA GCT AGC GAG CGA GAG 3’

Antisense: 3’ GAG GAT TTC CCC ACA GAC CG 5’

SREBP-1

Sense: 5’ AGC CCC ACT TCA TCA AGG C 3’

Antisense: 3’ GCT TCT CAA TGG CGT TGT GG 5’

2.2.2. Gradient PCR

Newly synthesized primers were dissolved in sterile ddH_2O at a concentration of 100 µM and were used for a gradient PCR reaction to determine the best temperature for different primer pairs. The reaction mix had a total volume of 50 µl/PCR tube and contained:

GoTaq® G2 Colorless Master Mix (Promega)	25 µl
10 µM Primer – Sense	5 µl
10 µM Primer – Antisense	5 µl
DNA	2 µl
dH_2O	13 µl
Total:	50 µl

Table 1: Reaction mix for the gradient PCR.

Settings for the PCR were:

Step	Temperature	Time
Initial denaturation	95°C	3 min
Quantification 41 cycles	95°C	30 s
	60°C	30 s
	72°C	1 min
Final extension	72°C	7 min
Hold	4°C	∞

Table 2: settings for the gradient PCR.

2.2.3. Gel electrophoresis:

After the PCR, 15 µl of reaction PCR product were mixed with 3 µl loading dye and loaded on a 1.2% agarose gel. As a DNA size marker, 10 µl Quick-Load Purple DNA Ladder (New England Biolabs) was used. The gel was pre-run at 20 V for 15 minutes and run at 68 V for 30 minutes in 1x TAE.

2.2.4. Gel elution and DNA isolation

Gel elution and DNA isolation was performed by using the Wizard® SV Gel and PCR Clean-Up System (Promega), following the manufacturer's instructions.

1. After gel electrophoresis, the 3 strongest bands were cut out of the gel and placed into a weighed 1.5 ml Eppendorf tube. 10 µl Membrane Binding Buffer were added per 10 mg of gel and it was subsequently dissolved at 50-65°C.
2. The dissolved gel was transferred to a SV Minicolumn, placed into a collection tube.
3. The mix was incubated for 1 minute at room temperature and then centrifuged at 16000 g for 1 minute.
4. The flowthrough was discarded and the Minicolumn was placed back into the collection tube.
5. 700 µl Membrane Wash Solution (diluted with ethanol) were added to the membrane and the Minicolumn was centrifuged at 16000 g for 1 minute.
6. The flowthrough was discarded and the step was repeated with 500 µl Membrane Wash Solution.
7. The flowthrough was once again discarded and the Minicolumn was recentrifuged for 1 minute with an open cap to let any residual ethanol evaporate.
8. The column was then transferred to a new 1.5 ml Eppendorf tube.
9. 50 µl nuclease free water were added to the Minicolumn and incubated for 1 minute, followed by centrifugation at 16000 g for 1 minute.
10. The eluted DNA was stored at -20°C.

2.3. Measuring of gene expression

2.3.1. Cell harvesting

Cells that have reached 90% confluence were harvested and frozen. First, the medium was removed and plates were put on ice. 300 µl 1x PBS of was added to the plates and the cells were scraped into a 1.5 ml Eppendorf tube with a rubber policeman. The tubes were then centrifuged for 5 minutes at 2.000 rpm, the PBS was removed and the pellets were frozen on dry ice and stored at -80°C.

2.3.2. RNA isolation

RNA was isolated with a peqGOLD Total RNA Kit (Peqlab Biotechnologie GmbH), according to the manufacturer's instructions. The frozen pellet was resuspended in 400 µl RNA Lysis buffer, loaded on a DNA Removing Column and centrifuged at 12.000 rcf for 1 minute. An equal volume of 70% ethanol was then added to the flow-through and mixed. The lysate was loaded onto a PerfectBind RNA Column (with a maximum of 750 µl at once) and centrifuged at 10.000 rcf for 1 minute. The flowthrough was discarded and 500 µl RNA Wash Buffer I were applied onto the RNA Column and the column was centrifuged at 10.000 rcf for 15 seconds, followed by washing with 600 µl RNA Wash Buffer II and centrifugation. The column was then dried by centrifugation at 12.000 rcf for 2 minutes. 50-100 µl RNase-free dH_2O were then directly applied to the matrix. The column was incubated at room temperature for 3 minutes, after which it was centrifuged at 5.000 rcf for 1 minute. The concentration of the eluted RNA was measured via NanoDrop and the RNA was frozen at -80°C.

2.3.3. cDNA synthesis

1. 3 µg of RNA and 1 µl of oligo(dT)18-primers were mixed with RNase free dH_2O to a total volume of 11 µl.
2. The mix was heated for 5 minutes at 70°C, followed by incubation on ice for 5 minutes.
3. 4 µl of Fermentas M-MuLV Reverse Transcriptase 5x Reaction Buffer, 2 µl dNTP mix (10mM), 1 µl RNase free dH_2O and 1 µl RiboLock RNase Inhibitor (Thermo Fisher Scientific) were added to the mix.
4. The mix was incubated at 37°C for 5 minutes.
5. 1 µl RevertAid Reverse Transcriptase was added to the mix and incubated for 1 hour at 42°C.
6. After incubation, the enzyme was deactivated by heating to 70°C for 1 minute.
7. The mix was then incubated on ice for 5 minutes and stored at -80°C.

2.3.4. Real-time RT-PCR

Real-time RT-PCR reaction mix per well:

dH_2O	7 µl
Primer sense (10 µM)	0.5 µl
Primer antisense (10 µM)	0.5 µl
LightCycler® 480 SYBR Green I Master (Roche)	9 µl
Total:	17 µl

Table 3: PCR reaction mix for one well.

The reaction mix was kept in the dark at 4°C and pipetted into the wells a 96-well plate. 1 µl sample cDNA was added to each well and the plate was sealed with sealing foil. The well was then centrifuged and the real-time PCR was performed using a Roche LightCycler 480.

Beta-actin was used as control. All samples and the control samples were measured in triplicates. For each gene, a standard curve was also measured by preparing samples with a known amount of cDNA, ranging from 10 µg to 0.001 µg, to calculate the efficiency of the reaction.

Step	**Temperature**	**Time**
	95°C	2 min
Quantification 45 cycles	95°C	20 s
	59°C	15 s
	72°C	40 s
Melting curves	95°C	15 s
	60°C	15 s
	95°C	Continuous acquisition
	40°C	20 s

Table 4: Settings for the real-time RT-PCR.

2.3.5. Statistical analysis

Statistical analysis of the measured steady state mRNA levels was performed by using a one sample student's t-test, which was carried out with the program SPSS.

2.4. Pinpointing of L-carnitine-regulated pathways

2.4.1. Cignal multi-pathway activity assay

The Cignal Assay was performed using a Cignal Finder™ 10-Pathway Reporter Array (Plate Format) (Qiagen), according to the manufacturer's instructions, with some slight modifications:

1. 50 µl of Opti-MEM® (Thermo Fisher Scientific Inc.) was added to each well on the plate. The reporter assay constructs were resuspended by tapping the plate and incubated for 5 minutes at room temperature.
2. A mix of 0.3 µl of ViaFect™ Transfection Reagent (Promega, Mannheim, Germany) and 50 µl of Opti-MEM® was prepared per well. The mix was incubated for 5 minutes at room temperature, after which it was added to the resuspended constructs.
3. The contents of the wells were mixed by gently tapping the plate for about 30 seconds, after which the plate was incubated for 20 minutes at room temperature to allow complex formation.
4. Cultured cells were washed with PBS and treated with 1-3 ml Trypsin-EDTA for 2-5 minutes in an incubator at 37°C and 7.5% CO_2. The cells were suspended in 7-9 ml of Opti-MEM® with 5% of foetal calf serum or dialysed foetal calf serum and counted with a CASY Cell Counter. After counting, the cells were centrifuged and resuspended in Opti-MEM® with 10% FCS/dialysed FCS and 1% NEAA*** to get a cell count of $6x10^5$ cells/ml.
5. After having incubated the plate for 20 minutes (as described under point 3), 50 µl of the cell suspension were added to each well of the plate and mixed by gently rocking the plate back and forth and left to right.
6. The plate was then incubated in an incubator at 37°C and 7.5% CO_2 for 24 hours.
7. After 24 hours, the medium in the wells was changed to complete growth medium (DMEM with 10% FCS/dialysed FCS, 0.1mM NEAA, 1mM Sodium pyruvate, 100

U/ml penicillin and 100 µg/ml streptomycin) for the control samples and to assay medium (Opti-MEM® containing 0.5% of dialysed FCS, 1% NEAA, 100 U/ml Penicillin and 100 µg/ml Streptomycin and 0 µM, 40 µM, 80 µM or 120 µM L-carnitine) in the other wells.

8. After 24 hours, the luciferase activity was measured by performing a luciferase assay.

2.4.2. Luciferase assay

The luciferase assay was carried out by using the Dual-Glo® Luciferase Assay System (Promega), according to the manufacturer's instructions:

1. Reagents were prepared by a) transferring the Dual-Glo® Luciferase Buffer to the Dual-Glo® Luciferase Substrate to create the Dual-Glo® Luciferase Reagent and b) diluting the needed amount of Dual-Glo® Stop & Glo® Substrate 1:100 in Dual-Glo® Stop & Glo® Buffer to a new container to create the Dual-Glo® Stop & Glo® Reagent.
2. 75 µl medium were removed from each well and 75 µl Dual-Glo® Luciferase Reagent were added.
3. The plate was incubated for at least 10 minutes and firefly luciferase activity was measured at 595 nm wavelength by using the Victor^3 V multilabel reader (PerkinElmer).
4. 75 µl Dual-Glo® Stop & Glo® Reagent were added to each well and the contents were mixed.
5. The plate was incubated for the same time as earlier (with at least 10 minutes) and renilla luciferase activity was measured at 480 nm wavelength by using the Victor^3 V multilabel reader (PerkinElmer).

2.5. Electrophoretic mobility shift assay and supershift assay

2.5.1. Metabolic conditions for cell cultivation

The WRL68 cells for the electrophoretic mobility shift and supershift assays were grown under following conditions:

- Normal (N): 7.5 x 10^5 cells were grown in 10 ml DMEM + 10% FCS + P/S + Qmax for 2 days.

- Dialysed (D): 1.7-2 x 10^6 cells were grown in 10 ml DMEM + 10% dialysed FCS (dialFCS) + P/S + Qmax for 48h, with a medium change after 24h.
- 40 µM L-carnitine: 1.7-2 x 10^6 cells were grown in 10 ml DMEM + 10% dialysed FCS (dialFCS) + P/S + Qmax for 48h, with a medium change after 24h. Cells were induced with 40 µM L-carnitine for 4h before harvest.
- 80 µM L-carnitine: 1.7-2 x 10^6 cells were grown in 10 ml DMEM + 10% dialysed FCS (dialFCS) + P/S + Qmax for 48h, with a medium change after 24h. Cells were induced with 80 µM L-carnitine for 4h before harvest.

2.5.2. List of antibodies

All antibodies were produced by Santa Cruz Biotechnology.

LXRα/β (H-7): sc-377260

PPARγ (E-8): sc-7273

PPARβ (F-10): sc-74517

PPARα (H-2): sc-398394

RXRβ$_2$ (MOK13-17): sc-56869

RXRβ1 (A-1): sc-376301

RXRα/β/γ (F-1): sc-46659

RXRγ (A-2): sc-365252

FXR1 (B-2): sc-374148

FXR2 (1G2): sc-32266

FXR (D-3): sc-25309

RARγ (H-6): sc-398065

2.5.3. Nuclear extract isolation

Isolation of nuclear extracts was performed as described by Siu et al. [99] in their protocol, with some small modifications:

1. Cells were cultured on 100 mm petri dishes until they reached 80-90% confluence.
2. The medium was removed and the cells were washed with 2-3 ml 1x PBS.
3. 2 ml of cell lysis buffer were added to each plate.
4. The cells were scraped from the plates into 2 ml Eppendorf tubes with a rubber policeman.
5. Nuclei were collected by centrifugation at 2500 g for 5 minutes at 4°C. The supernatant was removed without touching the pellet.
6. The pellet was resuspended in 300 µl nuclear extract buffer and incubated on a rocker platform for 1 hour at 4°C.
7. Debris was removed by centrifugation at 12000 g for 10 minutes at 4°C.
8. The supernatant was aliquoted into 3 Eppendorf tubes, 100 µl in each, and frozen in an ethanol cooling bath. 2 µl of the supernatant were used to measure protein concentration via Bradford assay.

Cell lysis buffer:

HEPES pH 7.6	20 mM
Glycerol	20%
NaCl	10 mM
$MgCl_2$	1.5 mM
EDTA	0.2 mM
Triton X	0.1%

The buffer was mixed to 90% and completed before use by adding dH_2O, PMSF, Complete Protease Inhibitor (Roche) and 1 mM DTT.

Nuclear extract buffer:

HEPES pH 7.6	20 mM
Glycerol	20%
NaCl	500 mM
$MgCl_2$	1.5 mM
EDTA	0.2 mM
Triton X	0.1%

The buffer was mixed to 90% and completed before use by adding dH_2O, PMSF, Complete Protease Inhibitor (Roche) and 1 mM DTT.

Bradford assay:

Protein concentration was measured by adding 2 µl of the nuclear extract to 800 µl water and 200 µl dye reagent. The mix was incubated for 5 minutes at room temperature. Absorbance was measured at 595 nm and the values were then used to calculate the concentration.

2.5.4. Preparation of spun columns

Columns for spun column chromatography were prepared by using 1 ml disposable syringes. The syringes were stuffed at the bottom with sterile siliconized glass wool to the 0.15 ml mark, inserted into 15 ml falcon tubes and filled with Sephadex G-50 in 1x TEN buffer (pH 8.0). The tubes were centrifuged for 5 minutes at 1500 rpm. The process was repeated until solid dry spun Sephadex reached to the 0.9 ml mark, followed by the final loading of 100 µl 1x TE buffer and one centrifugation for 5 minutes. The columns were sealed with parafilm and stored at 4°C until used for chromatography.

2.5.5. Radioactive labelling of oligonucleotides

oligo deoxynucleotide (100ng/µl)	1 µl
10x T4 polynucleotide kinase Buffer	5 µl
γ-32 ATP	4 µl
T4 polynucleotide kinase	1.5 µl
ddH_2O	38.5 µl
Total:	50 µl

The mix was incubated at 37°C for 30 minutes, after which it was stopped by adding 50 µl 1x TE buffer and mixing. 1 µl of the mix was used for Cherenkov activity measurement, while the rest was transferred to a spun column and centrifuged at 1500 rpm for 5 minutes. 1 µl of the mix was again used to control if the radioactive ^{32}P-labelwas successfully covalently introduced into the oligonucleotide. 2-3 µl of antisense oligonucleotide was added to the mix and heated to 90°C. The mix was then left for 30 minutes and room temperature and stored at 4°C.

2.5.6. Cherenkov counting for radioactivity measurement

1 µl of the radioactive mix before and after centrifugation was added to 99 µl of distilled water and measured using the TRI-CARB 2100TR Liquid Scintillation Analyzer.

2.5.7. Electrophoretic mobility shift and supershift assays

The radioactive oligonucleotides were used to prepare the reaction mix for the band shift and supershift assays:

5x Reaction Buffer	5 µl
sonicated salmon sperm DNA (5 µg/ml)	1 µl
ssODN (γ-^{32} ATP)	1 µl
10 µg nuclear extract	x µl
ddH_2O	y µl
antibody (for supershift assay)	1 µl
Total:	20 µl

The reaction mix was incubated in the dark on ice for 30 minutes, then it was immediately loaded on a nondenaturing polyacrylamide gel. For the estimation of the size of the

complexes, Thermo Scientific PageRuler and Thermo Scientific PageRuler Plus Prestained Protein Ladder were used as size markers. All assays were run on a band shift gel, made from:

30% Acrylamide-2% Bisacrylamide	3.18 ml
dH_2O	18.42 ml
10x TBE	1.44 ml
10% APS	120 µl
TEMED	24 µl
Total (for 2 gels):	25 ml

2.5.8. Optimization of electrophoresis conditions

All analyses were performed at 4°C in 1x TBE. The first band shifts were performed at 60V for 190 minutes. A test gel was run at 120V for 90 minutes, which showed to be an acceptable setting for the assay as it did not harm the complex and only resulted in faster migration of the bands, and repeated analyses were done using these settings. Assays of a series were always performed under the same conditions.

After electrophoresis, the gel had to be dried. For this purpose, it was transferred to a Whatman paper, covered with saran wrap and dried under vacuum for 1.5-2 hours at 75°C. The dried gels were then exposed to x-ray films from 1 hour and up to 5 days at -80°C.

3. Results

3.1. Simulation of hypercholesterolaemia in the cell culture

In order to mock hypercholesterolaemia, 3000 µl of Lipids Cholesterol Rich from adult bovine serum (Sigma-Aldrich) was added to a plate with cultured cells on the first try to reach cholesterol levels in the medium that are found in people with hypercholesterolaemia, but this amount proved to be too high and the cells died. Because of this, the added cholesterol was reduced to 250 µl, 500 µl and 1000 µl, with 1000 µl being the upper limit cells could still be propagated.

3.2. Real-time RT-PCR

3.2.1. Steady state mRNA levels of cells in a hyperglycaemic medium

3.2.1.1. OCTN1

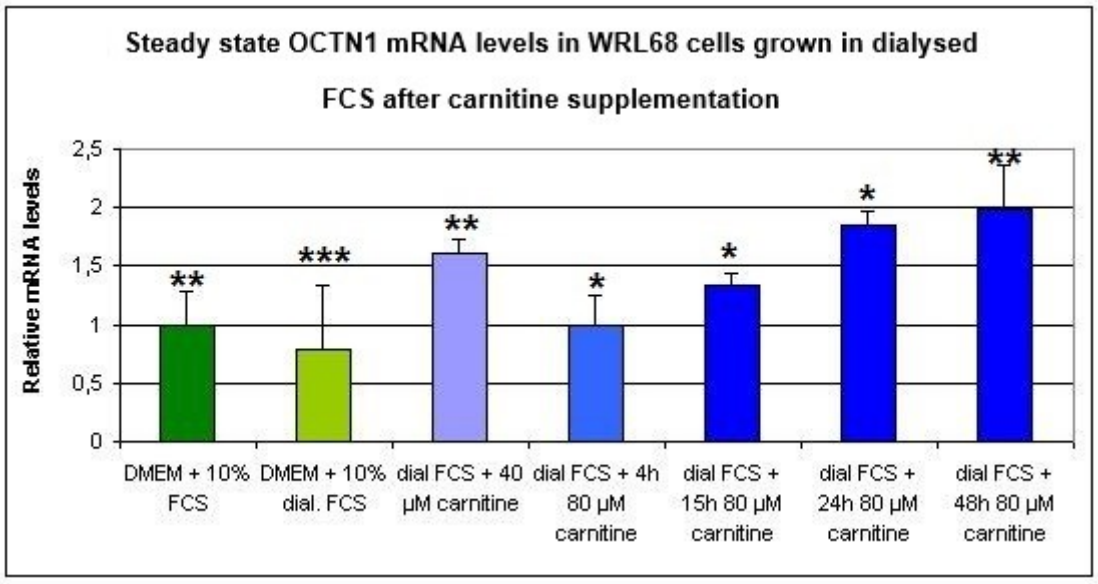

Figure 4: Analysis of OCTN1 steady state mRNA levels in WRL68 cells cultivated under L-carnitine deprivation and supplementation in a hyperglycaemic medium. Steady state OCTN1-mRNA levels were determined by real-time RT-PCR in WRL68 cells, cultivated in 10% dialysed FCS and supplemented with 40 µM and 80 µM L-carnitine (increasing supplementation durations) in comparison to un-supplemented and normal FCS. T-bars signify the standard deviation of each sample.

Expression of OCTN1 steady state mRNA levels in WRL68 cells, cultivated in DMEM medium with 10% “normal” undialysed FCS ($p<0.05$; indicated by **), were set at 1.0 to serve as basic reference level for all other treatment regimens (fig. 4). The OCTN1

mRNA amounts in cells kept under 10% dialysed FCS (= carnitine deficient medium) declined to 0.8 in relation to standard FCS with a statistical significance level of $p<0.5$ (indicated by ***). Subsequent supplementation of L-carnitine to the growth medium containing dialysed FCS raised OCTN1 expression back to normal extents or above, dependent on L-carnitine levels and duration of supplementation. Treatment with 40 µM for 4hrs lifted the mRNA steady state levels 1.6-fold above normal expression ($p<0.05$). In contrast, supplementation of 80 µM L-carnitine interestingly exerted a strict time dependent increase of steady mRNA levels. After 4hrs, OCTN1 expression was restored to that in WRL68 cells when cultivated in normal 10% FCS ($p<0.005$; indicated by *), however, after 15hrs a 1.3-fold ($p<0.005$), after 24hrs a 1.9-fold ($p<0.005$) and after 48hrs a 2.0-fold ($p<0.05$) peak in mRNA induction above the reference level in cells grown in 10% FCS could be recorded. Therefore, OCTN1 steady state mRNA levels reached values exceeding normal gene expression after addition of 80 µM L-carnitine, but only after continued cultivation for up to 48hrs.

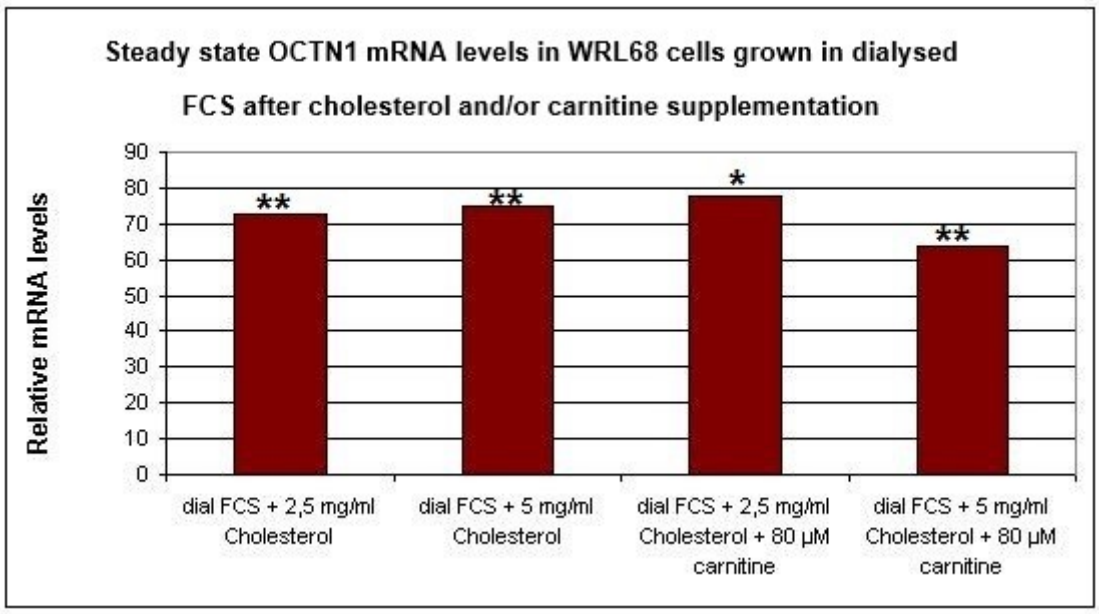

Figure 5: Analysis of OCTN1 steady state mRNA levels in WRL68 cells cultivated with cholesterol and L-carnitine supplementation. Steady state OCTN1-mRNA levels were determined by real-time RT-PCR in WRL68 cells, cultivated in 10% dialysed FCS and supplemented with 80 µM L-carnitine (increasing supplementation durations) in comparison to single cholesterol supplementation without L-carnitine. T-bars signify the standard deviation of each sample.

Addition of 2.5 mg/ml cholesterol (0.65 mM) to the cell culture medium containing 10% dialysed FCS increased expression of OCTN1 steady state mRNA levels in WRL68 cells approximately 72-fold over normal expression in 10% FCS ($p<0.05$), as seen in fig. 5.

However, doubling the cholesterol levels to 5.0 mg/ml final concentration (1.30 mM) caused only a slight additional surplus in OCTN1 mRNA increase of approximately 75-fold ($p<0.05$). Extra supplementation of 80 µM L-carnitine increased the extent of OCTN1 expression in the first case (78-fold over normal expression, $p<0.005$) and slightly lowered it in the second case (64-fold over normal expression, $p<0.05$).

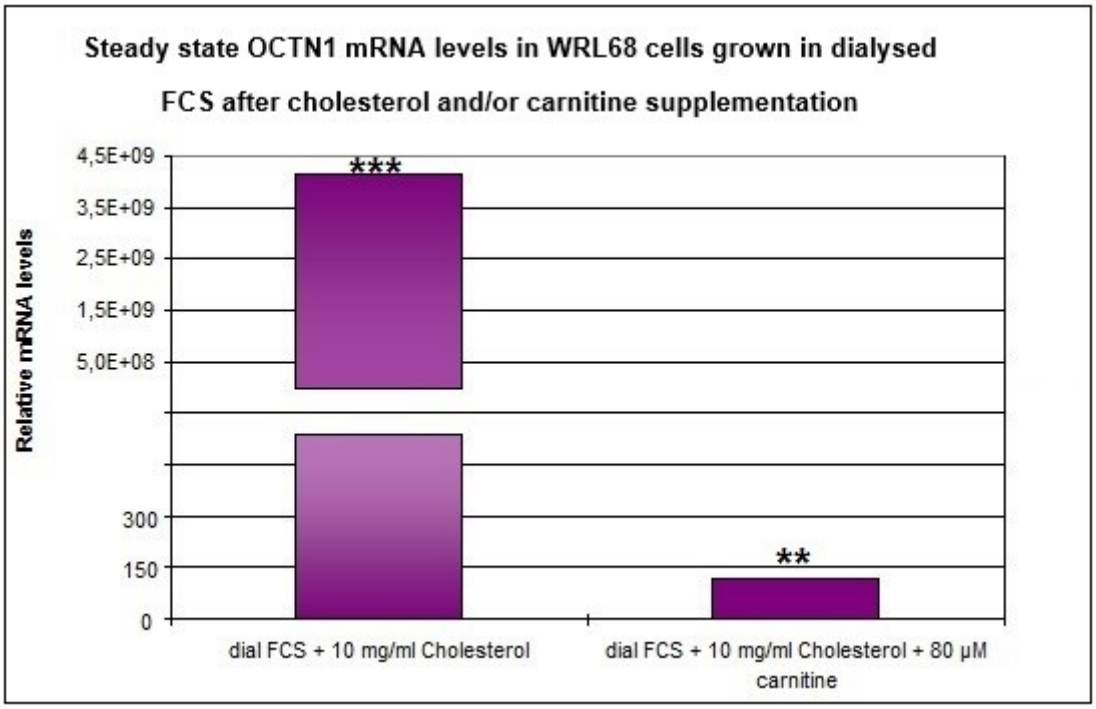

Figure 6: Analysis of OCTN1 steady state mRNA levels in WRL68 cells cultivated with supplementation of 10 mg/ml cholesterol and L-carnitine. Steady state OCTN1-mRNA levels were determined by real-time RT-PCR in WRL68 cells, cultivated in 10% dialysed FCS and supplemented with 80 µM L-carnitine (increasing supplementation durations) in comparison to cholesterol supplementation. T-bars signify the standard deviation of each sample.

Addition of 10 mg/ml cholesterol (2.59 mM) to the cell culture medium with dialysed FCS of WRL68 cells $4.2x10^9$-fold increased expression of OCTN1 steady state mRNA levels compared to expression normal FCS-containing cell culture medium ($p<0.5$) (fig. 6). This result in principle is an artificial one since such an enormous increase is physiologically not possible. But we observed comparable effects with the other genes by applying high concentrations of cholesterol in the medium. It is nevertheless a good indicator that cholesterol heavily affects gene expression, and that even these dramatic changes can be substantially remitted by L-carnitine. Subsequent supplementation with 80 µM L-carnitine successfully reduced the OCTN1 expression (132-fold over normal expression, $p<0.05$). Although this value still exceeded standard mRNA concentrations many fold

over normal extents, it is remarkable that L-carnitine was able to counteract this drastic induction of OCTN1 transcripts, caused by elevated cholesterol.

3.2.1.2. SLC35F2

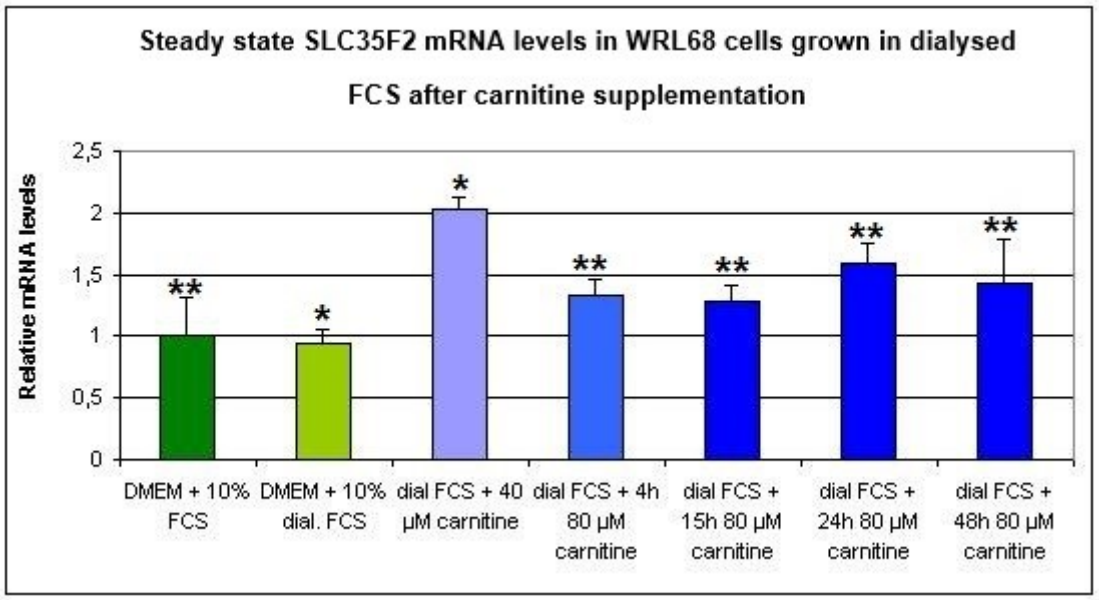

Figure 7: Analysis of SLC35F2 steady state mRNA levels in WRL68 cells cultivated under L-carnitine deprivation and supplementation in a hyperglycaemic medium. Steady state SLC35F2-mRNA levels were determined by real-time RT-PCR in WRL68 cells, cultivated in 10% dialysed FCS and supplemented with 40 µM and 80 µM L-carnitine (increasing supplementation durations) in comparison to un-supplemented and normal FCS. T-bars signify the standard deviation of each sample.

Expression of SLC35F2 steady state mRNA levels in WRL68 cells, cultivated in DMEM medium with 10% “normal” undialysed FCS ($p<0.05$; indicated by **), were set at 1.0 to serve as basic reference level for all other treatment regimens (fig. 7). The SLC35F2 mRNA amounts in cells kept under 10% dialysed FCS (= carnitine deficient medium) declined to 0.9 in relation to standard FCS with a statistical significance level of $p<0.005$ (indicated by *). Subsequent supplementation of L-carnitine to the growth medium containing dialysed FCS raised SLC35F2 expression above normal extents, dependent on L-carnitine levels and duration of supplementation. Treatment with 40 µM for 4hrs lifted the mRNA steady state levels 2-fold above normal expression ($p<0.005$), reaching the peak in induction. In contrast, supplementation of 80 µM L-carnitine showed a weaker effect in raising mRNA levels. After 4hrs a 1.3-fold ($p<0.05$), after 15hrs a 1.3-fold ($p<0.05$), after 24hrs a 1.6-fold ($p<0.05$) and after 48hrs a 1.4-fold ($p<0.05$) induction above the reference level in cells grown in 10% FCS could be recorded. Therefore, SLC35F2 steady state mRNA levels reached values exceeding normal gene expression

after addition 40 µM L-carnitine, while continued cultivation up to 48hrs with the addition of 80 µM L-carnitine was less successful.

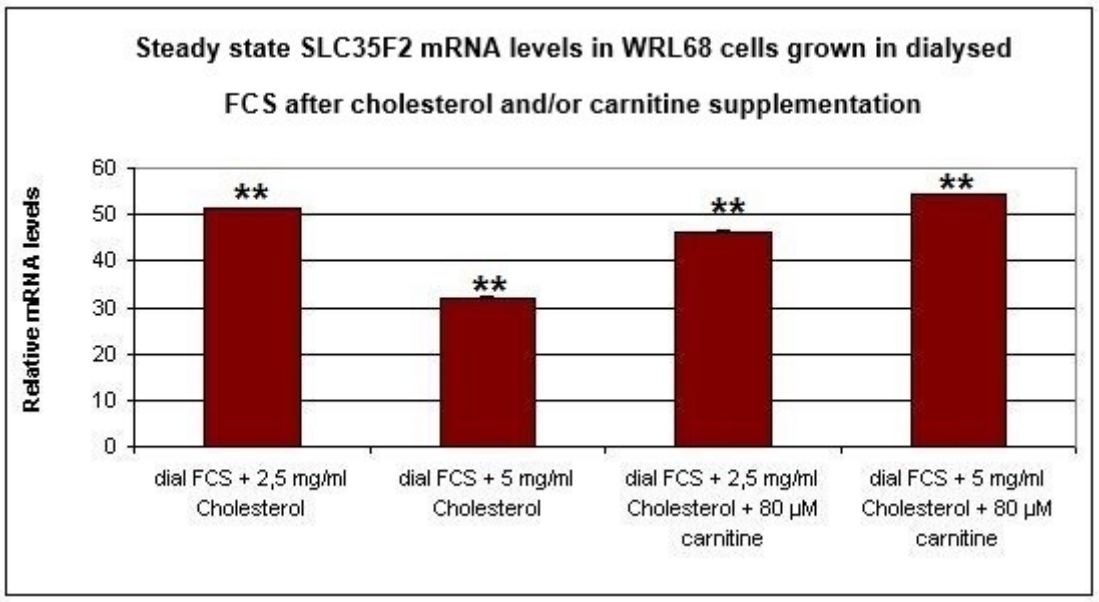

Figure 8: Analysis of SLC35F2 steady state mRNA levels in WRL68 cells cultivated with cholesterol and L-carnitine supplementation. Steady state SLC35F2-mRNA levels were determined by real-time RT-PCR in WRL68 cells, cultivated in 10% dialysed FCS and supplemented with 80 µM L-carnitine (increasing supplementation durations) in comparison to pure cholesterol supplementation. T-bars signify the standard deviation of each sample.

Addition of 2.5 mg/ml cholesterol (0.65 mM) to the cell culture medium containing 10% dialysed FCS increased expression of SLC35F2 steady state mRNA levels in WRL68 cells 51-fold over normal expression in 10% FCS ($p<0.05$), as seen in fig. 8Figure 8. However, doubling the cholesterol levels to 5.0 mg/ml final concentration (1.30 mM) caused only a 32-fold increase in OCTN1 mRNA ($p<0.05$). Extra supplementation of 80 µM L-carnitine decreased the extent of SLC35F2 expression in the first case (46-fold over normal expression, $p<0.05$), but increased it in the second case (54-fold over normal expression, $p<0.05$).

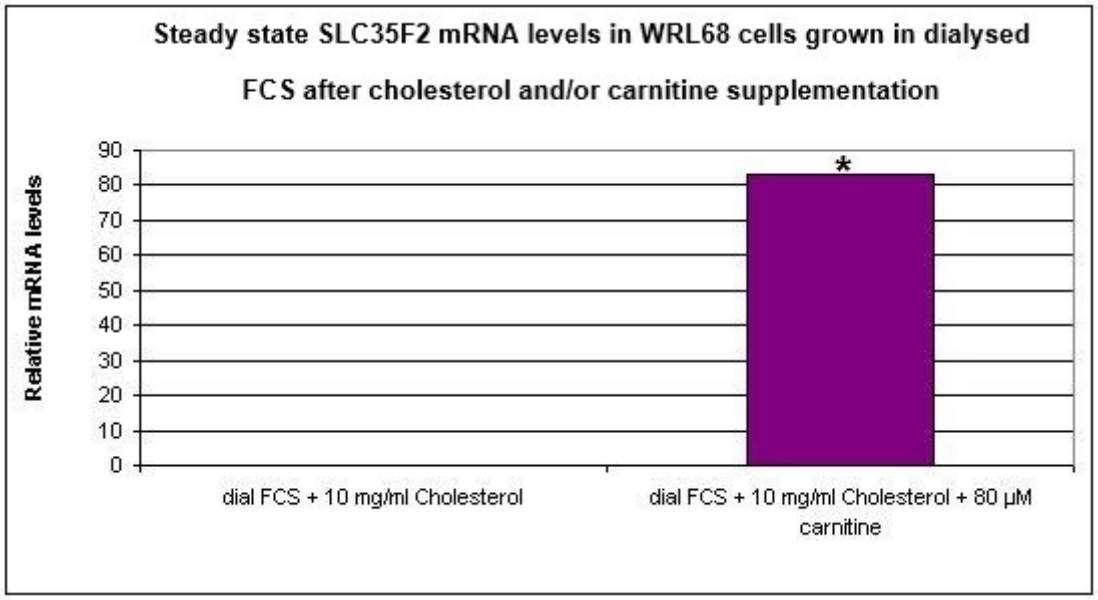

Figure 9: Analysis of SLC35F2 steady state mRNA levels in WRL68 cells cultivated with supplementation of 10 mg/ml cholesterol and L-carnitine. Steady state SLC35F2-mRNA levels were determined by real-time RT-PCR in WRL68 cells, cultivated in 10% dialysed FCS and supplemented with 80 µM L-carnitine (increasing supplementation durations) in comparison to cholesterol supplementation. T-bars signify the standard deviation of each sample.

In the treatment where 10 mg/ml cholesterol (2.59 mM) was added to the cell culture medium with dialysed FCS of WRL68 cells, no SLC35F2 steady state mRNA levels could be measured (fig. 9). Supplementation with 80 µM L-carnitine successfully raised the expression (83-fold above normal expression, $p<0.005$). The absence of detectable levels of steady state SLC35F2 mRNA in cells with cholesterol supplementation is probably due to inhibition of transcription by these cholesterol levels. Interestingly, L-carnitine is able to counteract this cholesterol effect and re-establish SLC35F2 gene expression.

3.2.1.3. Rac1

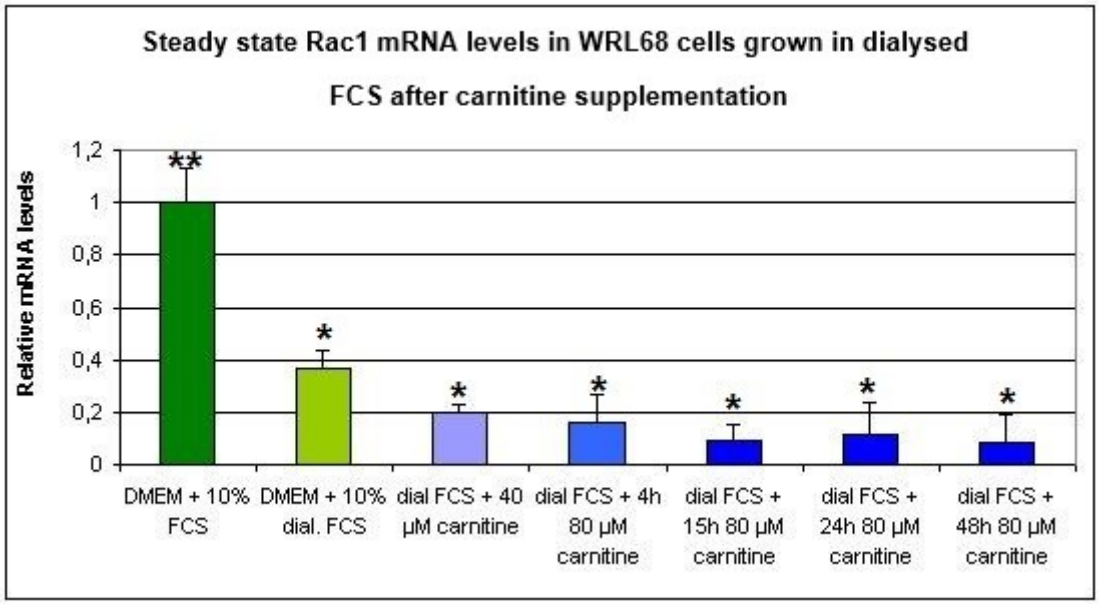

Figure 10: Analysis of Rac1 steady state mRNA levels in WRL68 cells cultivated under L-carnitine deprivation and supplementation in a hyperglycaemic medium. Steady state Rac1-mRNA levels were determined by real-time RT-PCR in WRL68 cells, cultivated in 10% dialysed FCS and supplemented with 40 µM and 80 µM L-carnitine (increasing supplementation durations) in comparison to un-supplemented and normal FCS. T-bars signify the standard deviation of each sample.

Expression of Rac1 steady state mRNA levels in WRL68 cells, cultivated in DMEM medium with 10% “normal” undialysed FCS ($p<0.05$; indicated by **), were set at 1.0 to serve as basic reference level for all other treatment regimens (fig. 10). The Rac1 mRNA amounts in cells kept under 10% dialysed FCS (= carnitine deficient medium) declined to 0.4 in relation to standard FCS with a statistical significance level of $p<0.005$ (indicated by *). Subsequent supplementation of L-carnitine to the growth medium containing dialysed FCS could not raise Rac1 expression back to normal extents or above, independent from L-carnitine levels or duration of supplementation. Treatment with 40 µM for 4hrs resulted in mRNA steady state levels 0.2-fold under normal expression ($p<0.005$). Supplementation of 80 µM L-carnitine resulted in similarly low levels, with recordings of 0.16-fold under normal expression after 4hrs ($p<0.005$), 0.09-fold after 15hrs ($p<0.005$), 0.1-fold after 24hrs ($p<0.005$) and 0.097-fold after 48hrs ($p<0.005$). Therefore, Rac1 steady state mRNA levels cannot be restored by L-carnitine in WRL68 cells.

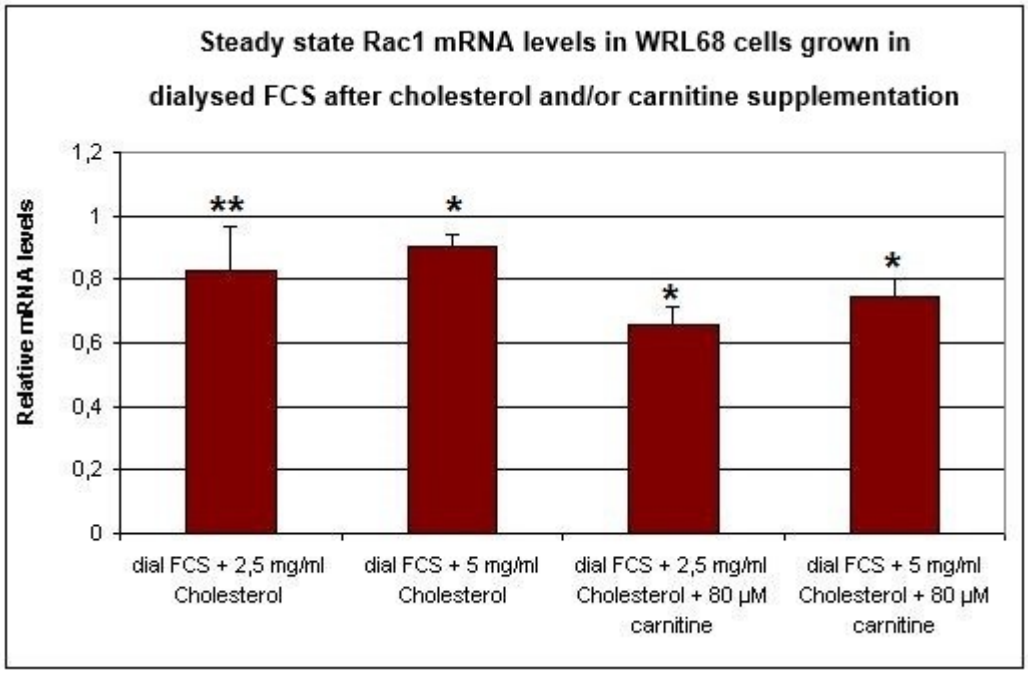

Figure 11: Analysis of Rac1 steady state mRNA levels in WRL68 cells cultivated with cholesterol and L-carnitine supplementation. Steady state Rac1-mRNA levels were determined by real-time RT-PCR in WRL68 cells, cultivated in 10% dialysed FCS and supplemented with 80 µM L-carnitine (increasing supplementation durations) in comparison to pure cholesterol supplementation. T-bars signify the standard deviation of each sample.

Addition of 2.5 mg/ml cholesterol (0.65 mM) to the cell culture medium containing 10% dialysed FCS decreased expression of Rac1 steady state mRNA levels in WRL68 cells approximately 0.8-fold under normal expression in 10% FCS ($p<0.05$), as seen in fig. 11. However, doubling the cholesterol levels to 5.0 mg/ml final concentration (1.30 mM) caused a slightly lower decrease in Rac1 mRNA of approximately 0.9-fold ($p<0.005$). Extra supplementation of 80 µM L-carnitine decreased the extent of Rac1 expression even further, close to 0.66-fold under normal expression ($p<0.005$) in the first case and approximately 0.75-fold under normal expression ($p<0.005$) in the second case.

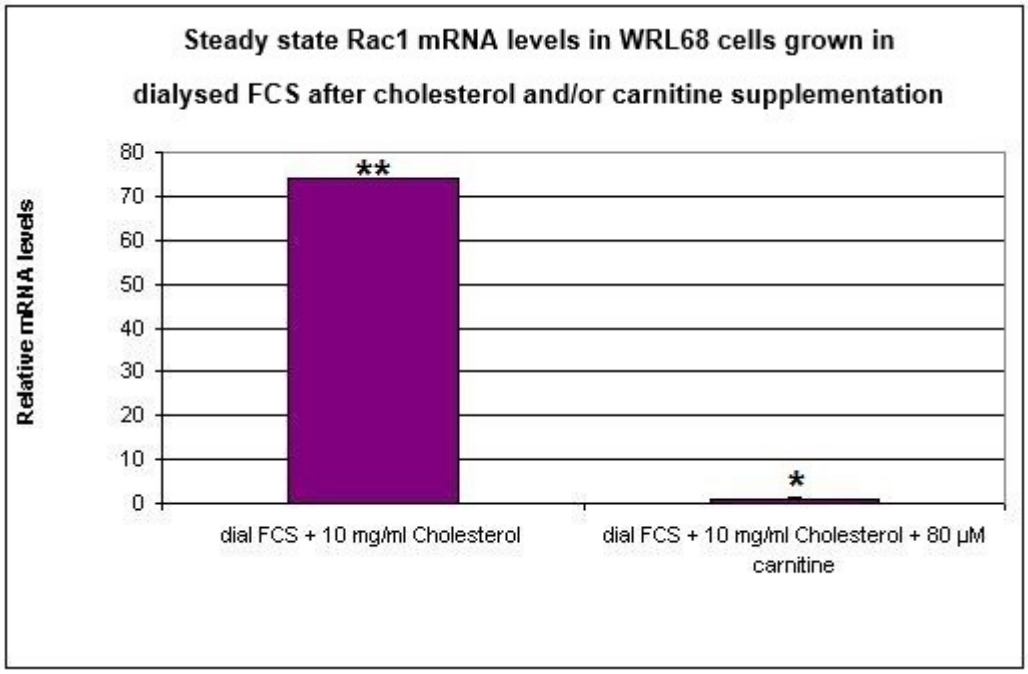

Figure 12: Analysis of Rac1 steady state mRNA levels in WRL68 cells cultivated with supplementation of 10 mg/ml cholesterol and L-carnitine. Steady state Rac1-mRNA levels were determined by real-time RT-PCR in WRL68 cells, cultivated in 10% dialysed FCS and supplemented with 80 µM L-carnitine (increasing supplementation durations) in comparison to cholesterol supplementation. T-bars signify the standard deviation of each sample.

Addition of 10 mg/ml cholesterol (2.59 mM) to the cell culture medium with 10% dialysed FCS of WRL68 cells 74-fold increased expression of Rac1 steady state mRNA levels compared to expression in normal FCS-containing cell culture medium ($p<0.05$) (see fig. 12). Subsequent supplementation with 80 µM L-carnitine reduced the expression of Rac1 to almost normal extents (1.1-fold over normal expression, $p<0.005$).

3.2.1.4. Rheb

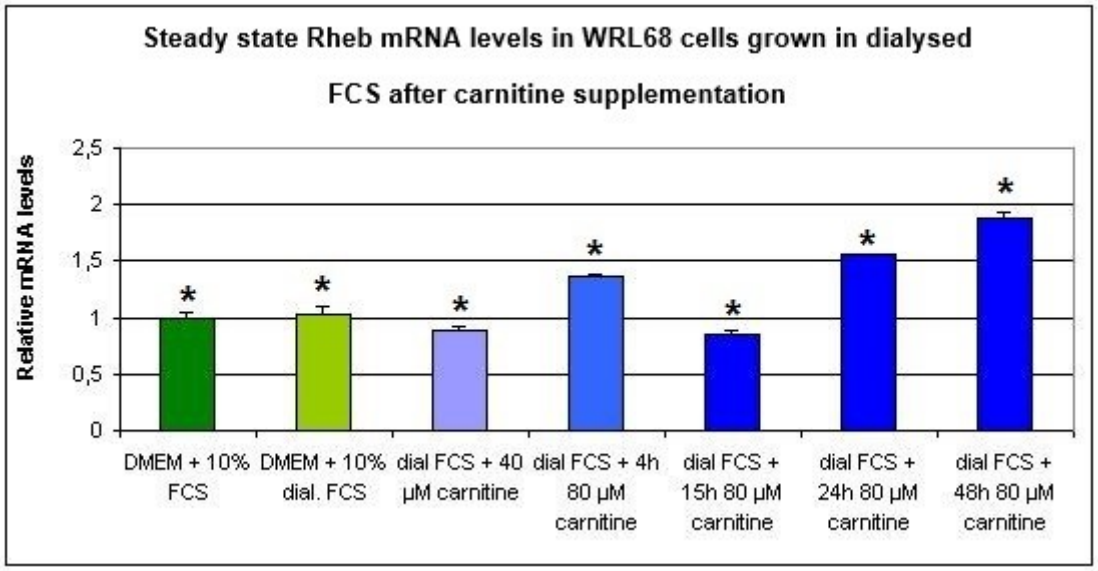

Figure 13: Analysis of Rheb steady state mRNA levels in WRL68 cells cultivated under L-carnitine deprivation and supplementation in a hyperglycaemic medium. Steady state Rheb-mRNA levels were determined by real-time RT-PCR in WRL68 cells, cultivated in 10% dialysed FCS and supplemented with 40 µM and 80 µM L-carnitine (increasing supplementation durations) in comparison to un-supplemented and normal FCS. T-bars signify the standard deviation of each sample.

Expression of Rheb steady state mRNA levels in WRL68 cells, cultivated in DMEM medium with 10% “normal” undialysed FCS ($p<0.005$; indicated by *), were set at 1.0 to serve as basic reference level for all other treatment regimens (fig. 13). The Rheb mRNA amounts in cells kept under 10% dialysed FCS (= carnitine deficient medium) increased to 1.03 in relation to standard FCS with a statistical significance level of $p<0.005$. Subsequent supplementation of L-carnitine to the growth medium containing dialysed FCS achieved mixed results and raised Rheb expression back to normal extents or above, dependent on L-carnitine levels and duration of supplementation. Treatment with 40 µM for 4hrs could not lift the mRNA steady state levels, resulting in recorded levels 0.9-fold below normal expression ($p<0.005$). In contrast, supplementation of 80 µM L-carnitine showed a time dependent behaviour in raising mRNA levels. After 4hrs, Rheb expression was raised to 1.4-fold above expression in WRL68 cells when cultivated in normal 10% FCS ($p<0.005$), but fell after 15hrs to 0.9 of normal expression ($p<0.005$). Steady state mRNA levels rose again after 24hrs to 1.6-fold ($p<0.005$) and after 48hrs to 1.9-fold above normal expression ($p<0.005$). Therefore, Rheb steady state mRNA levels reached values exceeding normal gene expression, but only after addition of 80 µM L-carnitine, while 40 µM L-carnitine was ineffective in raising expression.

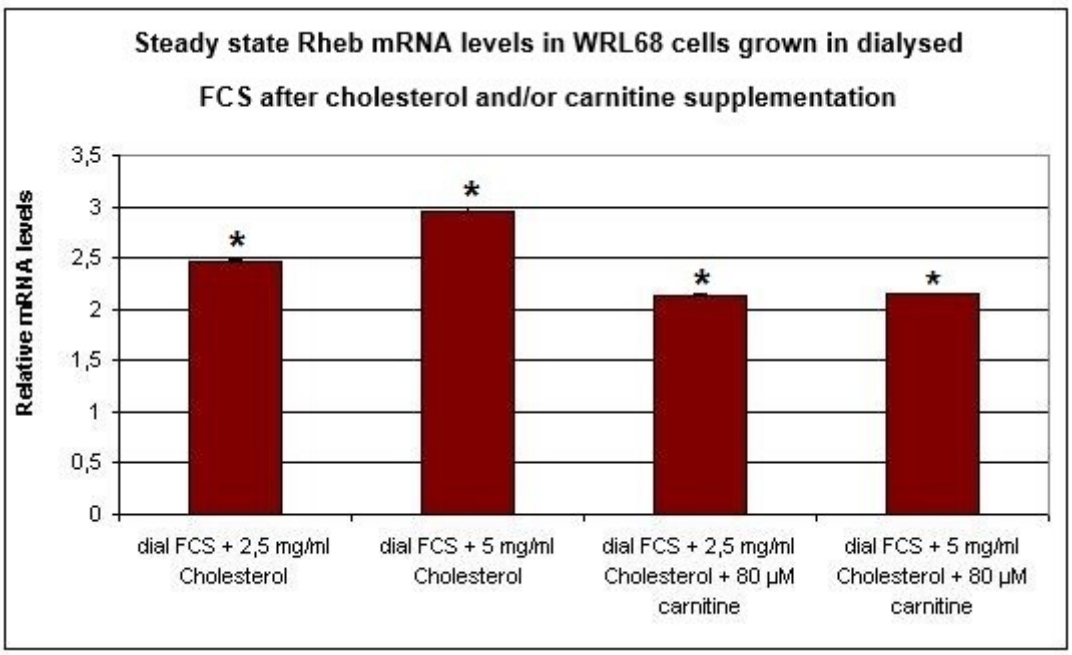

Figure 14: Analysis of Rheb steady state mRNA levels in WRL68 cells cultivated with cholesterol and L-carnitine supplementation. Steady state Rheb-mRNA levels were determined by real-time RT-PCR in WRL68 cells, cultivated in 10% dialysed FCS and supplemented with 80 µM L-carnitine (increasing supplementation durations) in comparison to pure cholesterol supplementation. T-bars signify the standard deviation of each sample.

Addition of 2.5 mg/ml cholesterol (0.65 mM) to the cell culture medium containing 10% dialysed FCS increased expression of Rheb steady state mRNA levels in WRL68 cells approximately 2.5-fold over normal expression in 10% FCS ($p<0.005$), as seen in fig. 14. Doubling the cholesterol levels to 5.0 mg/ml final concentration (1.30 mM) caused only a slight additional surplus in Rheb mRNA increase of approximately 3-fold ($p<0.005$). Extra supplementation of 80 µM L-carnitine lowered the extent of Rheb expression in both cases to approximately 2.1-fold over normal expression ($p<0.005$).

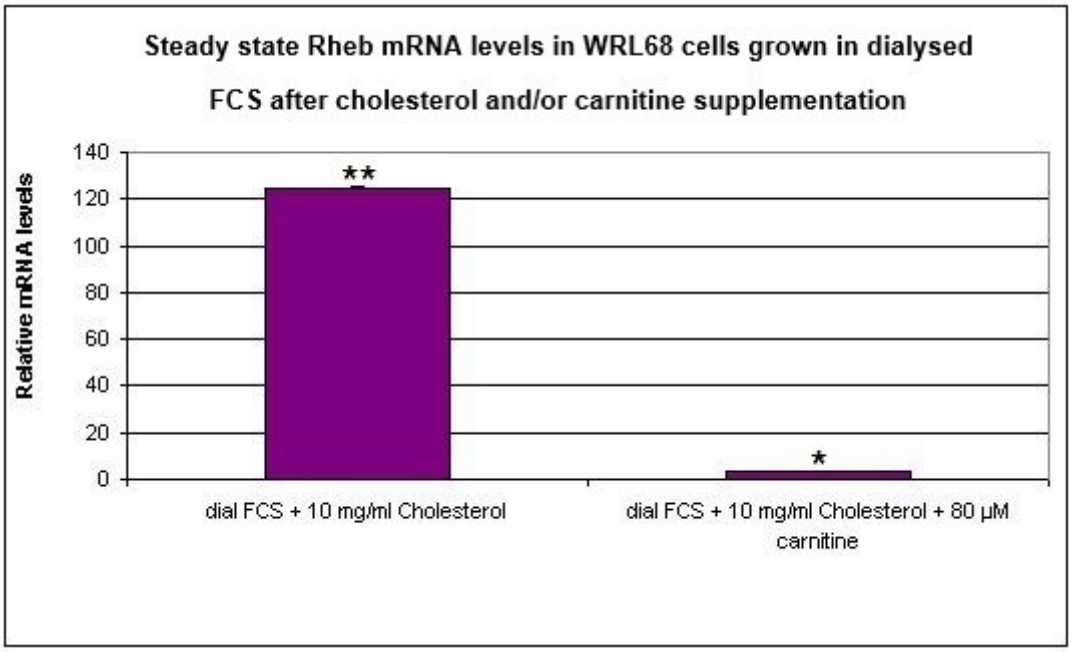

Figure 15: Analysis of Rheb steady state mRNA levels in WRL68 cells cultivated with supplementation of 10 mg/ml cholesterol and L-carnitine. Steady state Rheb-mRNA levels were determined by real-time RT-PCR in WRL68 cells, cultivated in 10% dialysed FCS and supplemented with 80 µM L-carnitine (increasing supplementation durations) in comparison to cholesterol supplementation. T-bars signify the standard deviation of each sample.

Addition of 10 mg/ml cholesterol (2.59 mM) to the cell culture medium with dialysed FCS of WRL68 cells increased expression of Rheb steady state mRNA levels 124-fold compared to expression normal FCS-containing cell culture medium ($p<0.5$; indicated by **) (fig. 15). Subsequent supplementation with 80 µM L-carnitine successfully reduced the Rheb expression (3.5-fold over normal expression, $p<0.005$), counteracting the induction of Rheb transcripts by elevated cholesterol levels.

3.2.1.5. GCN2

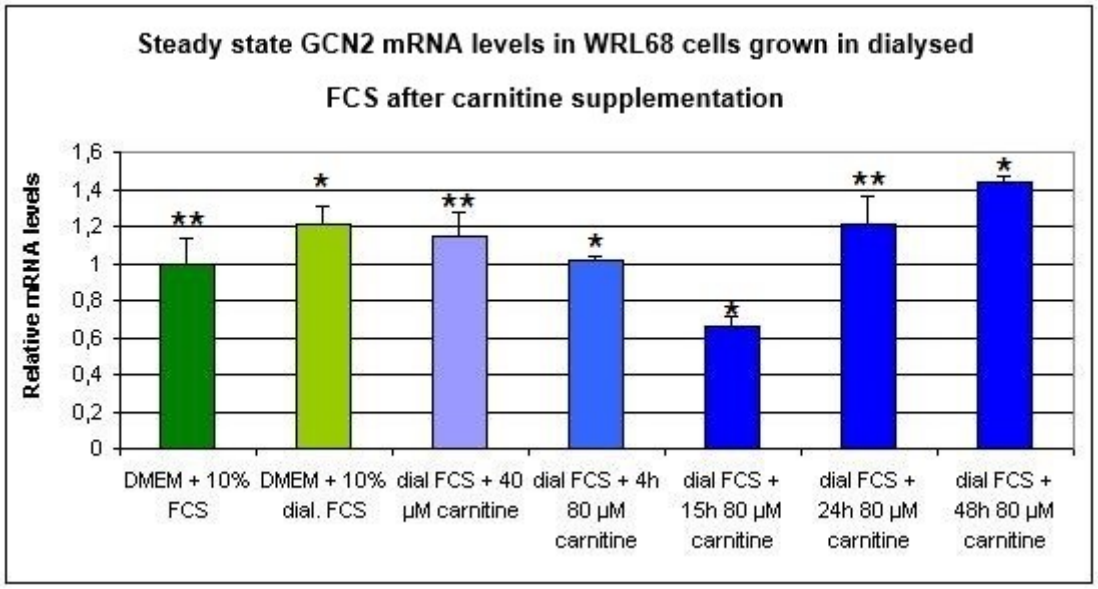

Figure 16: Analysis of GCN2 steady state mRNA levels in WRL68 cells cultivated under L-carnitine deprivation and supplementation in a hyperglycaemic medium. Steady state GCN2-mRNA levels were determined by real-time RT-PCR in WRL68 cells, cultivated in 10% dialysed FCS and supplemented with 40 µM and 80 µM L-carnitine (increasing supplementation durations) in comparison to un-supplemented and normal FCS. T-bars signify the standard deviation of each sample.

Expression of GCN2 steady state mRNA levels in WRL68 cells, cultivated in DMEM medium with 10% “normal” undialysed FCS ($p<0.05$; indicated by **), were set at 1.0 to serve as basic reference level for all other treatment regimens (fig. 16). The GCN2 mRNA amounts in cells kept under 10% dialysed FCS (= carnitine deficient medium) rose to 1.2 in relation to standard FCS with a statistical significance level of $p<0.005$ (indicated by *). Subsequent supplementation of L-carnitine to the growth medium containing dialysed FCS raised GCN2 expression back to normal extents or above in most cases, dependent on L-carnitine levels and duration of supplementation. Treatment with 40 µM for 4hrs lifted the mRNA steady state levels 1.15-fold above normal expression ($p<0.05$). In contrast, supplementation of 80 µM L-carnitine showed a weaker rise, with a recorded 1.02 after 4hrs ($p<0.005$) and even fell to 0.7 in relation to the reference level after 15hrs ($p<0.005$). However, after 24hrs a 1.2-fold ($p<0.05$) and after 48hrs a 1.44-fold ($p<0.005$) peak in mRNA induction above the reference level in cells grown in 10% FCS could be recorded. GCN2 steady state mRNA levels reached values exceeding normal gene expression after addition of 40 µM L-carnitine, but rose above dialysed levels after addition of 80 µM L-carnitine and a continued cultivation for 48hrs.

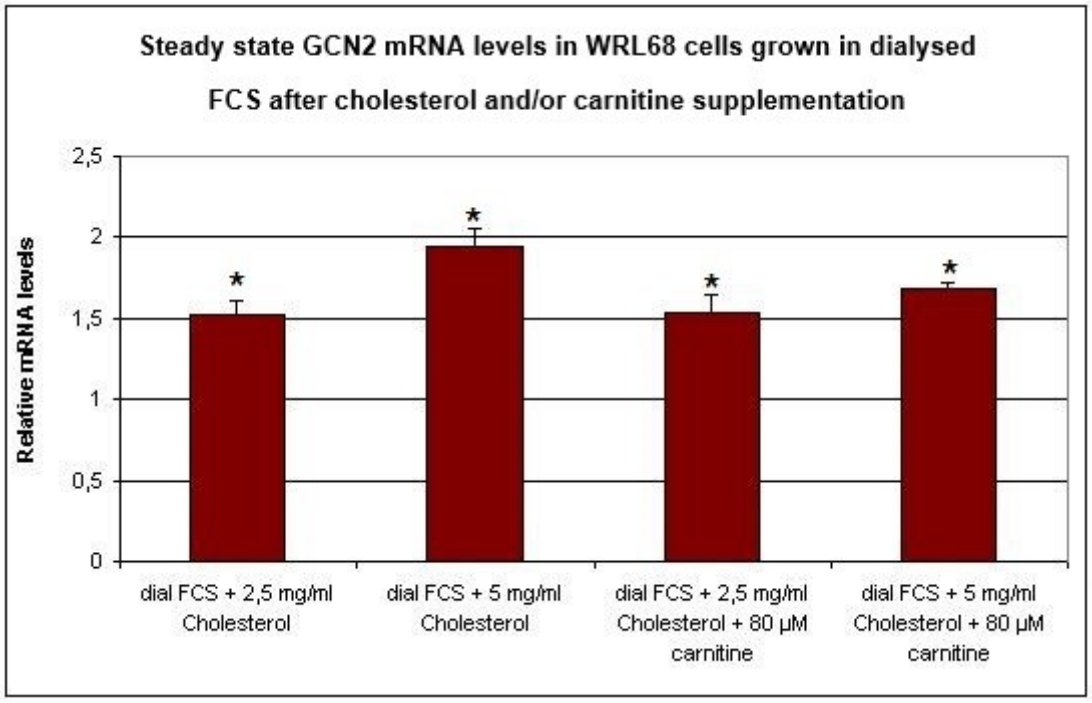

Figure 17: Analysis of GCN2 steady state mRNA levels in WRL68 cells cultivated with cholesterol and L-carnitine supplementation. Steady state GCN2-mRNA levels were determined by real-time RT-PCR in WRL68 cells, cultivated in 10% dialysed FCS and supplemented with 80 µM L-carnitine (increasing supplementation durations) in comparison to pure cholesterol supplementation. T-bars signify the standard deviation of each sample.

Addition of 2.5 mg/ml cholesterol (0.65 mM) to the cell culture medium containing 10% dialysed FCS increased expression of GCN2 steady state mRNA levels in WRL68 cells approximately 1.5-fold over normal expression in 10% FCS ($p<0.005$), as seen in fig. 17. However, doubling the cholesterol levels to 5.0 mg/ml final concentration (1.30 mM) caused only a slight additional surplus in GCN2 mRNA increase of approximately 1.9-fold ($p<0.005$). Extra supplementation of 80 µM L-carnitine could not change the extent of GCN2 expression in the first case (1.5-fold over normal expression, $p<0.005$) and slightly lowered it in the second case (1.7-fold over normal expression, $p<0.005$).

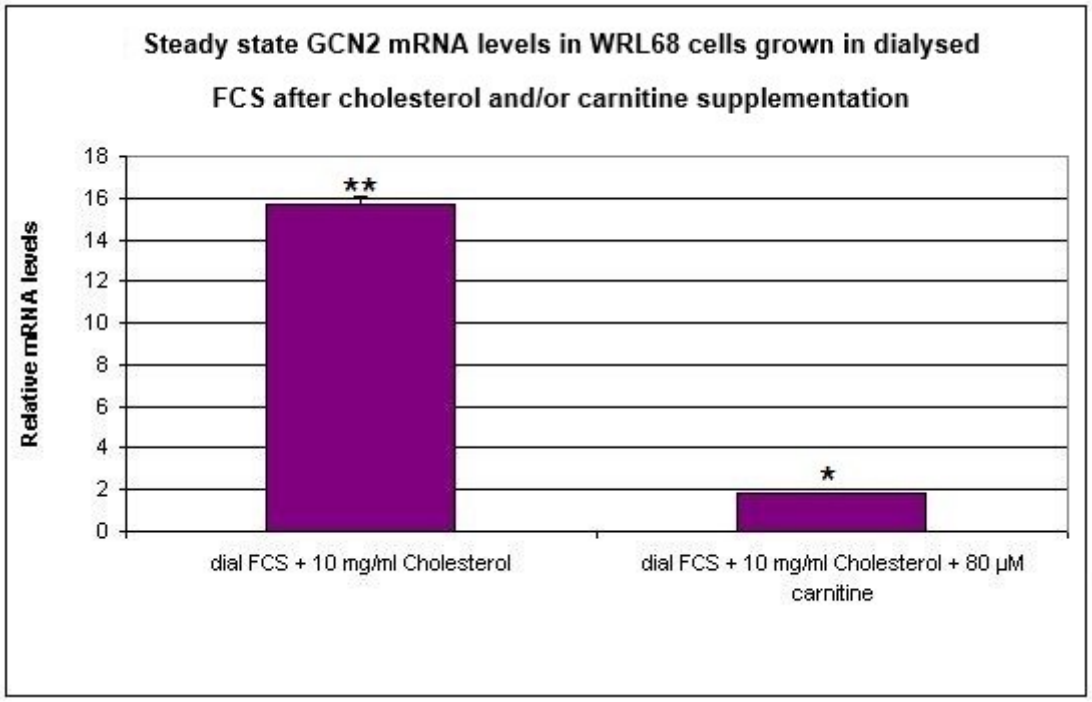

Figure 18: Analysis of GCN2 steady state mRNA levels in WRL68 cells cultivated with supplementation of 10 mg/ml cholesterol and L-carnitine. Steady state GCN2-mRNA levels were determined by real-time RT-PCR in WRL68 cells, cultivated in 10% dialysed FCS and supplemented with 80 µM L-carnitine (increasing supplementation durations) in comparison to cholesterol supplementation. T-bars signify the standard deviation of each sample.

Addition of 10 mg/ml cholesterol (2.59 mM) to the cell culture medium with dialysed FCS of WRL68 cells increased expression of GCN2 steady state mRNA levels almost 16-fold compared to expression normal FCS-containing cell culture medium ($p<0.05$) (fig. 18). Subsequent supplementation with 80 µM L-carnitine successfully reduced the GCN2 expression (1.8-fold over normal expression, $p<0.005$), counteracting the induction of GCN2 transcripts by elevated cholesterol levels.

3.2.1.6. PGC-1α

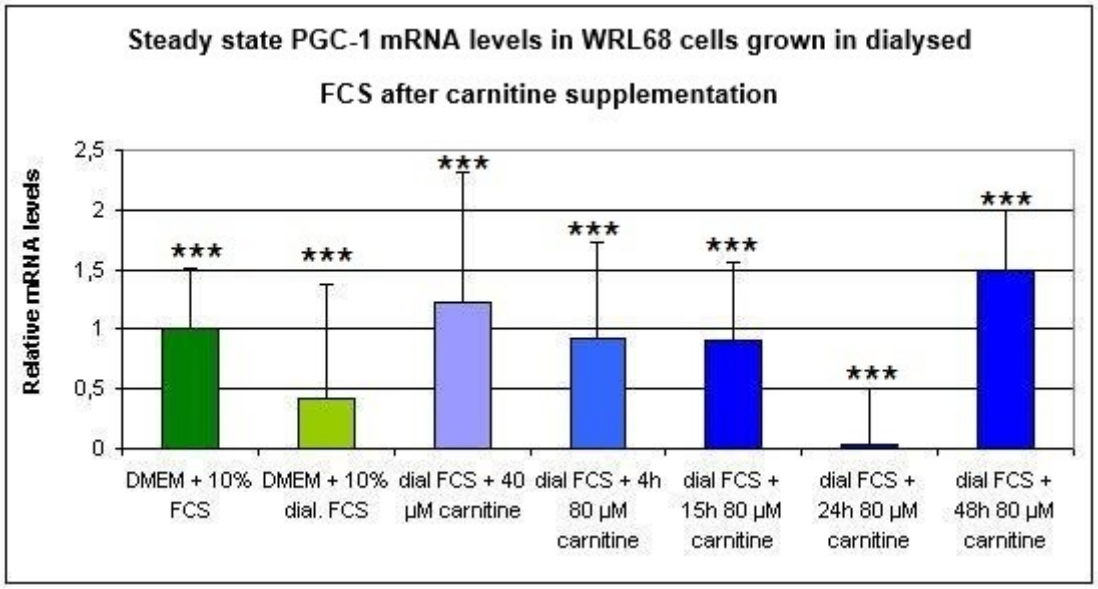

Figure 19: Analysis of PGC-1α steady state mRNA levels in WRL68 cells cultivated under L-carnitine deprivation and supplementation in a hyperglycaemic medium. Steady state PGC-1α-mRNA levels were determined by real-time RT-PCR in WRL68 cells, cultivated in 10% dialysed FCS and supplemented with 40 µM and 80 µM L-carnitine (increasing supplementation durations) in comparison to un-supplemented and normal FCS. T-bars signify the standard deviation of each sample.

Expression of PGC-1α steady state mRNA levels in WRL68 cells, cultivated in DMEM medium with 10% “normal” undialysed FCS ($p<0.5$; indicated by ***), were set at 1.0 to serve as basic reference level for all other treatment regimens (fig. 19). The PGC-1α mRNA amounts in cells kept under 10% dialysed FCS (= carnitine deficient medium) declined to 0.4 in relation to standard FCS with a statistical significance level of $p<0.5$. Subsequent supplementation of L-carnitine to the growth medium containing dialysed FCS had varying effects on PGC-1 expression, depending on L-carnitine levels and duration of supplementation. Treatment with 40 µM for 4 hrs lifted the mRNA steady state levels 1.2-fold above normal expression ($p<0.5$). In contrast, supplementation of 80 µM L-carnitine showed a strict time dependent exertion in raising mRNA levels. The recorded values were 0.9-fold below normal expression after 4hrs ($p<0.5$), 0.9-fold after 15hrs ($p<0.5$) and 0.03-fold after 24hrs ($p<0.5$), while after 48hrs of supplementation a 1.5-fold peak in mRNA induction above the reference level in cells grown in 10% FCS was measured ($p<0.5$). PGC-1α steady state mRNA levels reached values exceeding normal gene expression after addition of 40 µM L-carnitine, but in the case of supplementation of 80 µM L-carnitine rose above normal levels only after cultivation for 48hrs.

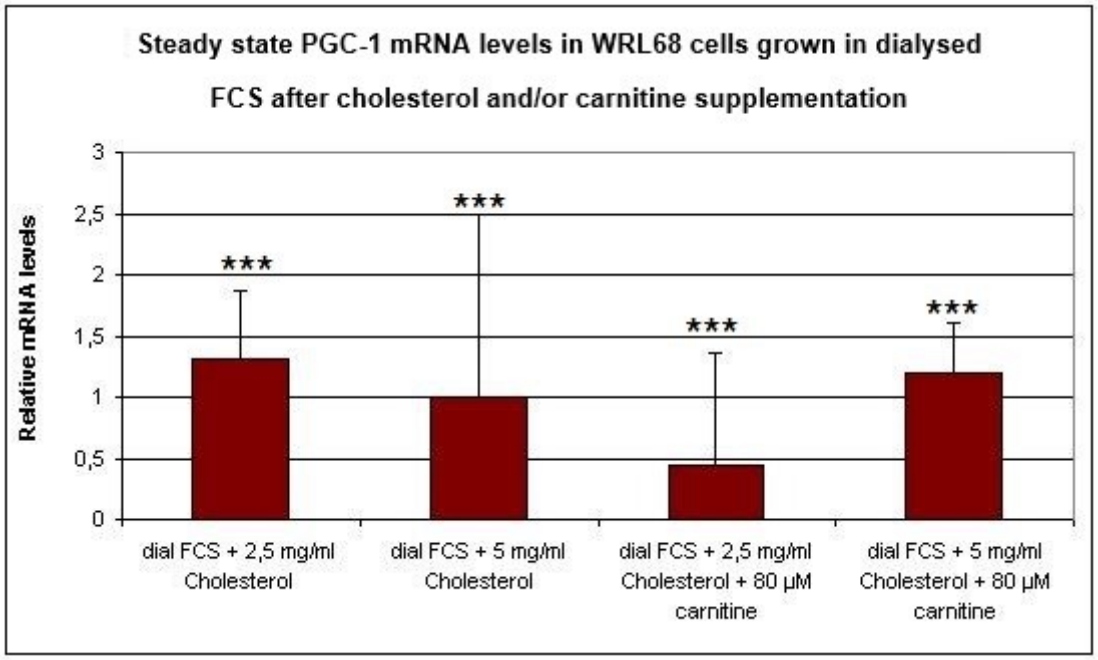

Figure 20: Analysis of PGC-1α steady state mRNA levels in WRL68 cells cultivated with cholesterol and L-carnitine supplementation. Steady state PGC-1α-mRNA levels were determined by real-time RT-PCR in WRL68 cells, cultivated in 10% dialysed FCS and supplemented with 80 µM L-carnitine (increasing supplementation durations) in comparison to pure cholesterol supplementation. T-bars signify the standard deviation of each sample.

Addition of 2.5 mg/ml cholesterol (0.65 mM) to the cell culture medium containing 10% dialysed FCS increased expression of PGC-1α steady state mRNA levels in WRL68 cells 1.3-fold over normal expression in 10% FCS ($p<0.5$), as seen in fig. 20. However, doubling the cholesterol levels to 5.0 mg/ml final concentration (1.30 mM) did not cause an increase in expression and was close to the reference level (0.99-fold under normal expression, $p<0.5$). Extra supplementation of 80 µM L-carnitine lowered the extent of PGC-1α expression in the first case (0.4-fold under normal expression, $p<0.5$) and slightly increased it in the second case (1.2-fold over normal expression, $p<0.5$).

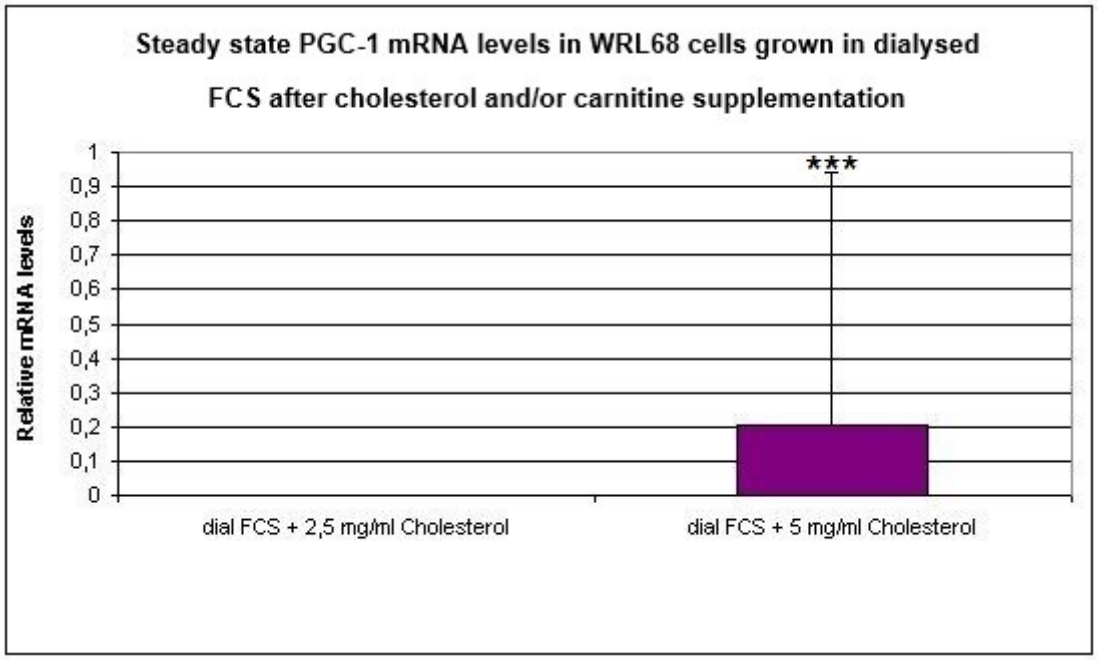

Figure 21: Analysis of PGC-1α steady state mRNA levels in WRL68 cells cultivated with supplementation of 10 mg/ml cholesterol and L-carnitine. Steady state PGC-1α-mRNA levels were determined by real-time RT-PCR in WRL68 cells, cultivated in 10% dialysed FCS and supplemented with 80 µM L-carnitine (increasing supplementation durations) in comparison to cholesterol supplementation. T-bars signify the standard deviation of each sample.

In the treatment where 10 mg/ml cholesterol (2.59 mM) was added to the cell culture medium with dialysed FCS of WRL68 cells, no PGC-1α steady state mRNA levels could be measured, which is very likely a result of inhibition by cholesterol (fig. 21). The measured expression in cells that were supplemented with 80 µM L-carnitine was 0.2-fold under the expression in normal FCS-containing cell culture medium ($p<0.5$).

3.2.1.7. SREBP-1

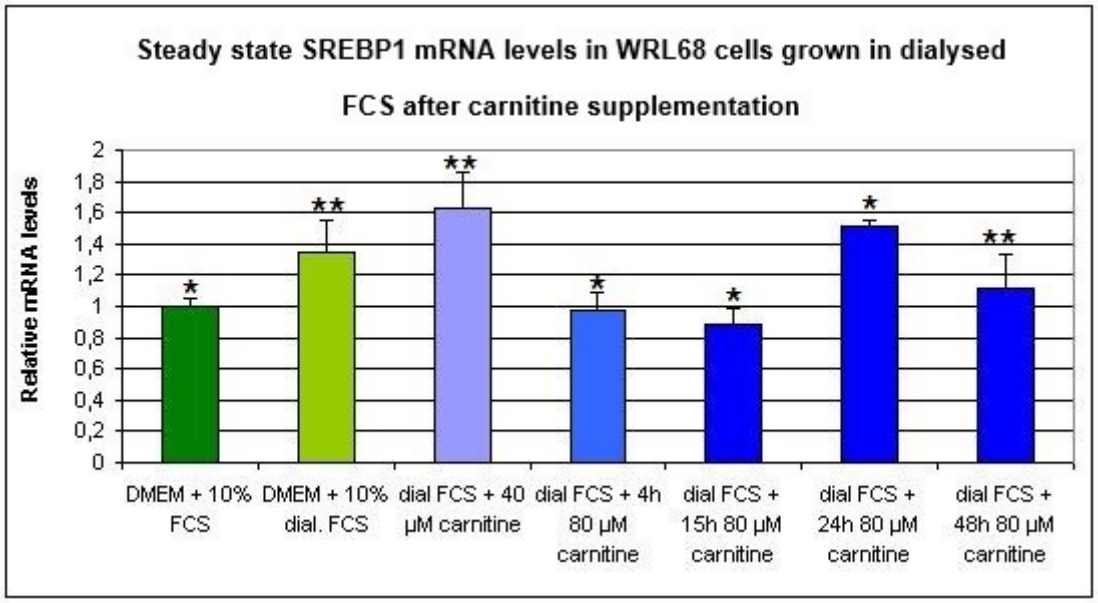

Figure 22: Analysis of SREBP-1 steady state mRNA levels in WRL68 cells cultivated under L-carnitine deprivation and supplementation in a hyperglycaemic medium. Steady state SREBP-1-mRNA levels were determined by real-time RT-PCR in WRL68 cells, cultivated in 10% dialysed FCS and supplemented with 40 µM and 80 µM L-carnitine (increasing supplementation durations) in comparison to un-supplemented and normal FCS. T-bars signify the standard deviation of each sample.

Expression of SREBP1 steady state mRNA levels in WRL68 cells, cultivated in DMEM medium with 10% “normal” undialysed FCS ($p<0.005$; indicated by *), were set at 1.0 to serve as basic reference level for all other treatment regimens (fig. 22). The SREBP1 mRNA amounts in cells kept under 10% dialysed FCS (= carnitine deficient medium) increased to 1.4 in relation to standard FCS with a statistical significance level of $p<0.05$ (indicated by **). Subsequent supplementation of L-carnitine to the growth medium containing dialysed FCS raised SREBP1 expression above normal extents, dependent on L-carnitine levels and was varying relative to the duration of supplementation. Treatment with 40 µM for 4 hrs lifted the mRNA steady state levels 1.6-fold above normal expression ($p<0.05$). In contrast, supplementation of 80 µM L-carnitine interestingly exhibited a strict time dependent influence in raising mRNA levels. SREBP1 expression was almost equal to that of WRL68 cells when cultivated in normal 10% FCS ($p<0.005$), however, it declined to 0.9 after 15hrs ($p<0.005$). Steady state mRNA levels increased to 1.5 after 24hrs ($p<0.005$), but fell to 1.1 after 48hrs ($p<0.05$). Therefore, 40 µM L-carnitine has the strongest capability to induce SREBP1, while addition of 80 µM L-carnitine becomes effective after 24hrs and declines after longer treatment.

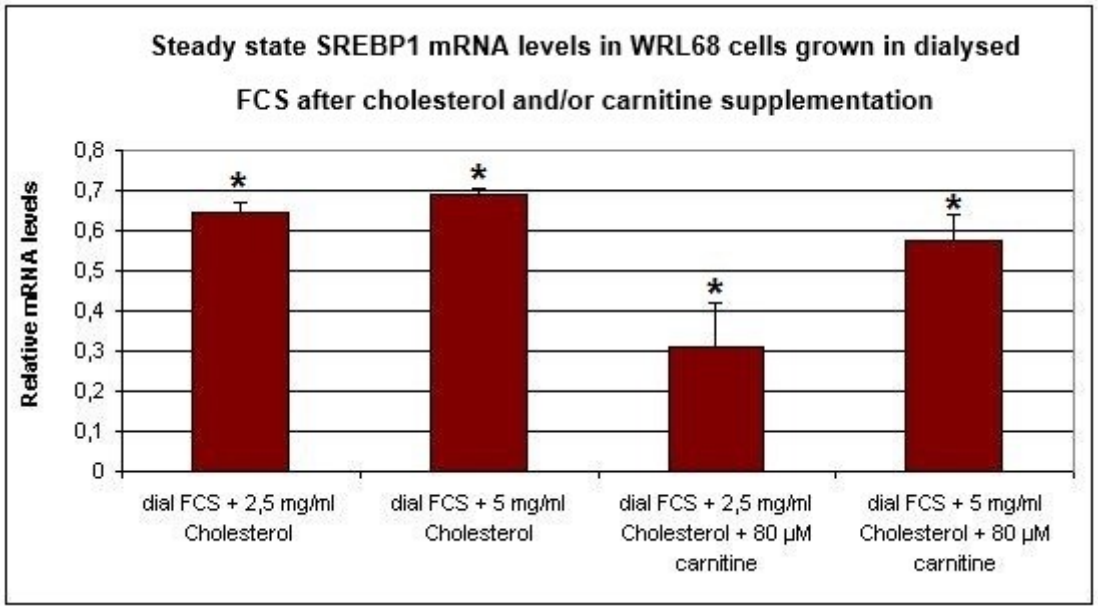

Figure 23: Analysis of SREBP-1 steady state mRNA levels in WRL68 cells cultivated with cholesterol and L-carnitine supplementation. Steady state SREBP-1-mRNA levels were determined by real-time RT-PCR in WRL68 cells, cultivated in 10% dialysed FCS and supplemented with 80 µM L-carnitine (increasing supplementation durations) in comparison to pure cholesterol supplementation. T-bars signify the standard deviation of each sample.

Addition of 2.5 mg/ml cholesterol (0.65 mM) to the cell culture medium containing 10% dialysed FCS decreased expression of SREBP1 steady state mRNA levels in WRL68 cells 0.6-fold under normal expression ($p<0.005$), while the doubling the cholesterol levels to 5.0 mg/ml final concentration (1.3 mM) decreased it 0.7-fold ($p<0.005$) (see fig. 23). Subsequent supplementation with 80 µM L-carnitine decreased the extent of SREBP1 expression, 0.3-fold under normal expression ($p<0.005$) in the first case and almost 0.6-fold under normal expression ($p<0.005$) in the second case.

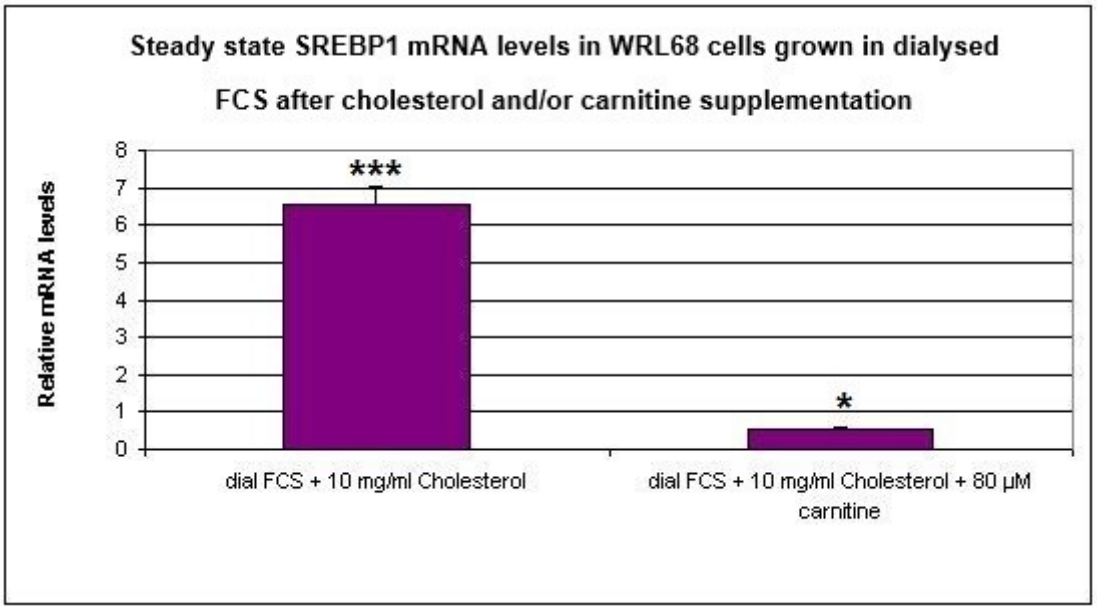

Figure 24: Analysis of SREBP-1 steady state mRNA levels in WRL68 cells cultivated with supplementation of 10 mg/ml cholesterol and L-carnitine. Steady state SREBP-1-mRNA levels were determined by real-time RT-PCR in WRL68 cells, cultivated in 10% dialysed FCS and supplemented with 80 µM L-carnitine (increasing supplementation durations) in comparison to cholesterol supplementation. T-bars signify the standard deviation of each sample.

Addition of 10 mg/ml cholesterol (2.59 mM) to the cell culture medium with 10% dialysed FCS of WRL68 cells 6.6-fold increased expression of SREBP-1 steady state mRNA levels compared to expression in normal FCS-containing cell culture medium ($p<0.5$) (shown in fig. 24). Subsequent supplementation with 80 µM L-carnitine reduced the expression of SREBP1 below normal extents (0.5 of normal expression, $p<0.005$).

3.2.2. Steady state mRNA levels of cells in a normoglycaemic medium

All following results were obtained using WRL68 cells, cultivated in low glucose DMEM (1000 mg/l glucose) with 10% dialysed or undialysed FCS.

3.2.1.1. OCTN1

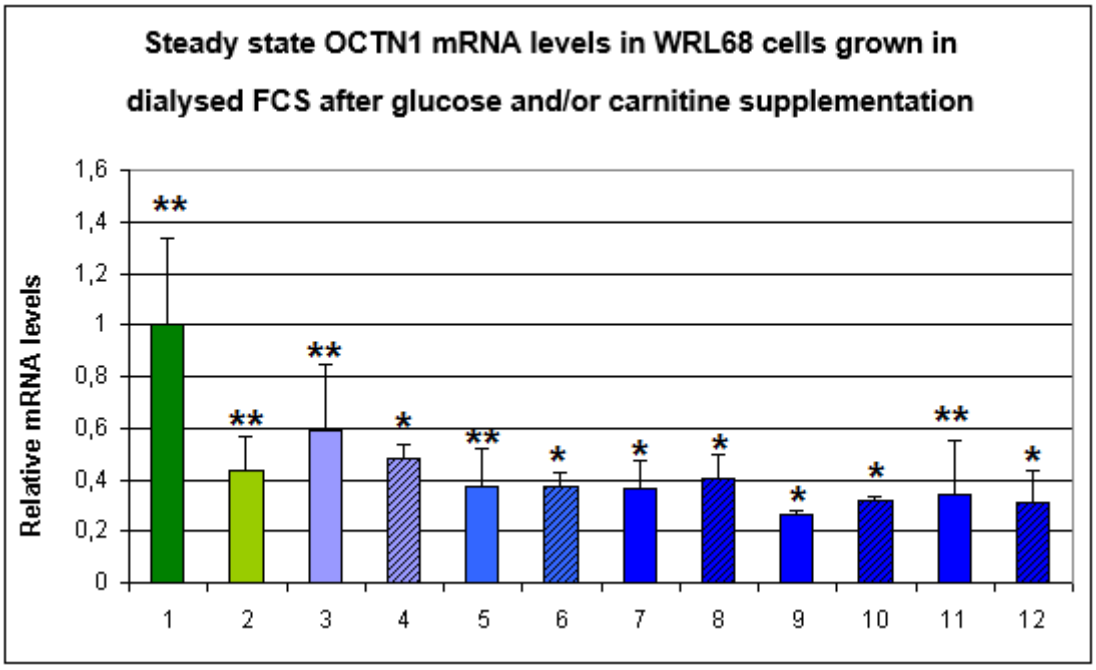

Figure 25: Analysis of OCTN1 steady state mRNA levels in WRL68 cells cultivated under L-carnitine deprivation and glucose and/or L-carnitine supplementation in a normoglycaemic medium. Steady state OCTN1-mRNA levels were determined by real-time RT-PCR in WRL68 cells, cultivated in 10% dialysed FCS and supplemented with 3500 µg/l glucose 40 µM and 80 µM L-carnitine (increasing supplementation durations) in comparison to un-supplemented and normal FCS. Legend: 1: normal FCS; 2: dialysed FCS (dialFCS); 3: dialFCS + 40µM L-carnitine for 4hrs; 4: dialFCS + 40µM L-carnitine and 3500 mg/l glucose for 4hrs; 5: dialFCS + 80µM L-carnitine for 4hrs; 6: dialFCS + 80µM L-carnitine and 3500 mg/l glucose for 4hrs; 7: dialFCS + 80µM L-carnitine for 15hrs; 8: dialFCS + 80µM L-carnitine and 3500 mg/l glucose for 15hrs; 9: dialFCS + 80µM L-carnitine for 24hrs; 10: dialFCS + 80µM L-carnitine and 3500 mg/l glucose for 24hrs; 11: dialFCS + 80µM L-carnitine for 48hrs; 12: dialFCS + 80µM L-carnitine and 3500 mg/l glucose for 48hrs.T-bars signify the standard deviation of each sample.

Expression of OCTN1 steady state mRNA levels in WRL68 cells, cultivated in DMEM medium with 10% “normal” undialysed FCS ($p<0.05$; indicated by **), were set at 1.0 to serve as basic reference level for all other treatment regimens (fig. 25). The OCTN1 mRNA amounts in cells kept under 10% dialysed FCS (= carnitine deficient medium) declined to 0.44 in relation to standard FCS with a statistical significance level of $p<0.05$. Subsequent supplementation of L-carnitine to the growth medium containing dialysed FCS could not raise OCTN1 expression back to normal extents or above, independent from L-carnitine or glucose levels and duration of supplementation. Treatment with 40 µM for 4hrs lifted mRNA steady state levels compared to the expression in cells in 10% dialysed FCS, but was still 0.59 of normal expression ($p<0.05$). Increase of glucose levels to 4500 mg/l for the duration of the supplementation lowered this expression to 0.48-fold below normal expression ($p<0.005$; indicated by *). Treatment with 80 µM L-carnitine

was less successful, with a slightly higher expression in most cases where glucose levels were raised to 4500 mg/l for the duration of the supplementation. After 4hrs, OCTN1 expression was 0.37-fold below normal expression ($p<0.05$) in low glucose and 0.38-fold below normal expression ($p<0.005$) in high glucose conditions. Expression after 15hrs was similar, with 0.37-fold below normal expression ($p<0.005$) in low glucose medium and 0.40-fold below normal expression ($p<0.005$) with raised glucose levels. Steady state mRNA levels fell even further after 24hrs of supplementation to 0.26-fold below normal expression ($p<0.005$) in low glucose and 0.32-fold below normal expression ($p<0.005$) with increased glucose levels and after 48hrs to 0.34-fold below normal expression ($p<0.05$) in low glucose medium and 0.31-fold below normal expression ($p<0.005$) at increased glucose levels.

3.2.1.2. SLC35F2

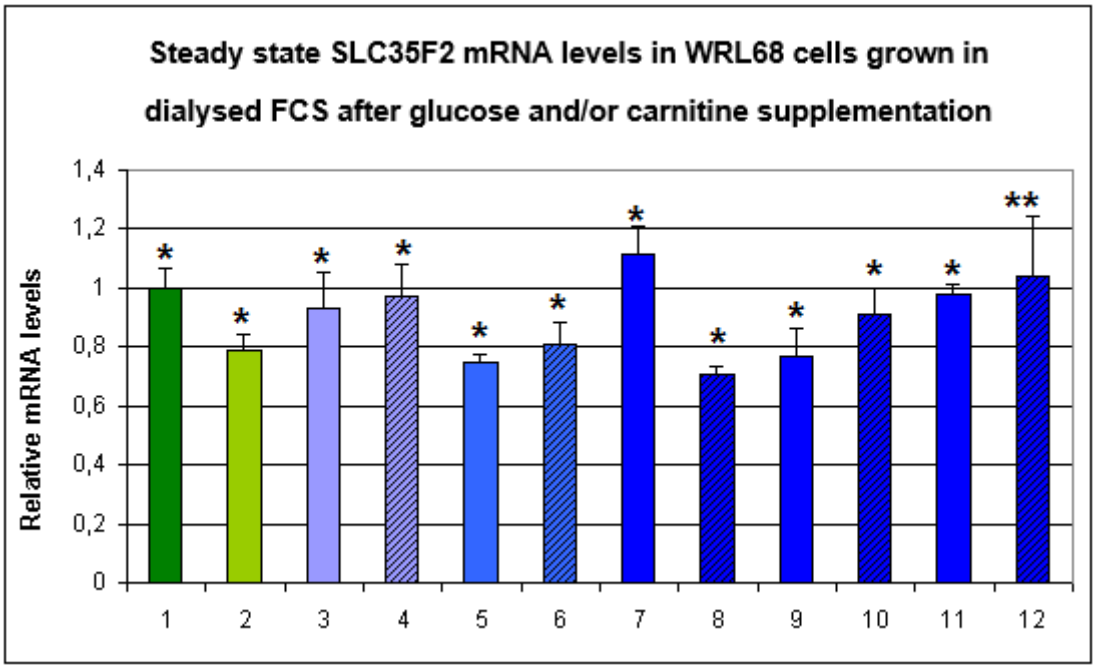

Figure 26: Analysis of SLC35F2 steady state mRNA levels in WRL68 cells cultivated under L-carnitine deprivation and glucose and/or L-carnitine supplementation in a normoglycaemic medium. Steady state SLC35F2-mRNA levels were determined by real-time RT-PCR in WRL68 cells, cultivated in 10% dialysed FCS and supplemented with 3500 µg/l glucose 40 µM and 80 µM L-carnitine (increasing supplementation durations) in comparison to un-supplemented and normal FCS. Legend: 1: normal FCS; 2: dialysed FCS (dialFCS); 3: dialFCS + 40µM L-carnitine for 4hrs; 4: dialFCS + 40µM L-carnitine and 3500 mg/l glucose for 4hrs; 5: dialFCS + 80µM L-carnitine for 4hrs; 6: dialFCS + 80µM L-carnitine and 3500 mg/l glucose for 4hrs; 7: dialFCS + 80µM L-carnitine for 15hrs; 8: dialFCS + 80µM L-carnitine and 3500 mg/l glucose for 15hrs; 9: dialFCS + 80µM L-carnitine for 24hrs; 10: dialFCS + 80µM L-carnitine and 3500 mg/l glucose for 24hrs; 11: dialFCS + 80µM L-carnitine for 48hrs; 12: dialFCS + 80µM L-carnitine and 3500 mg/l glucose for 48hrs.T-bars signify the standard deviation of each sample.

Expression of SLC35F2 steady state mRNA levels in WRL68 cells, cultivated in DMEM medium with 10% “normal” undialysed FCS ($p<0.005$; indicated by *), were set at 1.0 to serve as basic reference level for all other treatment regimens (fig. 26). The SLC35F2 mRNA amounts in cells kept under 10% dialysed FCS (= carnitine deficient medium) declined to 0.79 in relation to standard FCS with a statistical significance level of $p<0.005$. Subsequent supplementation of L-carnitine to the growth medium containing dialysed FCS achieved mixed results, but could not raise SLC35F2 expression above normal extents under most conditions. Treatment with 40 µM for 4hrs lifted the mRNA steady state levels back to almost normal values, with 0.9-fold of normal expression ($p<0.005$) in low glucose medium and approximately 1-fold of normal expression ($p<0.005$) when glucose levels were raised to 4500 mg/l. In contrast, supplementation of 80 µM L-carnitine showed a time-dependent effect in shifting steady state mRNA levels, up to slightly higher expression in cells where glucose levels were raised for the duration of the supplementation. After 4hrs, SLC35F2 expression was 0.71-fold below normal expression ($p<0.005$) in low glucose and 0.81-fold below normal expression ($p<0.005$) under high glucose conditions. Expression spiked after 15hrs to 1.11-fold above the reference level ($p<0.005$) in low glucose medium, but fell to 0.71-fold below normal expression ($p<0.005$) with raised glucose levels. Steady state mRNA levels started to gradually rise after 24hrs of supplementation to 0.77-fold below normal expression ($p<0.005$) in low glucose and 0.91-fold below normal expression ($p<0.005$) with increased glucose levels and after 48hrs to 0.98-fold below normal expression ($p<0.05$) in low glucose medium and 1.04-fold above normal expression ($p<0.05$) at increased glucose levels.

3.2.1.3. Rac1

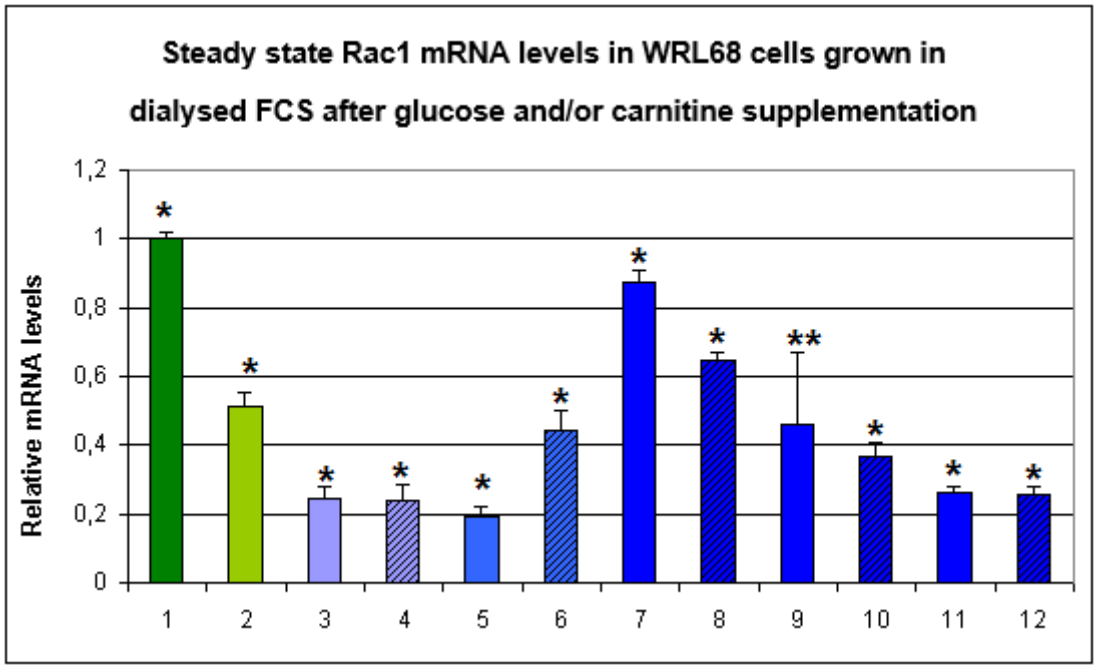

Figure 27: Analysis of Rac1 steady state mRNA levels in WRL68 cells cultivated under L-carnitine deprivation and glucose and/or L-carnitine supplementation in a normoglycaemic medium. Steady state Rac1-mRNA levels were determined by real-time RT-PCR in WRL68 cells, cultivated in 10% dialysed FCS and supplemented with 3500 µg/l glucose 40 µM and 80 µM L-carnitine (increasing supplementation durations) in comparison to un-supplemented and normal FCS. Legend: 1: normal FCS; 2: dialysed FCS (dialFCS); 3: dialFCS + 40µM L-carnitine for 4hrs; 4: dialFCS + 40µM L-carnitine and 3500 mg/l glucose for 4hrs; 5: dialFCS + 80µM L-carnitine for 4hrs; 6: dialFCS + 80µM L-carnitine and 3500 mg/l glucose for 4hrs; 7: dialFCS + 80µM L-carnitine for 15hrs; 8: dialFCS + 80µM L-carnitine and 3500 mg/l glucose for 15hrs; 9: dialFCS + 80µM L-carnitine for 24hrs; 10: dialFCS + 80µM L-carnitine and 3500 mg/l glucose for 24hrs; 11: dialFCS + 80µM L-carnitine for 48hrs; 12: dialFCS + 80µM L-carnitine and 3500 mg/l glucose for 48hrs.T-bars signify the standard deviation of each sample.

Expression of Rac1 steady state mRNA levels in WRL68 cells, cultivated in DMEM medium with 10% “normal” undialysed FCS ($p<0.005$; indicated by *), were set at 1.0 to serve as basic reference level for all other treatment regimens (fig. 27). The Rac1 mRNA amounts in cells kept under 10% dialysed FCS (= carnitine deficient medium) declined to 0.51 in relation to standard FCS with a statistical significance level of $p<0.005$. Subsequent supplementation of L-carnitine to the growth medium containing dialysed FCS could not raise Rac1 expression back to normal extents or above, independent from L-carnitine or glucose levels and duration of supplementation. Treatment with 40 µM for 4hrs resulted in mRNA steady state levels 0.25-fold below normal expression ($p<0.005$) under normal conditions and 0.24-fold below normal expression ($p<0.005$) when extra glucose was added. In contrast, supplementation of 80 µM L-carnitine showed a time-dependent effect on steady state mRNA levels. The measured extents after 4hrs under

normal conditions were 0.19-fold below normal levels ($p<0.005$), while they increased to 0.45-fold below normal levels ($p<0.005$) when glucose was added for the duration of the supplementation. The strongest effect was recorded after 15hrs of supplementation at low levels of glucose with 0.88-fold below normal expression ($p<0.005$) and 0.64-fold below normal expression ($p<0.005$) with raised glucose levels. Rac1 steady state levels declined after longer supplementation, to 0.46-fold under normal extents ($p<0.05$; indicated by **) under normal conditions and to 0.37-fold below normal expression ($p<0.005$) with raised glucose levels after 24hrs and to 0.26-fold under normal extents ($p<0.005$) under normal conditions and to 0.25-fold below normal expression ($p<0.005$) with raised glucose levels after 48hrs. These results indicate that L-carnitine cannot raise Rac1 expression above normal extents in low glucose medium. While supplementation of L-carnitine at elevated glucose levels resulted in a marked increased expression after 4hrs compared to conditions where L-carnitine was given under low glucose. Therefore L-carnitine alone was more successful as additive after prolonged treatments at higher glucose levels in reducing mRNA steady state expression levels.

3.2.1.4. Rheb

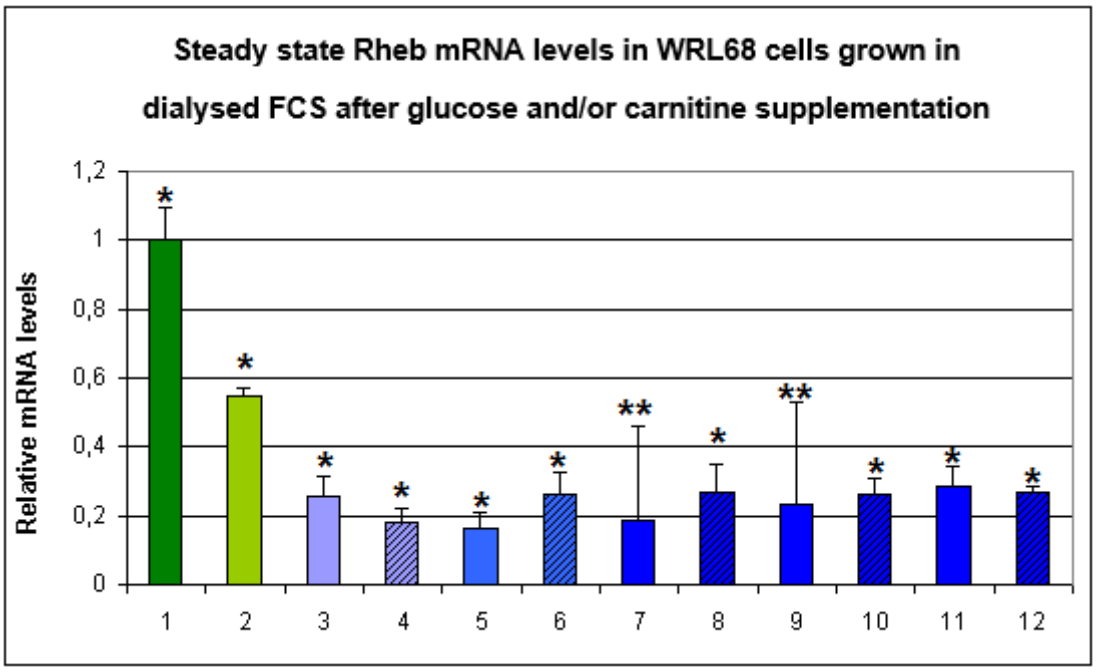

Figure 28: Analysis of Rheb steady state mRNA levels in WRL68 cells cultivated under L-carnitine deprivation and glucose and/or L-carnitine supplementation in a normoglycaemic medium. Steady state Rheb-mRNA levels were determined by real-time RT-PCR in WRL68 cells, cultivated in 10% dialysed FCS and supplemented with 3500 µg/l glucose 40 µM and 80 µM L-carnitine (increasing supplementation durations) in comparison to un-supplemented and normal FCS. Legend: 1: normal FCS; 2: dialysed FCS (dialFCS); 3: dialFCS + 40µM L-carnitine for 4hrs; 4: dialFCS + 40µM L-carnitine and 3500 mg/l glucose for 4hrs; 5: dialFCS + 80µM L-carnitine for 4hrs; 6: dialFCS + 80µM L-carnitine and 3500 mg/l glucose for 4hrs;

7: dialFCS + 80µM L-carnitine for 15hrs; 8: dialFCS + 80µM L-carnitine and 3500 mg/l glucose for 15hrs; 9: dialFCS + 80µM L-carnitine for 24hrs; 10: dialFCS + 80µM L-carnitine and 3500 mg/l glucose for 24hrs; 11: dialFCS + 80µM L-carnitine for 48hrs; 12: dialFCS + 80µM L-carnitine and 3500 mg/l glucose for 48hrs.T-bars signify the standard deviation of each sample.

Expression of Rheb steady state mRNA levels in WRL68 cells, cultivated in DMEM medium with 10% “normal” undialysed FCS ($p<0.005$; indicated by *), were set at 1.0 to serve as basic reference level for all other treatment regimens (fig. 28). The Rheb mRNA amounts in cells kept under 10% dialysed FCS (= carnitine deficient medium) declined to 0.55 in relation to standard FCS with a statistical significance level of $p<0.005$. Subsequent supplementation of L-carnitine to the growth medium containing dialysed FCS could not increase Rheb expression back to normal extents or even above extents in dialysed FCS, independent from L-carnitine or glucose levels and duration of supplementation. Treatment with 40 µM for 4hrs could not lift the mRNA steady state levels, resulting in recorded levels of 0.25-fold below normal expression ($p<0.005$), while increasing the glucose levels to 4500 mg/l additionally lowered them to 0.18-fold below normal expression ($p<0.005$). Supplementation of 80 µM L-carnitine achieved similarly low results, with recordings of 0.16-fold below normal expression ($p<0.005$) under normal conditions and 0.26-fold below normal expression ($p<0.005$) with increased glucose levels after 4hrs, 0.18-fold below normal expression ($p<0.05$; indicated by **) under normal conditions and 0.27-fold below normal expression ($p<0.005$) with increased glucose levels after 15hrs, 0.24-fold below normal expression ($p<0.05$) under normal conditions and 0.26-fold below normal expression ($p<0.005$) with increased glucose levels after 24hrs and 0.28-fold below normal expression ($p<0.005$) under normal conditions and 0.27-fold below normal expression ($p<0.005$) with increased glucose levels after 48hrs. L-carnitine was not able to induce Rheb steady state mRNA levels in cells that were grown in low glucose medium. It is interesting to note that supplementation of 80 µM L-carnitine generally increased gene expression when paired with higher glucose levels compared to only L-carnitine. In the case of Rheb steady state transcript levels higher, glucose levels in contrast lowered them when paired with 40 µM L-carnitine supplementation.

3.2.1.5. GCN2

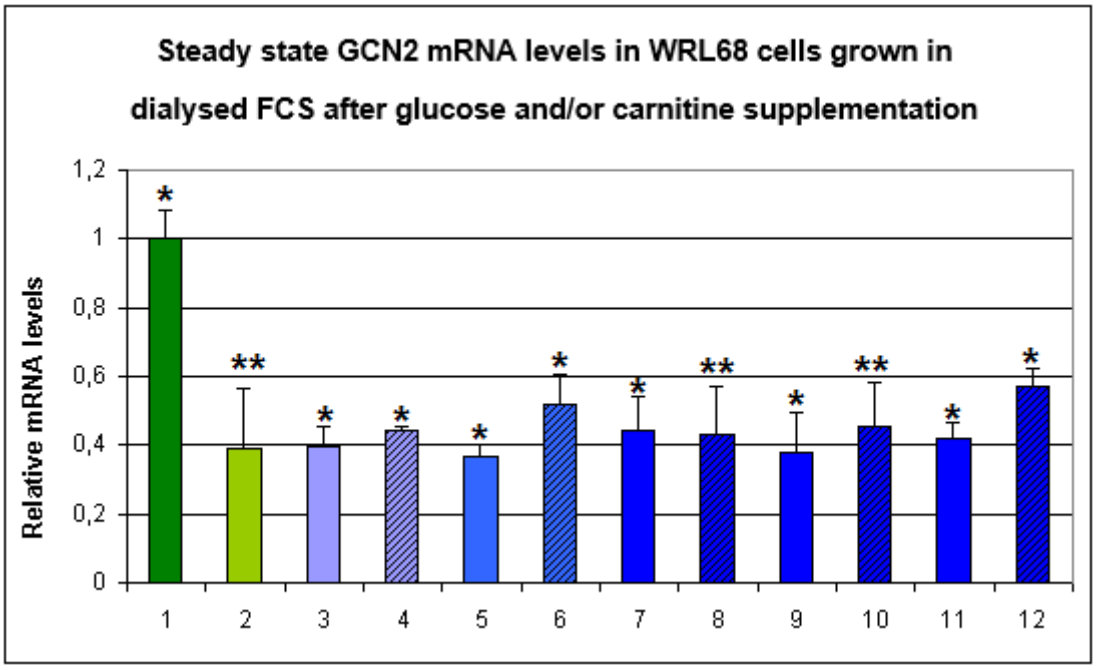

Figure 29: Analysis of GCN2 steady state mRNA levels in WRL68 cells cultivated under L-carnitine deprivation and glucose and/or L-carnitine supplementation in a normoglycaemic medium. Steady state GCN2-mRNA levels were determined by real-time RT-PCR in WRL68 cells, cultivated in 10% dialysed FCS and supplemented with 3500 µg/l glucose 40 µM and 80 µM L-carnitine (increasing supplementation durations) in comparison to un-supplemented and normal FCS. Legend: 1: normal FCS; 2: dialysed FCS (dialFCS); 3: dialFCS + 40µM L-carnitine for 4hrs; 4: dialFCS + 40µM L-carnitine and 3500 mg/l glucose for 4hrs; 5: dialFCS + 80µM L-carnitine for 4hrs; 6: dialFCS + 80µM L-carnitine and 3500 mg/l glucose for 4hrs; 7: dialFCS + 80µM L-carnitine for 15hrs; 8: dialFCS + 80µM L-carnitine and 3500 mg/l glucose for 15hrs; 9: dialFCS + 80µM L-carnitine for 24hrs; 10: dialFCS + 80µM L-carnitine and 3500 mg/l glucose for 24hrs; 11: dialFCS + 80µM L-carnitine for 48hrs; 12: dialFCS + 80µM L-carnitine and 3500 mg/l glucose for 48hrs.T-bars signify the standard deviation of each sample.

Expression of GCN2 steady state mRNA levels in WRL68 cells, cultivated in DMEM medium with 10% “normal” undialysed FCS ($p<0.005$; indicated by *), were set at 1.0 to serve as basic reference level for all other treatment regimens (fig. 29). The GCN2 mRNA amounts in cells kept under 10% dialysed FCS (= carnitine deficient medium) declined to 0.39 in relation to standard FCS with a statistical significance level of $p<0.05$ (indicated by **). Subsequent supplementation of L-carnitine to the growth medium containing dialysed FCS could not raise GCN2 expression back to normal extents in dialysed FCS, independent from L-carnitine or glucose levels and duration of supplementation. Treatment with 40 µM for 4hrs could not lift the mRNA steady state levels, resulting in recorded levels of 0.40-fold below normal expression ($p<0.005$), while increasing the glucose levels to 4500 mg/l increased them to 0.44-fold below normal expression ($p<0.005$). Supplementation of 80 µM L-carnitine achieved similarly low results, with

recordings of 0.37-fold below normal expression ($p<0.005$) under normal conditions and 0.52-fold below normal expression ($p<0.005$) with increased glucose levels after 4hrs, 0.44-fold below normal expression ($p<0.005$) under normal conditions and 0.43-fold below normal expression ($p<0.05$; indicated by **) with increased glucose levels after 15hrs, 0.38-fold below normal expression ($p<0.05$) under normal conditions and 0.45-fold below normal expression ($p<0.05$) with increased glucose levels after 24hrs and 0.42-fold below normal expression ($p<0.005$) under normal conditions and 0.57-fold below normal expression ($p<0.005$) with increased glucose levels after 48hrs. L-carnitine was unable to raise GCN2 steady state mRNA levels in cells that were grown in low glucose medium. Generally, addition of glucose to the treatment of cells with L-carnitine increased mRNA expression levels compared to supplementation only with L-carnitine.

3.2.1.6. PGC-1

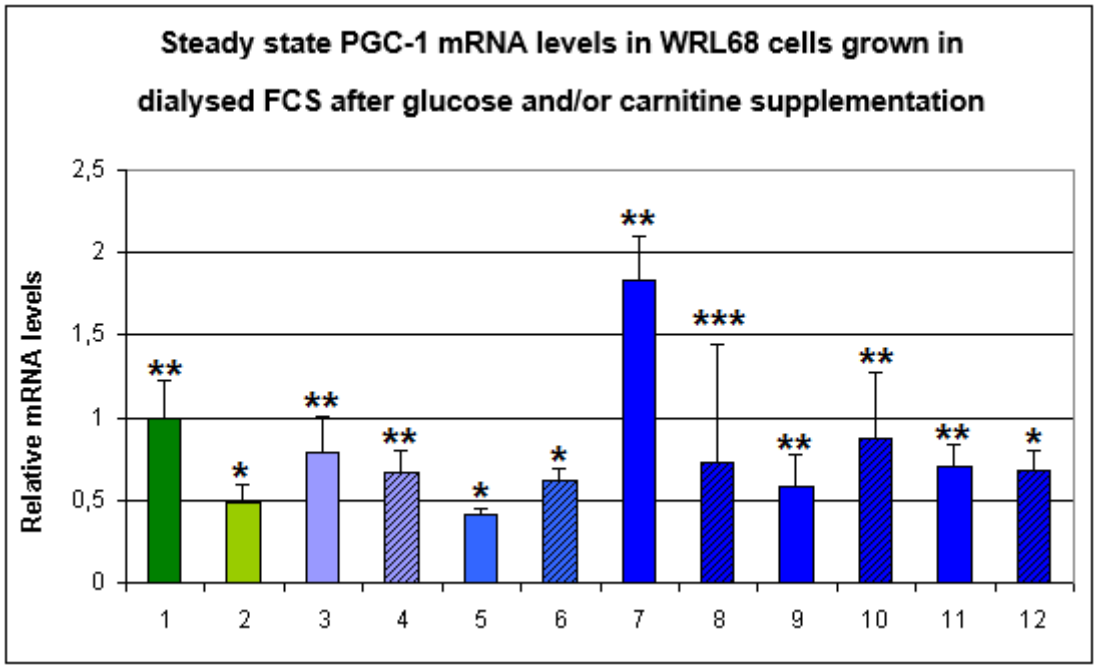

Figure 30: Analysis of PGC-1 steady state mRNA levels in WRL68 cells cultivated under L-carnitine deprivation and glucose and/or L-carnitine supplementation in a normoglycaemic medium. Steady state PGC-1-mRNA levels were determined by real-time RT-PCR in WRL68 cells, cultivated in 10% dialysed FCS and supplemented with 3500 µg/l glucose 40 µM and 80 µM L-carnitine (increasing supplementation durations) in comparison to un-supplemented and normal FCS. Legend: 1: normal FCS; 2: dialysed FCS (dialFCS); 3: dialFCS + 40µM L-carnitine for 4hrs; 4: dialFCS + 40µM L-carnitine and 3500 mg/l glucose for 4hrs; 5: dialFCS + 80µM L-carnitine for 4hrs; 6: dialFCS + 80µM L-carnitine and 3500 mg/l glucose for 4hrs; 7: dialFCS + 80µM L-carnitine for 15hrs; 8: dialFCS + 80µM L-carnitine and 3500 mg/l glucose for 15hrs; 9: dialFCS + 80µM L-carnitine for 24hrs; 10: dialFCS + 80µM L-carnitine and 3500 mg/l glucose for 24hrs; 11: dialFCS + 80µM L-carnitine for 48hrs; 12: dialFCS + 80µM L-carnitine and 3500 mg/l glucose for 48hrs. T-bars signify the standard deviation of each sample.

Expression of PGC-1α steady state mRNA levels in WRL68 cells, cultivated in DMEM medium with 10% “normal” undialysed FCS ($p<0.05$; indicated by **), were set at 1.0 to serve as basic reference level for all other treatment regimens (fig. 30). The PGC-1α mRNA amounts in cells kept under 10% dialysed FCS (= carnitine deficient medium) declined to 0.48 in relation to standard FCS with a statistical significance level of $p<0.005$ (indicated by *). Subsequent supplementation of L-carnitine to the growth medium containing dialysed FCS had varying effects on PGC-1α expression, depending on L-carnitine levels and duration of supplementation. Treatment with 40 µM for 4hrs resulted in mRNA steady state levels 0.78-fold below normal expression ($p<0.05$) under normal conditions and declined to 0.67-fold below normal expression ($p<0.05$) when extra glucose was added. In contrast, supplementation of 80 µM L-carnitine showed a dependence on time of treatment and glucose levels in affecting mRNA levels. The measured extents after 4hrs under normal conditions were 0.41-fold below normal levels ($p<0.005$), while they increased to 0.61-fold below normal levels ($p<0.005$) when glucose was added for the duration of the supplementation. The strongest effect was recorded after 15hrs of supplementation at low levels of glucose, where mRNA steady state levels rose 1.83-fold above normal amounts ($p<0.05$), but reached only levels of 0.73-fold below normal expression ($p<0.5$; indicated by ***) under higher glucose conditions. After 24hrs of supplementation, PGC-1α steady state levels reached levels of 0.58-fold below normal extents ($p<0.05$) under normal conditions and rose to 0.88-fold below normal expression ($p<0.05$) with raised glucose levels. The recorded levels after 48hrs of treatment were 0.70-fold below normal expression ($p<0.05$) under normal conditions and 0.68-fold below normal expression ($p<0.005$) with raised glucose levels after 48hrs.

3.2.1.7. SREBP1

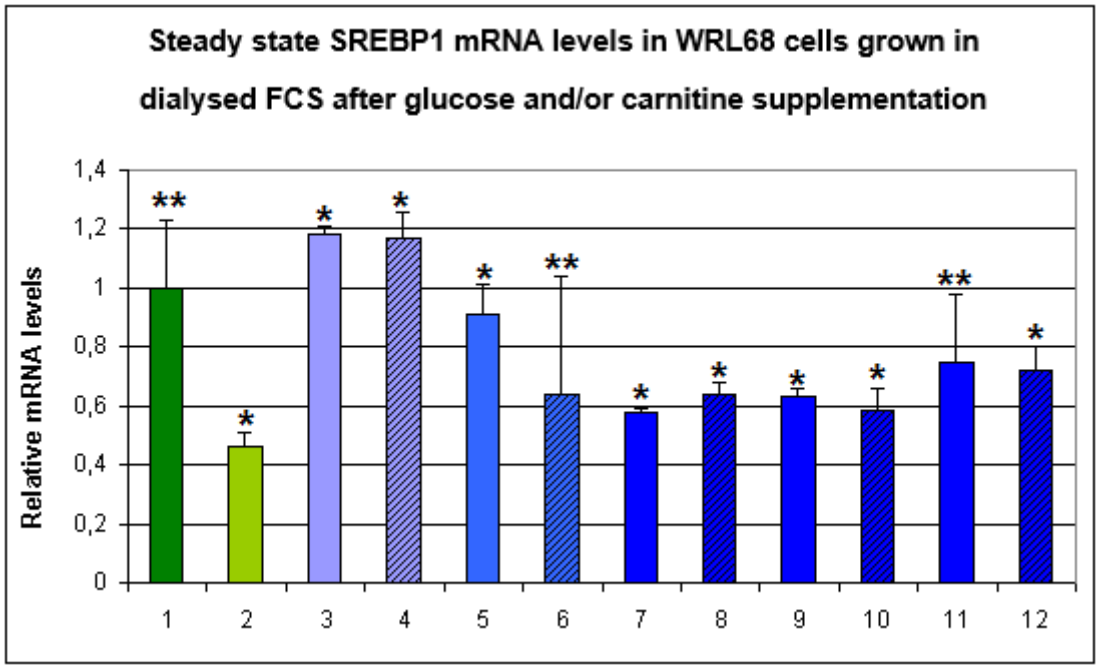

Figure 31: Analysis of SREBP1 steady state mRNA levels in WRL68 cells cultivated under L-carnitine deprivation and glucose and/or L-carnitine supplementation in a normoglycaemic medium. Steady state SREBP1-mRNA levels were determined by real-time RT-PCR in WRL68 cells, cultivated in 10% dialysed FCS and supplemented with 3500 µg/l glucose 40 µM and 80 µM L-carnitine (increasing supplementation durations) in comparison to un-supplemented and normal FCS. Legend: 1: normal FCS; 2: dialysed FCS (dialFCS); 3: dialFCS + 40µM L-carnitine for 4hrs; 4: dialFCS + 40µM L-carnitine and 3500 mg/l glucose for 4hrs; 5: dialFCS + 80µM L-carnitine for 4hrs; 6: dialFCS + 80µM L-carnitine and 3500 mg/l glucose for 4hrs; 7: dialFCS + 80µM L-carnitine for 15hrs; 8: dialFCS + 80µM L-carnitine and 3500 mg/l glucose for 15hrs; 9: dialFCS + 80µM L-carnitine for 24hrs; 10: dialFCS + 80µM L-carnitine and 3500 mg/l glucose for 24hrs; 11: dialFCS + 80µM L-carnitine for 48hrs; 12: dialFCS + 80µM L-carnitine and 3500 mg/l glucose for 48hrs.T-bars signify the standard deviation of each sample.

Expression of SREBP1 steady state mRNA levels in WRL68 cells, cultivated in DMEM medium with 10% “normal” undialysed FCS ($p<0.05$; indicated by **), were set at 1.0 to serve as basic reference level for all other treatment regimens (fig. 31). The SREBP1 mRNA amounts in cells kept under 10% dialysed FCS (= carnitine deficient medium) decreased to 0.46 in relation to standard FCS with a statistical significance level of $p<0.005$ (indicated by *). Subsequent supplementation of L-carnitine to the growth medium containing dialysed FCS had varying effects on SREBP1 expression, depending on L-carnitine levels. Treatment with 40 µM for 4hrs lifted the mRNA steady state levels 1.18-fold above normal expression ($p<0.005$) under normal conditions and to 1.17-fold above normal expression ($p<0.005$) when extra glucose was added. In contrast, supplementation of 80 µM L-carnitine could not raise mRNA levels above normal extents. The measured transcript amounts after 4hrs under normal conditions were 0.91-fold

below normal levels ($p<0.005$), while they decreased to 0.64-fold below normal levels ($p<0.05$) when glucose was added for the duration of the supplementation. Therefore, 40 µM L-carnitine has the strongest capability to induce SREBP1 transcripts, while addition of 80 µM L-carnitine becomes effective after 24hrs and declines after longer treatment. After 15hrs of supplementation at low levels of glucose, mRNA extents reached values 0.58-fold below normal levels ($p<0.005$) and increased to 0.64-fold below normal expression ($p<00.5$) with raised glucose levels. After 24hrs of supplementation, SREBP1 steady state levels reached levels of 0.63-fold below normal extents ($p<0.005$) under normal conditions and declined to 0.58-fold below normal expression ($p<0.005$) with raised glucose levels. The recorded levels after 48hrs of treatment were 0.75-fold below normal expression ($p<0.05$) under normal conditions and 0.72-fold below normal expression ($p<0.005$) with raised glucose levels after 48hrs. These results show that 40 µM L-carnitine can successfully raise SREBP1 steady state mRNA levels in cells that were grown in low glucose medium, while 80 µM L-carnitine is most effective after a short treatment and starts to rise again after longer duration of supplementation. Increasing the glucose levels to 4500 mg/l resulted in lower mRNA extents in most cases.

3.3. Pinpointing of L-carnitine regulated pathways

3.3.1. Oestrogen pathway

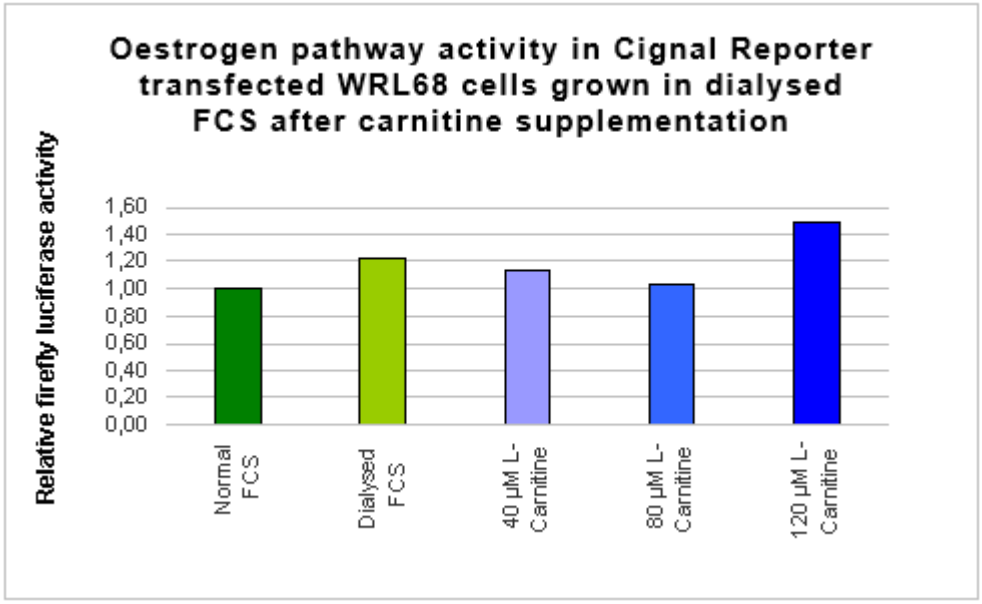

Figure 32: Analysis of the oestrogen pathway in WRL68 cells cultivated under L-carnitine deprivation and supplementation. Pathway activity was determined by measuring firefly luciferase luminescence in transfected WRL68 cells, cultivated in 10% dialysed FCS and supplemented with 40 µM, 80 µM and 120 µM L-carnitine in comparison to un-supplemented and normal FCS.

Activity of the oestrogen pathway in WRL68 cells, cultivated in DMEM medium with 10% "normal" undialysed FCS, measured through firefly luciferase activity, was set at 1.0 to serve as basic reference level for all other treatment regimens (fig. 32). Activity in cells kept under 10% dialysed FCS (= carnitine deficient medium) increased to 1.2 in contrast to normal extents. Subsequent supplementation of varying concentrations of L-carnitine for 4 hours successfully raised activity, depending on used L-carnitine concentration. Supplementation of 40 µM L-carnitine increased activity to 1.1-fold above normal values. In contrast, supplementation of 80 µM L-carnitine resulted in a slight decrease above normal activity. The peak in activity was reached after supplementation of 120 µM L-carnitine with an increase to 1.5-fold above normal activity. These findings show that carnitine deficiency increases the activity of the oestrogen pathway. Supplementation of L-carnitine was able to increase the activity above normal levels, the pronounced effect was exerted by supraphysiological 120 µM L-carnitine concentrations that induced the oestrogen pathway signalling even above those recorded at dialysed levels.

3.3.2. Androgen pathway

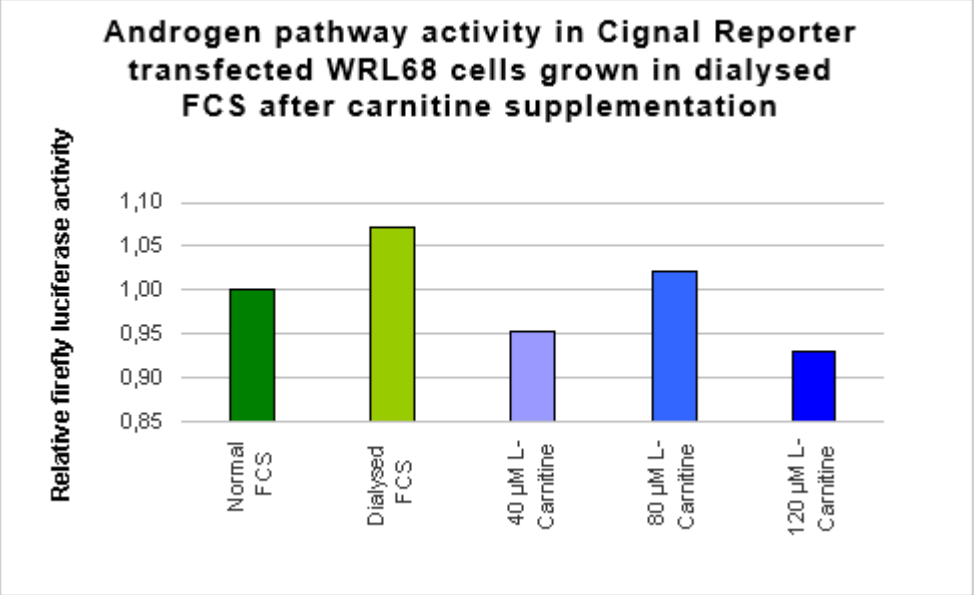

Figure 33: Analysis of the androgen pathway in WRL68 cells cultivated under L-carnitine deprivation and supplementation. Pathway activity was determined by measuring firefly luciferase luminescence in transfected WRL68 cells, cultivated in 10% dialysed FCS and supplemented with 40 µM, 80 µM and 120 µM L-carnitine in comparison to un-supplemented and normal FCS.

Activity of the androgen pathway in WRL68 cells, cultivated in DMEM medium with 10% "normal" undialysed FCS, measured through firefly luciferase activity, was set at 1.0 to serve as basic reference level for all other treatment regimens (fig. 33). Activity in cells kept under 10% dialysed FCS (= carnitine deficient medium) increased to 1.1 in contrast to normal extents. Subsequent supplementation of increasing concentrations of L-carnitine for 4 hours successfully achieved mixed results, but could not raise activity above levels in the carnitine deficient medium. Activity after supplementation of 40 µM L-carnitine lowered the androgen pathway to 0.95 of normal activity. In contrast, supplementation of 80 µM L-carnitine resulted in a slight increase above normal activity. Supplementation of 120 µM L-carnitine once again resulted in a decrease of activity to 0.9 of normal values. These results indicate that carnitine deficiency increases the activity of the androgen pathway, in contrast only supplementation of 80 µM L-carnitine was able to reinstall the pathway activity observed in normal cells, while 40 µM below and 120 µM above slightly reduced the androgen signalling.

3.3.3. PPAR pathway

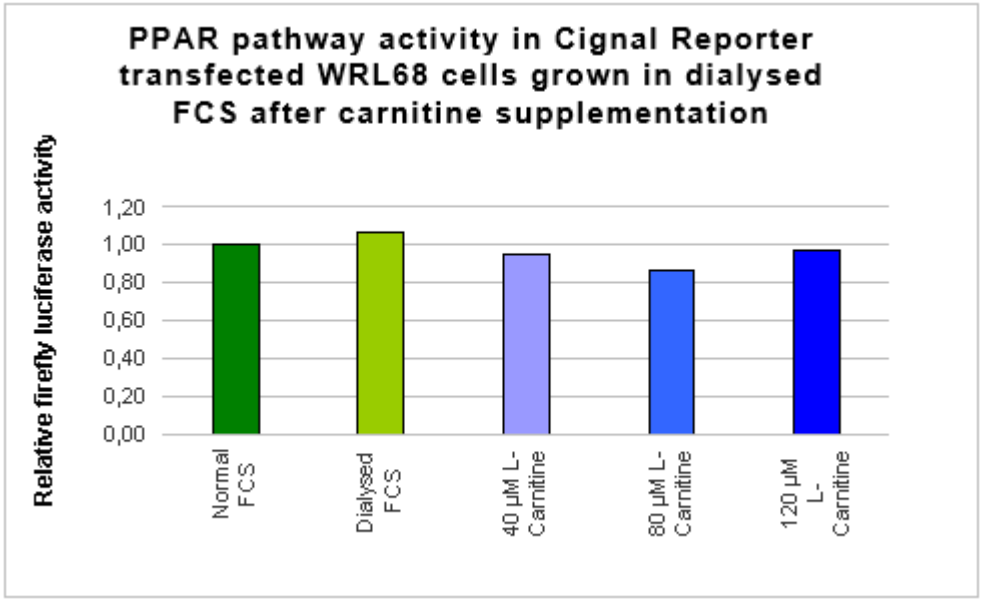

Figure 34: Analysis of the PPAR pathway in WRL68 cells cultivated under L-carnitine deprivation and supplementation. Pathway activity was determined by measuring firefly luciferase luminescence in transfected WRL68 cells, cultivated in 10% dialysed FCS and supplemented with 40 µM, 80 µM and 120 µM L-carnitine in comparison to un-supplemented and normal FCS.

Activity of the PPAR pathway in WRL68 cells, cultivated in DMEM medium with 10% "normal" undialysed FCS, measured through firefly luciferase activity, was set at 1.0 to serve as basic reference level for all other treatment regimens (fig. 34). Activity in cells kept under 10% dialysed FCS (= carnitine deficient medium) increased to 1.1in contrast to normal extents. Subsequent supplementation of varying concentrations of L-carnitine for 4 hours could not raise activity above normal levels. Activity after supplementation of 40 µM L-carnitine decreased to 0.9 of that under normal conditions, and decreased even further to 0.9-fold below normal levels after supplementation of 80 µM L-carnitine, while supplementation of 120 µM L-carnitine was able to restore the PPAR pathway very close to normal values at 0.96 of control. These results indicate that carnitine deficiency increases the activity of the PPAR pathway, while supplementation of L-carnitine in contrast lowers it below normal levels.

3.3.4. Retinoic acid pathway

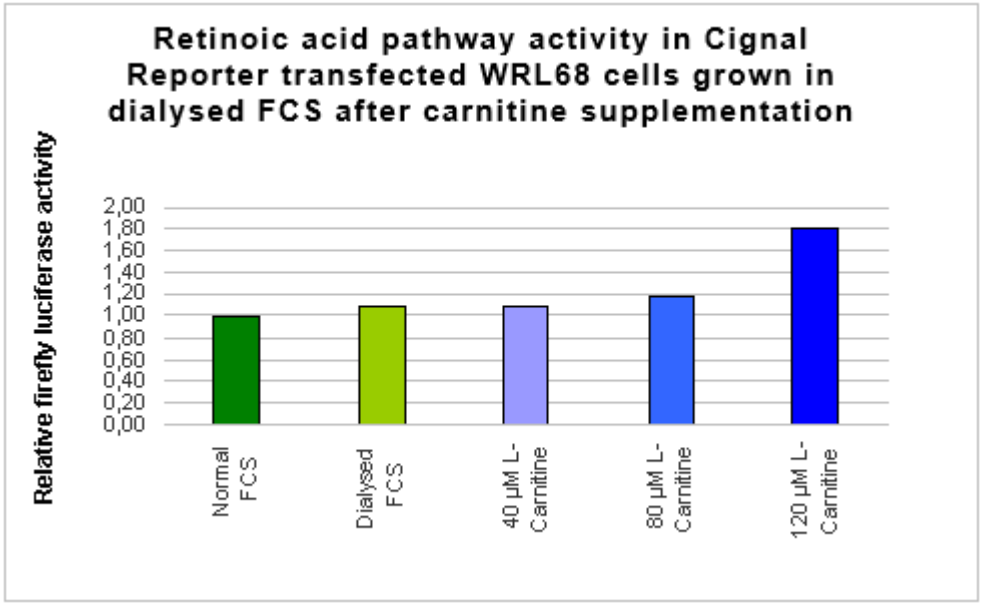

Figure 35: Analysis of the retinoic acid pathway in WRL68 cells cultivated under L-carnitine deprivation and supplementation. Pathway activity was determined by measuring firefly luciferase luminescence in transfected WRL68 cells, cultivated in 10% dialysed FCS and supplemented with 40 µM, 80 µM and 120 µM L-carnitine in comparison to un-supplemented and normal FCS.

Activity of the retinoic acid pathway in WRL68 cells, cultivated in DMEM medium with 10% “normal” undialysed FCS, measured through firefly luciferase activity, was set at 1.0 to serve as basic reference level for all other treatment regimens (fig. 35). Activity in cells kept under 10% dialysed FCS (= carnitine deficient medium) increased to 1.1 in contrast to normal extents. Subsequent supplementation of varying concentrations of L-carnitine for 4 hours increased activity, depending on concentration. Activity after supplementation of 40 µM L-carnitine increased to 1.1-fold above normal levels. Higher concentrations of L-carnitine exerted the strongest effect upon activity. Supplementation with 80 µM L-carnitine increased it to 1.2-fold above normal levels and 120 µM L-carnitine increased it to 1.8-fold above normal values. These results indicate that carnitine deficiency slightly increases the activity of the retinoic acid pathway and is further increased by supplementation of L-carnitine. High supplementation levels at 120 µM L-carnitine had the pronounced strongest effect upon the retinoic acid pathway.

3.3.5. *Vitamin D pathway*

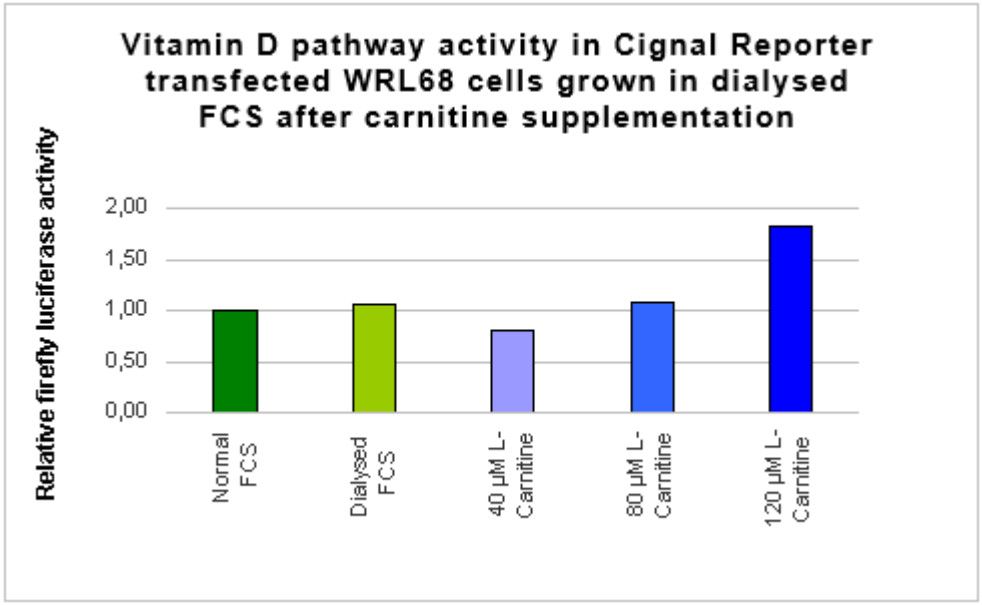

Figure 36: Analysis of the vitamin D pathway in WRL68 cells cultivated under L-carnitine deprivation and supplementation. Pathway activity was determined by measuring firefly luciferase luminescence in transfected WRL68 cells, cultivated in 10% dialysed FCS and supplemented with 40 µM, 80 µM and 120 µM L-carnitine in comparison to un-supplemented and normal FCS.

Activity of the vitamin D pathway in WRL68 cells, cultivated in DMEM medium with 10% "normal" undialysed FCS, measured through firefly luciferase activity, was set at 1.0 to serve as basic reference level for all other treatment regimens (fig. 36). Recorded activity in cells kept under 10% dialysed FCS (= carnitine deficient medium) was close to normal activity, with a 1.1-fold increase above normal activity. Subsequent supplementation of increasing concentrations of L-carnitine for 4 hours exerted a concentration-dependent effect on the vitamin D pathway activity. Supplementation of 40 µM L-carnitine lowered activity to 0.8-fold below normal values. But supplementation of 80 µM L-carnitine successfully raised firefly luciferase activity to 1.1-fold above normal extents. Supplementation of 120 µM L-carnitine was the most effective in raising activity with a recorded peak of 1.8-fold above normal activity. These findings show that carnitine deficiency has a weak lowering or inducing effect on the vitamin D pathway activity. Interestingly, this pathway function damped at physiological L-carnitine levels but when supplemented in physiological as well as supraphysiological concentrations its activity is remarkably induced.

3.3.6. Glucocorticoid pathway

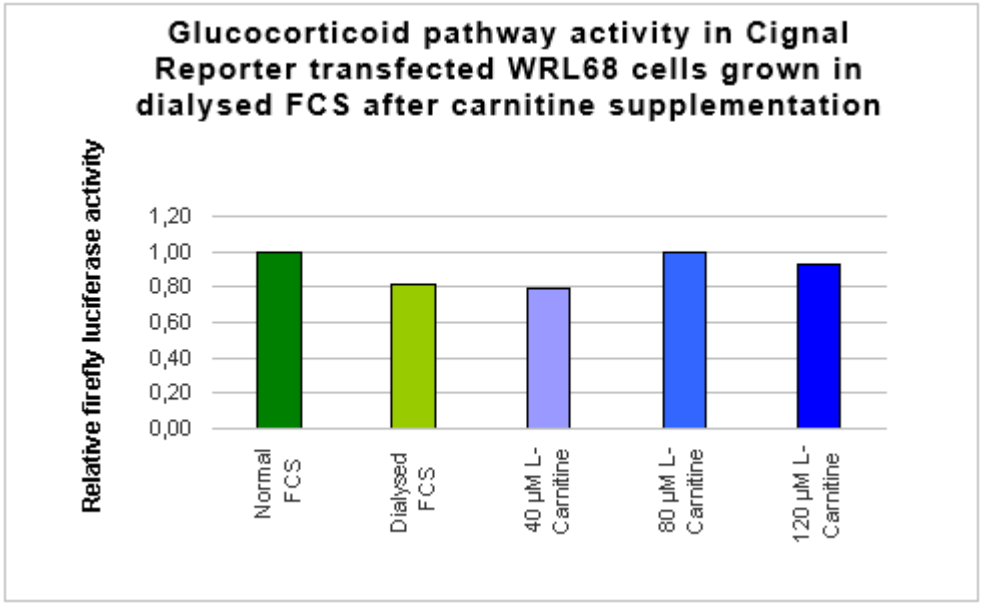

Figure 37: Analysis of the glucocorticoid pathway in WRL68 cells cultivated under L-carnitine deprivation and supplementation. Pathway activity was determined by measuring firefly luciferase luminescence in transfected WRL68 cells, cultivated in 10% dialysed FCS and supplemented with 40 µM, 80 µM and 120 µM L-carnitine in comparison to un-supplemented and normal FCS.

Activity of the glucocorticoid pathway in WRL68 cells, cultivated in DMEM medium with 10% “normal” undialysed FCS, measured through firefly luciferase activity, was set at 1.0 to serve as basic reference level for all other treatment regimens (fig. 37). Measured activity in cells kept under 10% dialysed FCS (= carnitine deficient medium) decreased to 0.8 of normal activity. Subsequent supplementation of increasing concentrations of L-carnitine for 4 hours had restoring effects, especially at higher carnitine levels. Treatment with 40 µM was not sufficient and resulted in measured firefly activity of 0.8-fold below normal extents. But supplementation of 80 µM L-carnitine restored activity to normal levels, while 120 µM L-carnitine once again lowered it to 0.9. These findings show that carnitine deficiency results in lower pathway activity that can be restored by L-carnitine, but only at higher supplementation levels of 80 µM L-carnitine.

3.3.7. *Progesterone pathway*

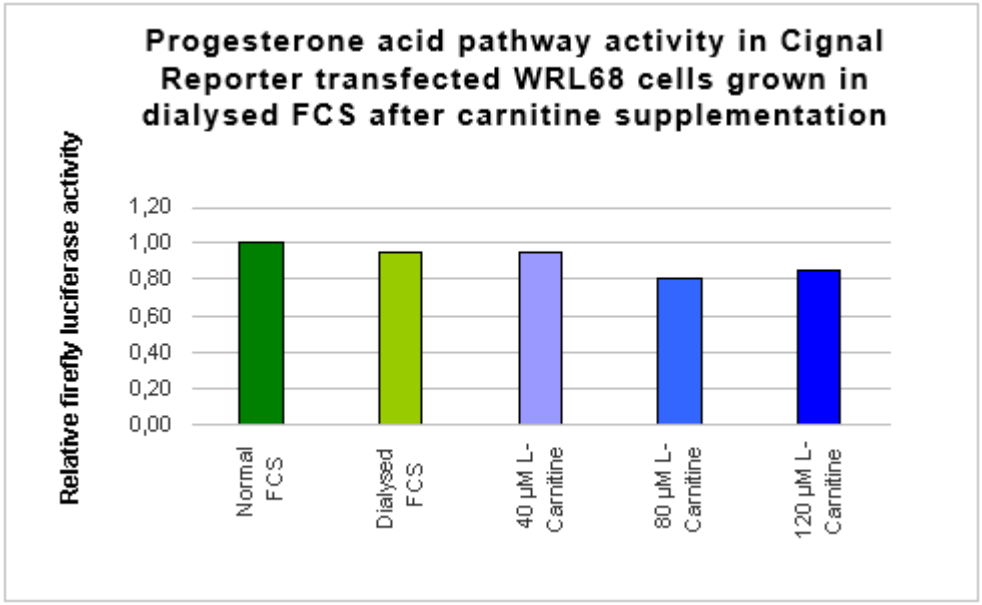

Figure 38: Analysis of the progesterone pathway in WRL68 cells cultivated under L-carnitine deprivation and supplementation. Pathway activity was determined by measuring firefly luciferase luminescence in transfected WRL68 cells, cultivated in 10% dialysed FCS and supplemented with 40 µM, 80 µM and 120 µM L-carnitine in comparison to un-supplemented and normal FCS.

Activity of the progesterone pathway in WRL68 cells, cultivated in DMEM medium with 10% “normal” undialysed FCS, measured through firefly luciferase activity, was set at 1.0 to serve as basic reference level for all other treatment regimens (fig. 38). Recorded activity in cells kept under 10% dialysed FCS (= carnitine deficient medium) was close to normal activity at 0.95-fold below normal extents. Subsequent supplementation of varying concentrations of L-carnitine for 4 hours was not able to restore activity to normal values. Treatment with 40 µM was the most effective and resulted in a value of 0.95-fold below normal extents. Supplementation of 80 µM L-carnitine was less effective, with recorded 0.8 of normal activity, while supplementation of 120 µM L-carnitine resulted in a slight increase to 0.9 of normal activity. These findings show that progesterone pathway activity is only minimally influenced by carnitine deficiency and is mainly mitigated by L-carnitine supplementation, especially at supraphysiological levels.

3.3.8. *Retinoid X pathway*

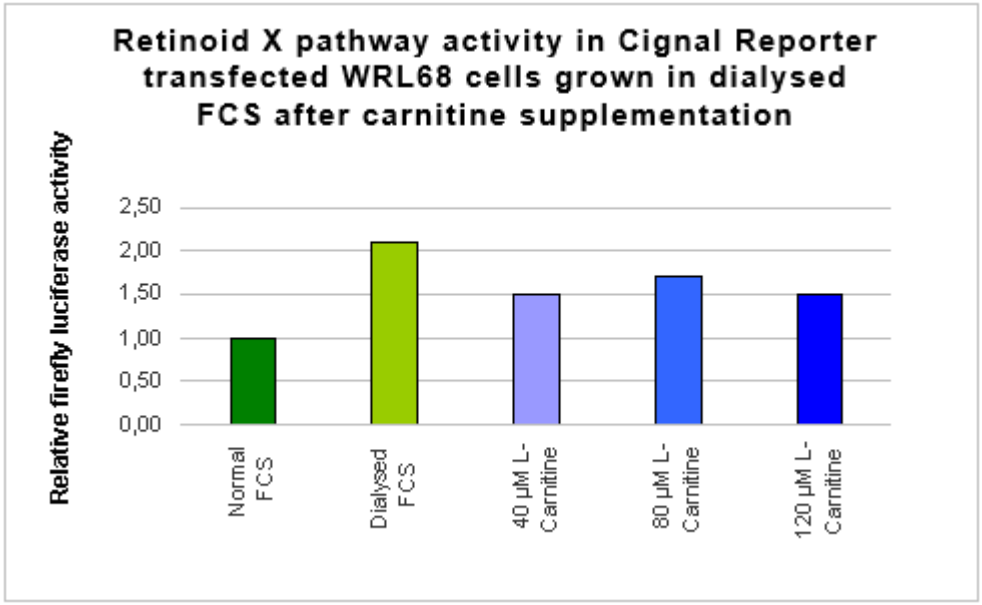

Figure 39: Analysis of the retinoid X pathway in WRL68 cells cultivated under L-carnitine deprivation and supplementation. Pathway activity was determined by measuring firefly luciferase luminescence in transfected WRL68 cells, cultivated in 10% dialysed FCS and supplemented with 40 µM, 80 µM and 120 µM L-carnitine in comparison to un-supplemented and normal FCS.

Activity of the retinoid X pathway in WRL68 cells, cultivated in DMEM medium with 10% "normal" undialysed FCS, measured through firefly luciferase activity, was set at 1.0 to serve as basic reference level for all other treatment regimens (fig. 39). Activity in cells kept under 10% dialysed FCS (= carnitine deficient medium) increased 2.1-fold in contrast to normal extents. Subsequent supplementation of varying concentrations of L-carnitine for 4 hours was able to lower activity compared to that in the carnitine deficient medium. Activity after supplementation of 40 µM L-carnitine was 1.5-fold above normal levels, while the recorded level after supplementation of 80 µM L-carnitine was 1.7-fold above normal extents. Supplementation of 120 µM L-carnitine once again lead to a weaker increase with 1.5-fold above normal values. These results indicate that carnitine deficiency increases the activity of the retinoid X pathway, but supplementation of L-carnitine leads to its normalization.

3.3.9. *Liver X pathway*

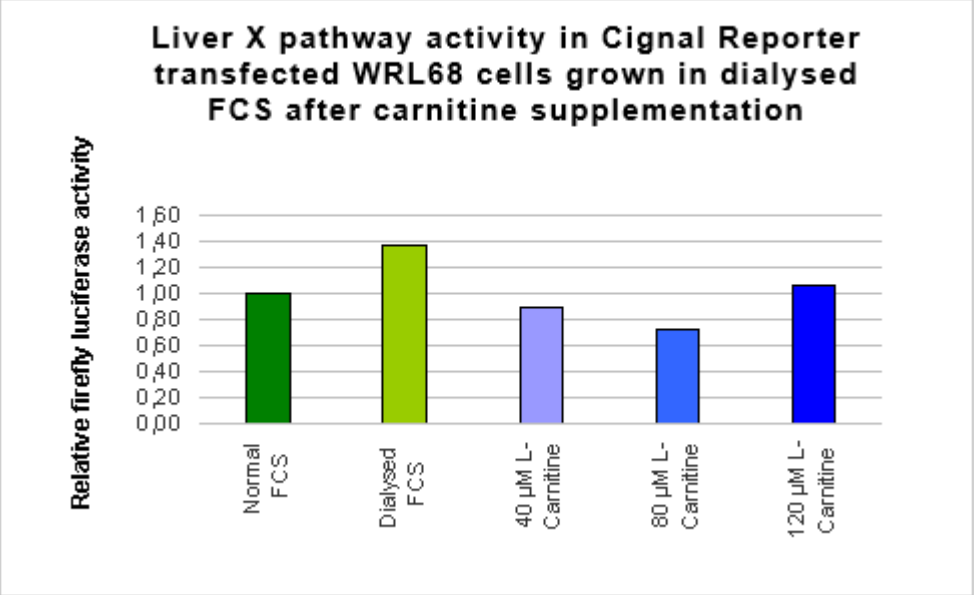

Figure 40: Analysis of the liver X pathway in WRL68 cells cultivated under L-carnitine deprivation and supplementation. Pathway activity was determined by measuring firefly luciferase luminescence in transfected WRL68 cells, cultivated in 10% dialysed FCS and supplemented with 40 µM, 80 µM and 120 µM L-carnitine in comparison to un-supplemented and normal FCS.

Activity of the liver X pathway in WRL68 cells, cultivated in DMEM medium with 10% "normal" undialysed FCS, measured through firefly luciferase activity, was set at 1.0 to serve as basic reference level for all other treatment regimens (fig. 40). Activity in cells kept under 10% dialysed FCS (= carnitine deficient medium) increased up to 1.4-fold compared to normal extents. Subsequent supplementation of varying concentrations of L-carnitine for 4 hours achieved mixed results, depending on concentration. Activity after supplementation of 40 µM L-carnitine decreased to 0.9 of that under normal conditions, and decreased even further to 0.7-fold below normal levels after supplementation of 80 µM L-carnitine. In contrast, supplementation of 120 µM L-carnitine successfully increased activity 1.1-fold above normal values. These results indicate that carnitine deficiency increases the activity of the liver X pathway, while supplementation of L-carnitine shifts it closer to normal levels.

3.3.10. *Hepatocyte nuclear factor 4 (HNF4) pathway*

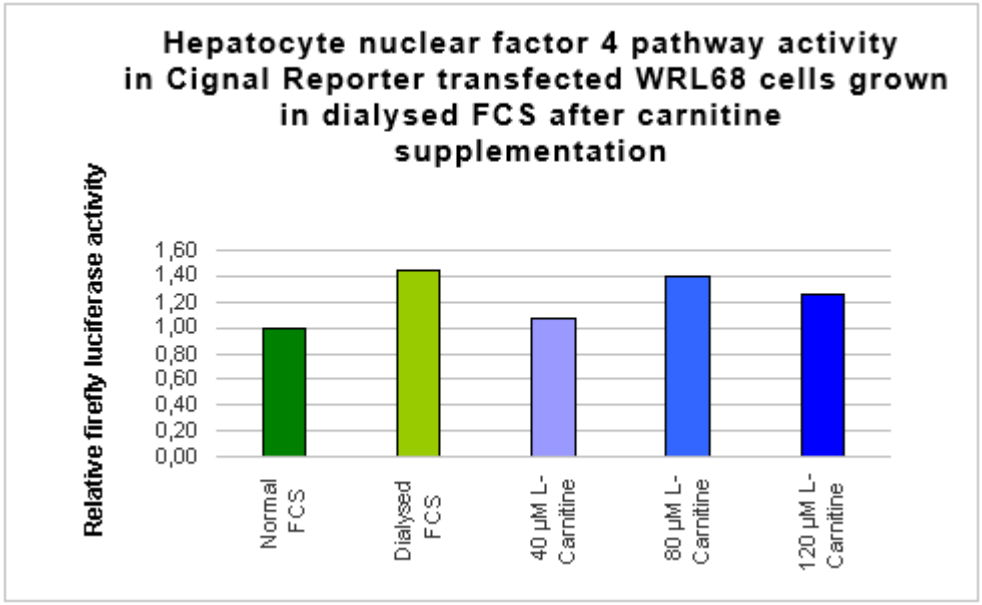

Figure 41: Analysis of the HNF4 pathway in WRL68 cells cultivated under L-carnitine deprivation and supplementation. Pathway activity was determined by measuring firefly luciferase luminescence in transfected WRL68 cells, cultivated in 10% dialysed FCS and supplemented with 40 µM, 80 µM and 120 µM L-carnitine in comparison to un-supplemented and normal FCS.

Activity of the HNF4 pathway in WRL68 cells, cultivated in DMEM medium with 10% "normal" undialysed FCS, measured through firefly luciferase activity, was set at 1.0 to serve as basic reference level for all other treatment regimens (fig. 41). Activity in cells kept under 10% dialysed FCS (= carnitine deficient medium) increased to 1.5 in contrast to normal extents. Subsequent supplementation of varying concentrations of L-carnitine for 4 hours raised activity in all cases. Activity after supplementation of 40 µM L-carnitine increased to 1.1-fold above normal conditions, and increased even further to 1.4-fold above normal levels after supplementation of 80 µM L-carnitine. Supplementation of 120 µM L-carnitine decreased activity back to 1.3-fold above normal values. These results indicate that carnitine deficiency increases the activity of the HNF4 pathway, in contrast supplementation of L-carnitine lowers it. Interestingly, low L-carnitine levels are the most effective in normalizing HNF4 pathway activity, while supraphysiological levels lead to an increase in expression.

3.4. Electrophoretic mobility shift assays (EMSA)

Band shift assays were performed using nuclear protein extracts, obtained from WRL68 cells that were grown in DMEM with 10% undialysed (normal) FCS or in DMEM with 10% dialysed FCS (dialFCS). Subsequently, some plates were supplemented with 40 µM or 80 µM L-carnitine for 4 hours. Nuclear extracts were isolated as described in Materials and methods (2.5.3 Nuclear extract isolation). The isolated protein extracts were incubated with ^{32}P-labelled oligonucleotides of putative promoter binding elements, derived from theoretical analysis of the CrAT promoter (1.5 Carnitine acetyltransferase), and with increasing concentrations of unlabelled "cold" acetyl-L-carnitine (ALC) (0 µM, 20 µM, 40 µM, 80 µM or 120 µM). The rationale behind this was to investigate a noncovalent interaction of unlabelled ALC with the promoter complex of specific transcription factors that have been proven to be involved in the "carnitine effect".

3.4.1. Analysis of the putative hRARRXR binding site

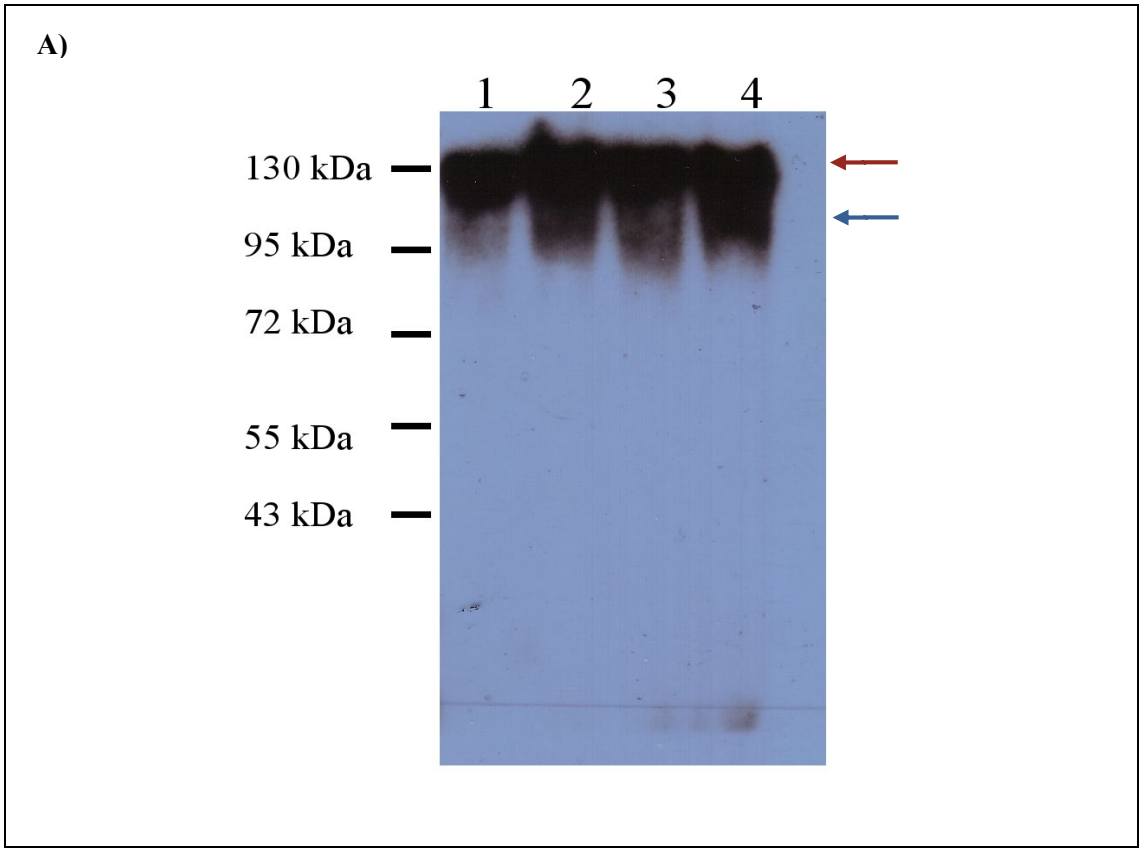

B)

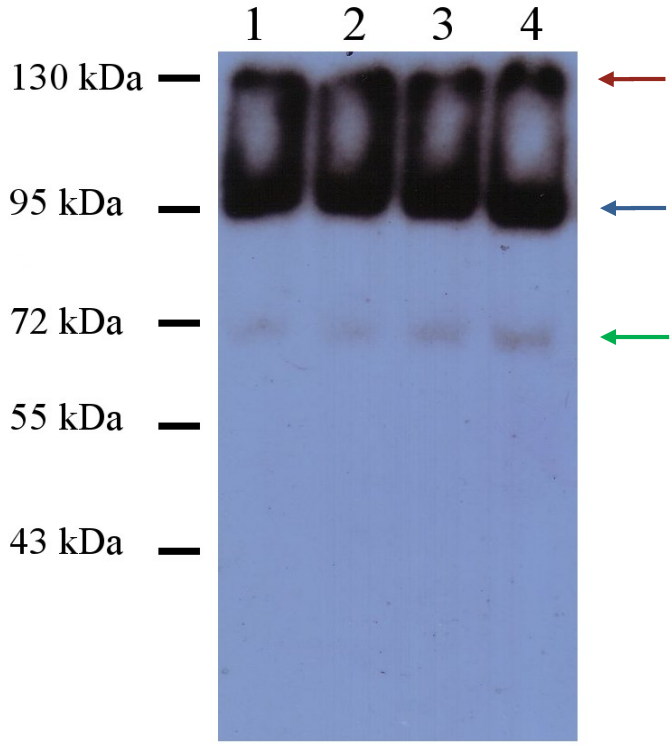
1
2
3
4
130 kDa
95 kDa
72 kDa
55 kDa
43 kDa

C)

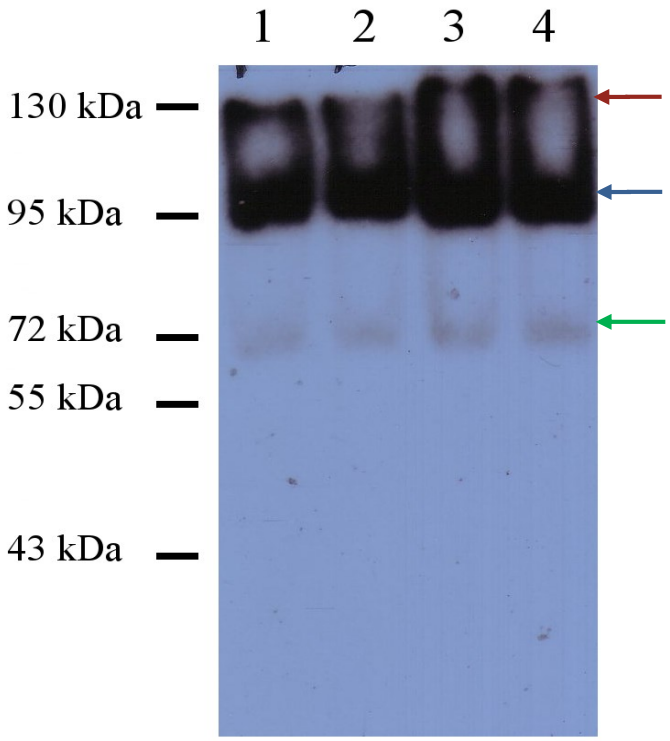
1
2
3
4
130 kDa
95 kDa
72 kDa
55 kDa
43 kDa

D)

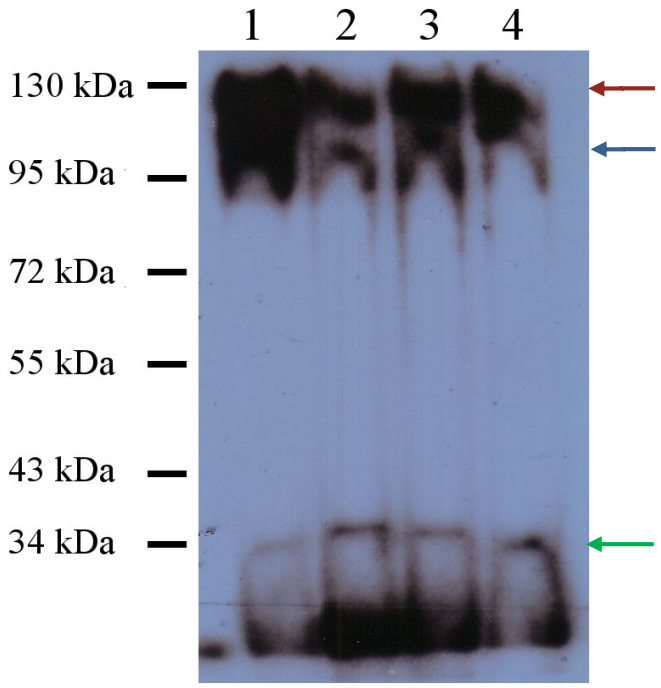

E)

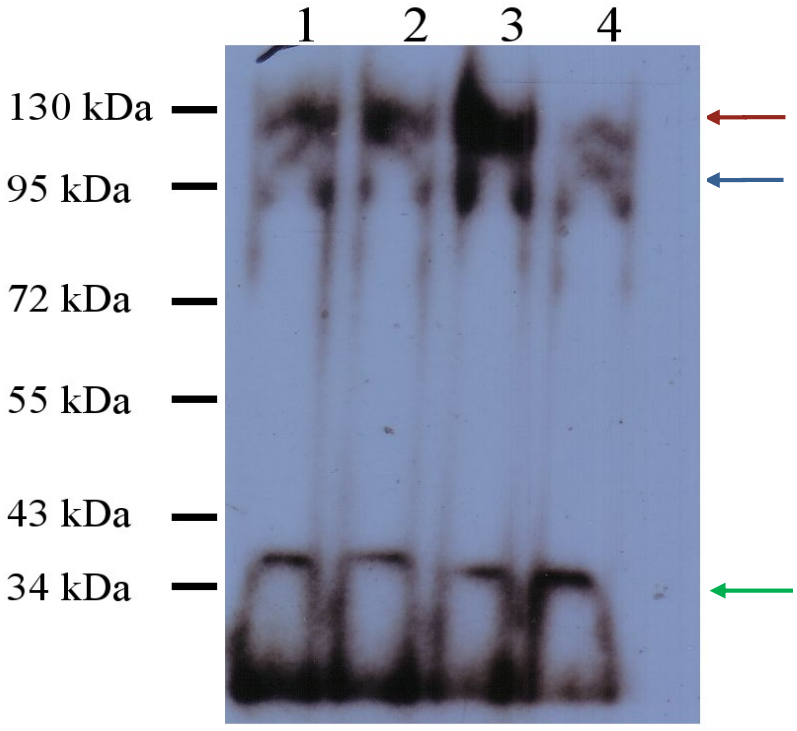

A) Band shift analysis without ALC

B) Band shift analysis with 20 µM ALC

C) Band shift analysis with 40 µM ALC

D) Band shift analysis with 80 µM ALC

E) Band shift analysis with 120 µM ALC

Lanes:

1: DMEM + 10% FCS

2: DMEM + 10% dialysed FCS (dialFCS)

3: dialFCS + 40 µM L-carnitine

4: dialFCS + 80 µM L-carnitine

Figure 42: Band shift analysis of the putative RARRXR binding site with increasing concentrations of added acetyl-L-carnitine (ALC).

The results of the RARRXR band shift analysis presented in fig. 42 are:

A) This electrophoretic mobility shift assay was performed without the addition of "cold" unlabelled acetyl-L-carnitine (ALC) to the reaction mix. It resulted in a marked band shift of at least two bands, one major with a size of about 130 kDa and a second smaller one underneath. Smaller protein complexes migrated further down in the range of the 95 kDa marker, but no additional bands could be resolved.

B) Addition of 20 µM acetyl-L-carnitine to the band shift reaction mix resulted in a downshift of the original upper shift band to a size of about 95 kDa, and the appearance of a faint band with the size of about 72 kDa, which turned out to be stronger in cases where the extract was obtained from L-carnitine-supplemented cells.

C) Appending of 40 µM unlabelled acetyl-L-carnitine to the reaction mix generated a similar result as seen with 20 µM acetyl-L-carnitine, leading to the weakening of the original band at 130 kDa and a marked downshift, gaining a size of about 95 kDa. The new band at 72 kDa did also appear in this case.

D) In the analysis where 80 µM acetyl-L-carnitine was appended to the reaction mix, the faint band at 72 kDa disappeared, independent from the treatment regimen. The original upper shift-band was also strengthened and the 95 kDa band was weakened when using extracts from WRL68 cells cultivated in DMEM with 10% dialysed FCS (lane 2), while supplementation of 40 µM L-carnitine prior to extraction seems to have prevented a stronger weakening (lane 3). Using extracts from cells that were supplemented with 80 µM L-carnitine resulted in an upshift of the original 95 kDa band or the appearance of a

new band (lane 4). Appending of 80 µM unlabelled ALC also resulted in the appearance of a faint band near the 34 kDa marker all cases.

E) In the band shift where 120 µM acetyl-L-carnitine was appended to the reaction mix all bands lost in intensity compared to the parallel reactions. The band at the 95 kDa marker disappeared in all cases, whereas the marked 130 kDa band shift resolved into 2 distinct bands. The band at the 34 kDa marker that appeared when using extracts that were supplemented with 80 µM acetyl-L-carnitine before extraction also appeared stronger (lane 4).

A compilation of all observed effects in the band shift analyses of RARRXR is given in table 5.

Table 5: Signal intensities and migration patterns of the mobility shift bands for RARRXR.

hRARRXR							
		Band size [kDa]					
Appended ALC	**Nuclear Extract**	130	95	72	55	43	34
No ALC	N	****					
	Dial	****					
	40	****					
	80	****					
20 µM	N	***	****	*			
	Dial	***	****	*			
	40	***	****	*			
	80	***	****	*			
40 µM	N	**	****				
	Dial	**	****				
	40	**	****				
	80	**	****				
80 µM	N	***	****				*
	Dial	**	**				*
	40	***	**				*
	80	**	*				*
120 µM	N	**	**				*
	Dial	**	**				*
	40	***	*				*
	80	*	*				*

Legend to table 5: N – protein extract from cells grown in normal cell culture medium (DMEM and 10% FCS); D – protein extract from cells kept in dialysed medium (DMEM and 10% dialysed FCS); 40 – protein extract from cells grown in medium with 10% dialysed FCS and supplemented with 40 µM L-carnitine; 80 – protein extract from cells cultivated in medium with 10% dialysed FCS and supplemented with 80 µM L-carnitine; * - very weak band; ** - weak band; *** - strong band; **** - very strong band.

3.4.2. Analysis of the putative glucocorticoid α (GR α) binding site

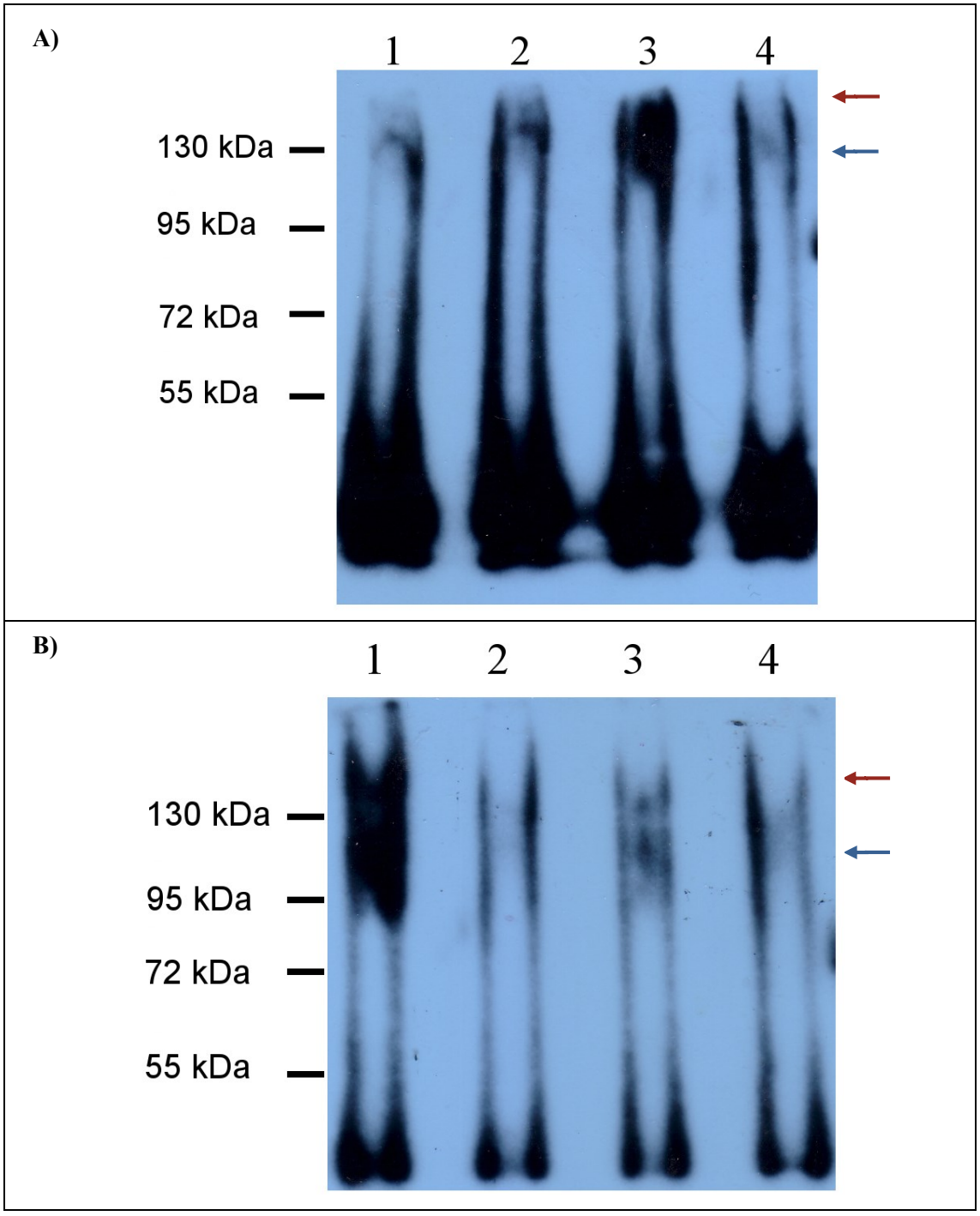

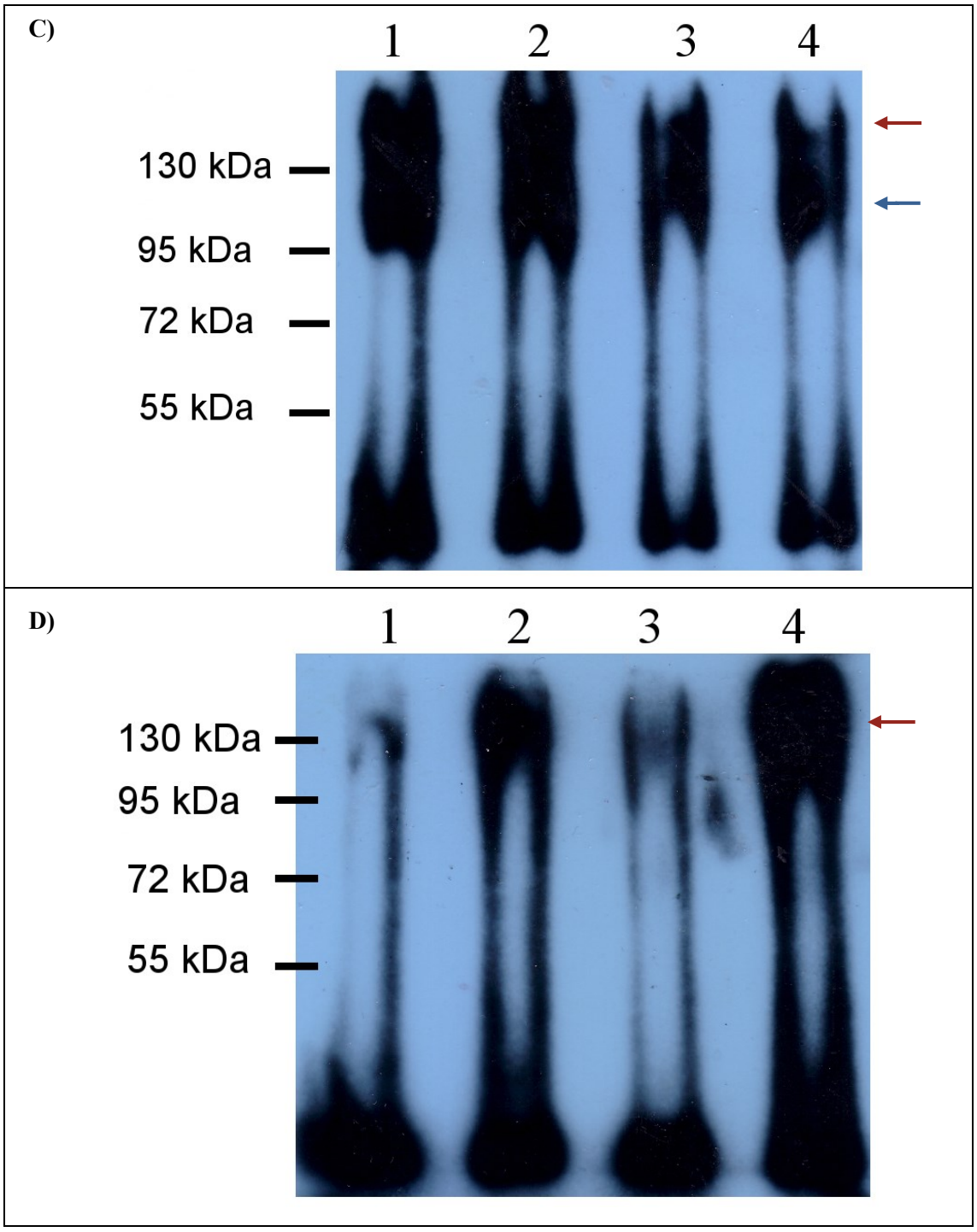
C)
1
2
3
4
130 kDa
95 kDa
72 kDa
55 kDa
D)
1
2
3
4
130 kDa
95 kDa
72 kDa
55 kDa

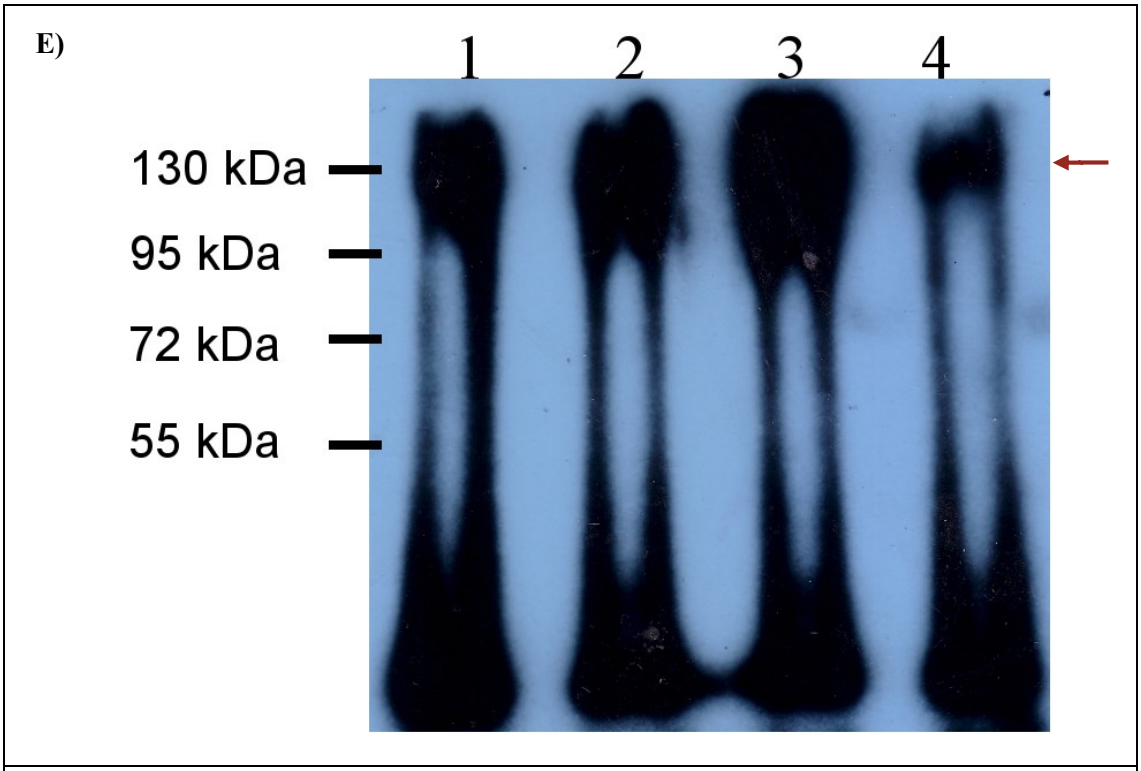

A) Band shift analysis without ALC

B) Band shift analysis with 20 µM ALC

C) Band shift analysis with 40 µM ALC

D) Band shift analysis with 80 µM ALC

E) Band shift analysis with 120 µM ALC

Lanes:

1: DMEM + 10% FCS

2: DMEM + 10% dialysed FCS (dialFCS)

3: dialFCS + 40 µM L-carnitine

4: dialFCS + 80 µM L-carnitine

Figure 43: Band shift analysis of the putative glucocorticoid binding site with different concentrations of added acetyl-L-carnitine (ALC).

The results of the RARRXR band shift analysis presented in fig. 43 are:

A) For a control, unlabelled acetyl-L-carnitine (ALC) was omitted from the reaction mix. The band shift assay generated a faint band with a size of about 150 kDa and a more pronounced band at 130 kDa using extracts from WRL68 cells cultivated in DMEM with 10% FCS (lane 1). Both bands gradually intensified when nuclear extracts from WRL68 cells were used that had been previously cultivated in medium containing 10% dialysed FCS plus L-carnitine supplementation (lanes 3 and 4). They were strongest with 40 µM L-carnitine (lane 3). Supplementation of 80 µM L-carnitine resulted in extracts where the upper band disappeared, while the 95 kDa band was very faint (lane 4).

B) Addition of 20 µM acetyl-L-carnitine to the reaction mix resulted in an intensification of the bands and a downshift of the original upper shift band at 150 kDa down to 130 kDa and a downshift of the original lower shift band at 130 kDa down to the ~110 kDa marker when extracts were isolated from WRL68 cells cultivated in DMEM with 10% FCS (lane 1). However, extracts from cells cultivated in dialFCS primarily resulted in a marked weakening of all band shift signals, especially a very faint band at the 130 kDa marker (lane 2). Unlabelled ALC weakened the bands similarly in the 40 µM L-carnitine extracts, accompanied by a downshift (lane 3) compared to lane 1 where no unlabelled ALC was appended (fig. 43A). The weakened band in lane 4 (80 µM L-carnitine extract) also shifted down.

C) Appending of 40 µM unlabelled acetyl-L-carnitine to the reaction mix resulted in the strengthening of the bands when normal extract was used, and also led to the reappearance of the original upper shift band (lane 1). In all the lanes where dialFCS extracts were used, the results were similar to lane 1. Bandshifts intensified compared to those presented in panels A and B. The 40 µM and 80 µM L-carnitine extracts generated an upper shift in the size range of 150 kDa and a lower shift band slightly below the 130 kDa marker (lanes 3 and 4), in both cases with a signal intensity much stronger than those presented in panels A and B.

D) Appending of 80 µM acetyl-L-carnitine to the reaction mix resulted in the disappearance of all except the 130 kDa band in the case of the normal extract (lane 1). In lane 2 where the dialFCS extract was used, the lower shift band at ~110 kD disappeared, resulting in at least one remaining band near or above the 130 kDa marker. In lane 3 where the 40 µM L-carnitine extract was used once again a weakened band could be resolved, leading to a similar result as presented in fig. 43B. A similar effect could be observed with the extract from cells previously cultivated with 80 µM L-carnitine, where the lower shift band at ~110 kDa disappeared, compared to the other results.

E) Appending of 120 µM unlabelled acetyl-L-carnitine to the reaction mix resulted in the re-strengthening of the upper shift band in the lane with the normal extract (lane 1) and the disappearance of the lower shift band, similar to the bands shift assay where 80 µM unlabelled ALC was appended. The bands in the dialFCS extract (lane 2) and the 40 µM L-carnitine extract were similar to those in the normal extracts, signifying a stronger signal than after appending 80 µM cold ALC. Appending 120 µM ALC to the 80 µM L-carnitine resulted in a weakening of the signal above the 130 kDa marker, compared to the band shift assay with 80 µM ALC, but also resulted in only that one band (lane 4).

A compilation of all observed effects in the band shift analyses of GRα is given in table 6.

Table 6: Signal intensities and migration patterns of the mobility shift bands for GRα.

GRα							
		Band size [kDa]					
Appended ALC	**Nuclear Extract**	~150	130	~110	95	72	55
No ALC	N		*				
	Dial	*	**				
	40	*	***				
	80		*				
20 µM	N	**		***			
	Dial						
	40	*		*			
	80			*			
40 µM	N	****		****			
	Dial	****		****			
	40	***		***			
	80	**		***			
80 µM	N		*				
	Dial		**				
	40		*				
	80		****				
120 µM	N		****				
	Dial		****				
	40		****				
	80		***				

Legend to table 6: N – protein extract from cells grown in normal cell culture medium (DMEM and 10% FCS); D – protein extract from cells kept in dialysed medium (DMEM and 10% dialysed FCS); 40 – protein extract from cells grown in medium with 10% dialysed FCS and supplemented with 40 µM L-carnitine; 80 – protein extract from cells cultivated in medium with 10% dialysed FCS and supplemented with 80 µM L-carnitine; * - very weak band; ** - weak band; *** - strong band; **** - very strong band.

3.4.3. Analysis of the putative PPAR binding site

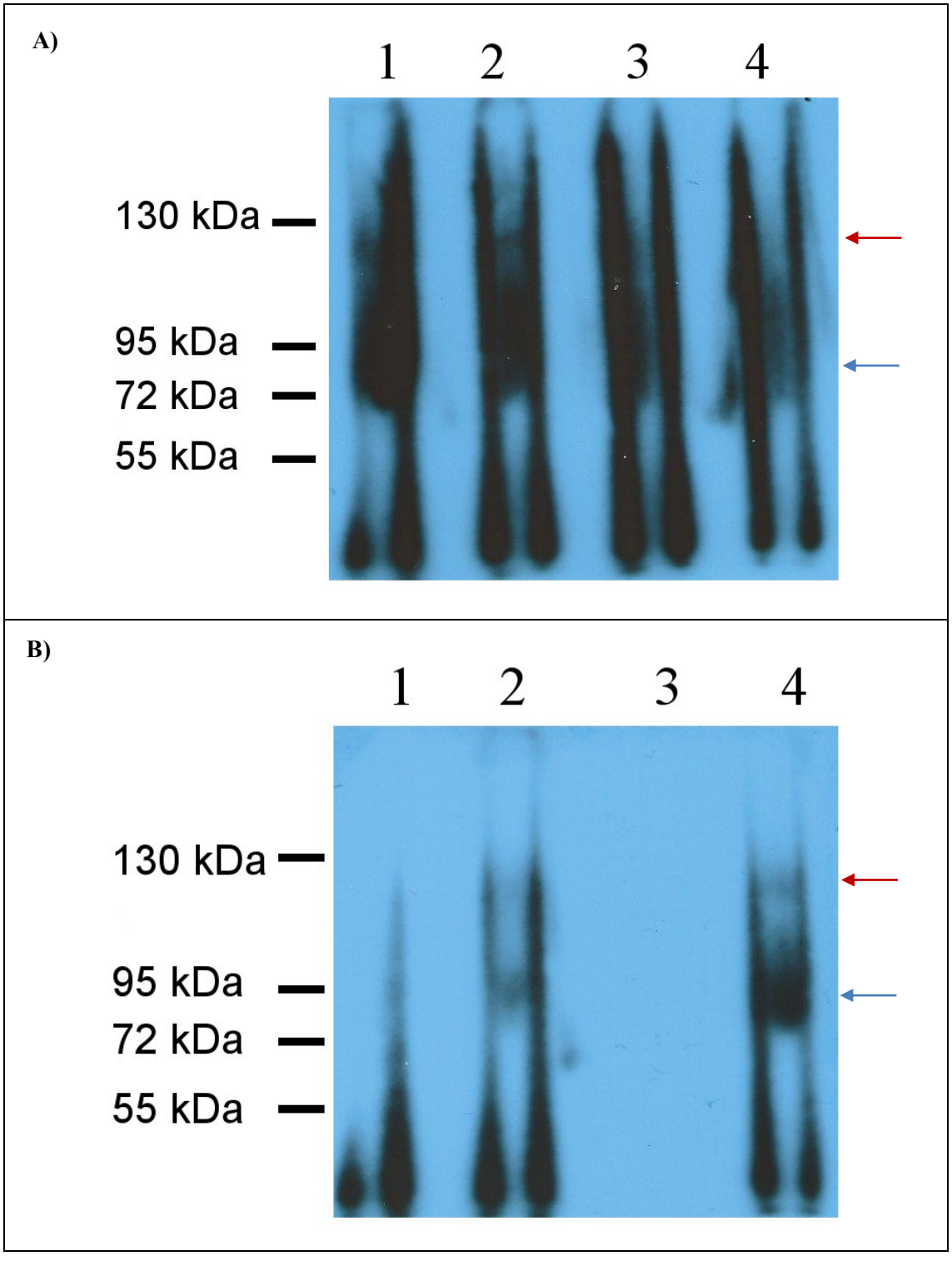

C)

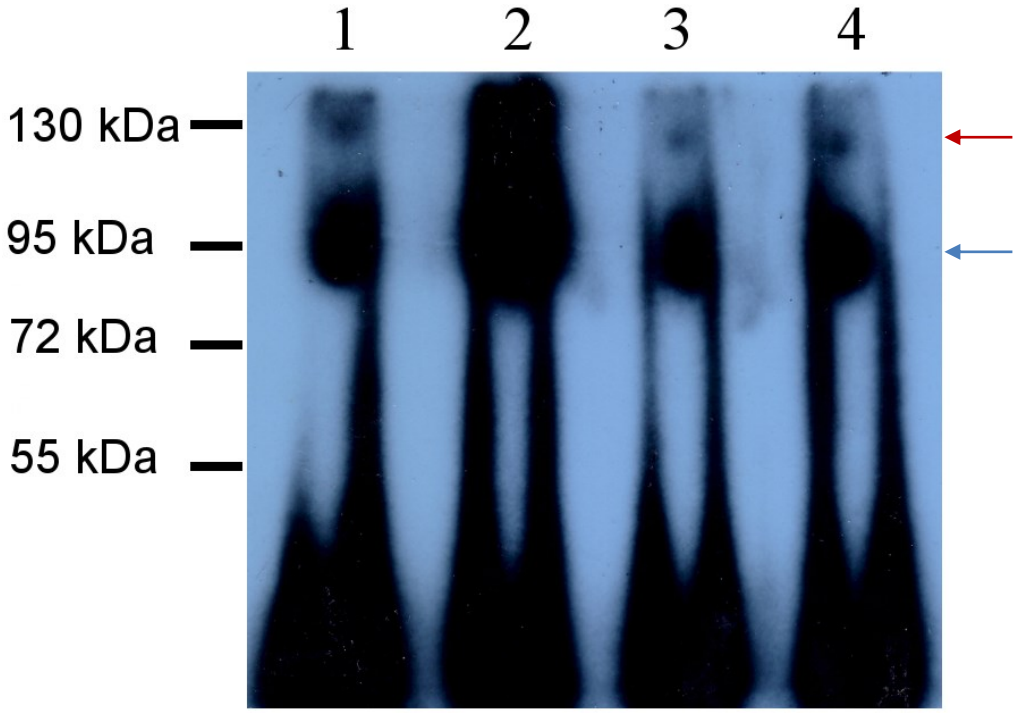
1
2
3
4
130 kDa
95 kDa
72 kDa
55 kDa

D)

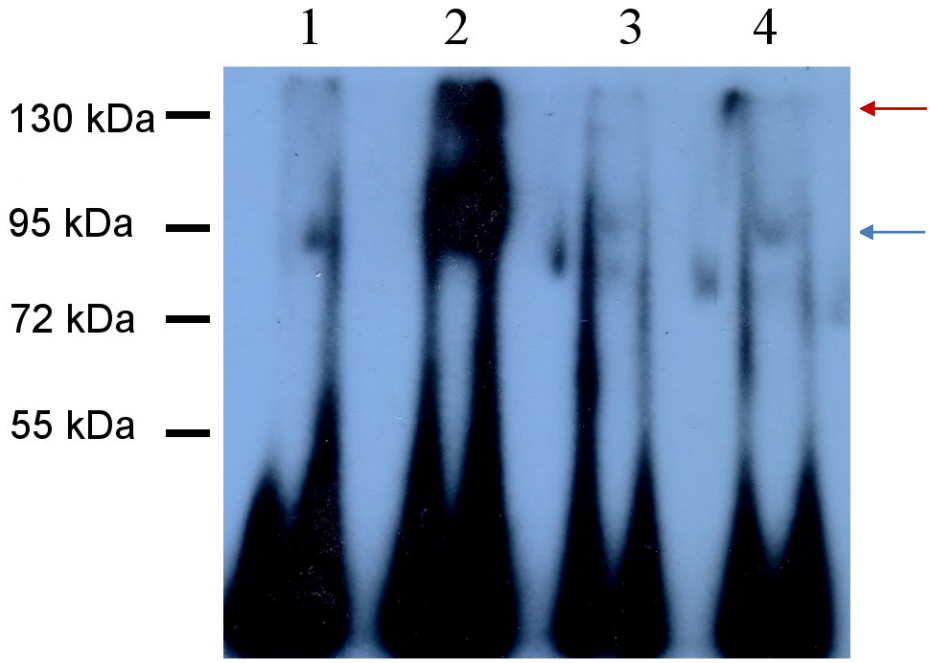
1
2
3
4
130 kDa
95 kDa
72 kDa
55 kDa

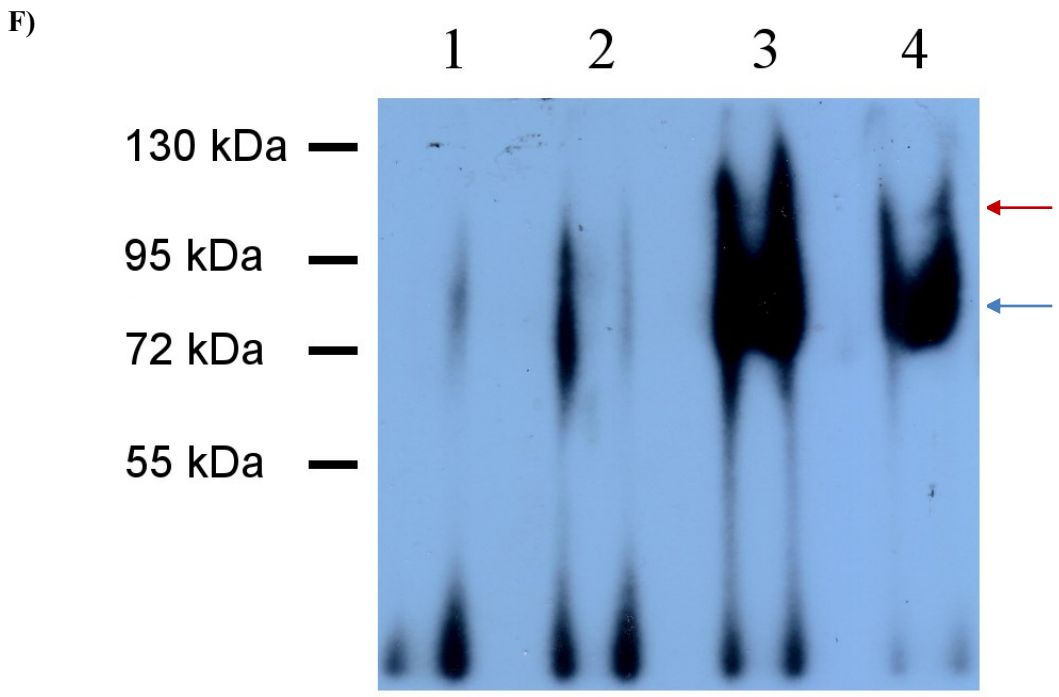

A) Band shift analysis without ALC

B) Band shift analysis with 20 µM ALC

C) Band shift analysis with 40 µM ALC

D) Band shift analysis with 80 µM ALC

E) Band shift analysis with 120 µM ALC

Lanes:

1: DMEM + 10% FCS

2: DMEM + 10% dialysed FCS (dialFCS)

3: dialFCS + 40 µM L-carnitine

4: dialFCS + 80 µM L-carnitine

Figure 44: Band shift analysis of the putative PPAR binding site with different concentrations of added acetyl-L-carnitine (ALC).

The results of the RARRXR band shift analysis presented in fig. 44 are:

A) In the mobility shift assay where unlabelled acetyl-L-carnitine (ALC) was omitted from the reaction mix, in all lanes at least one band at below the 95 kDa marker was visible, with a possible upper shift band slightly below the 130 kDa marker.

B) Appending of 20 µM unlabelled ALC resulted in no changes, showing an upper and a lower shift bands in the lanes with the dialyzed sample and the 80 µM sample, similar to (fig. 44A). In the lane loaded with a normal nuclear extract and the lane with a 40 µM extract no band shifts were visible.

C) Appending of 40 µM unlabelled ALC to the reaction mix resulted in the appearance of the same lower and upper shift bands as in the first two cases (A and B), but with a stronger signal than in the mobility shift assay with 20 µM ALC. However, the strongest signal could be observed in the lane where a nuclear extract isolated from cells cultivated in dialFCS was loaded (lane 2).

D) Appending of 80 µM unlabelled ALC to the reaction mix resulted in a faint band migrating at the 95 kDa marker generated in those lanes where nuclear extracts from cells kept in normal serum (lane 1) and supplemented with 40 µM L-carnitine (lane 3) and 80 µM L-carnitine (lane 4) were separated. The band shift signal turned out to be the strongest in the lane where an extract from cells cultivated with dialFCS (lane 2) were loaded, as well as in the analysis with 40 µM ALC was appended (fig. 44C). In this case, a new upper shift band with a size of 130 kDa could be resolved.

E) Appending of 120 µM unlabelled ALC to the reaction mix resulted in no bands in the lanes with the normal (lane 1) and dialFCS (lane 2) extracts, and the disappearance of the 130 kDa band in all lanes. In the lane with the 40 µM L-carnitine extract (lane 3), a large signal could be detected, which contained an upper shift band in the size range of the 95 kDa marker and a lower shift band slightly above the 72 kDa marker. In the lane with the 80 µM L-carnitine extract (lane 4), the signal was weaker than in the previous lane, containing at least the lower shift band.

A compilation of all observed effects in the band shift analyses of PPAR is given in table 7.

Table 7: Signal intensities and migration patterns of the mobility shift bands for PPAR.

PPAR				
		Band size [kDa]		
Appended ALC	**Nuclear Extract**	130	95	72
No ALC	N	***	****	
	Dial	**	***	
	40	*	**	
	80	*		
20 µM	N			
	Dial	*	*	
	40			
	80	*	**	
40 µM	N	**	****	
	Dial	****	****	
	40	*	***	
	80	*	***	
80 µM	N	*	*	
	Dial	***	****	
	40	*	*	
	80	*	*	
120 µM	N			
	Dial		*	
	40		*	****
	80		*	***

Legend to table 7: N – protein extract from cells grown in normal cell culture medium (DMEM and 10% FCS); D – protein extract from cells kept in dialysed medium (DMEM and 10% dialysed FCS); 40 – protein extract from cells grown in medium with 10% dialysed FCS and supplemented with 40 µM L-carnitine; 80 – protein extract from cells cultivated in medium with 10% dialysed FCS and supplemented with 80 µM L-carnitine; * - very weak band; ** - weak band; *** - strong band; **** - very strong band.

3.4.4. Analysis of the putative Hepatocyte Nuclear Factor 4 (HNF4) binding site

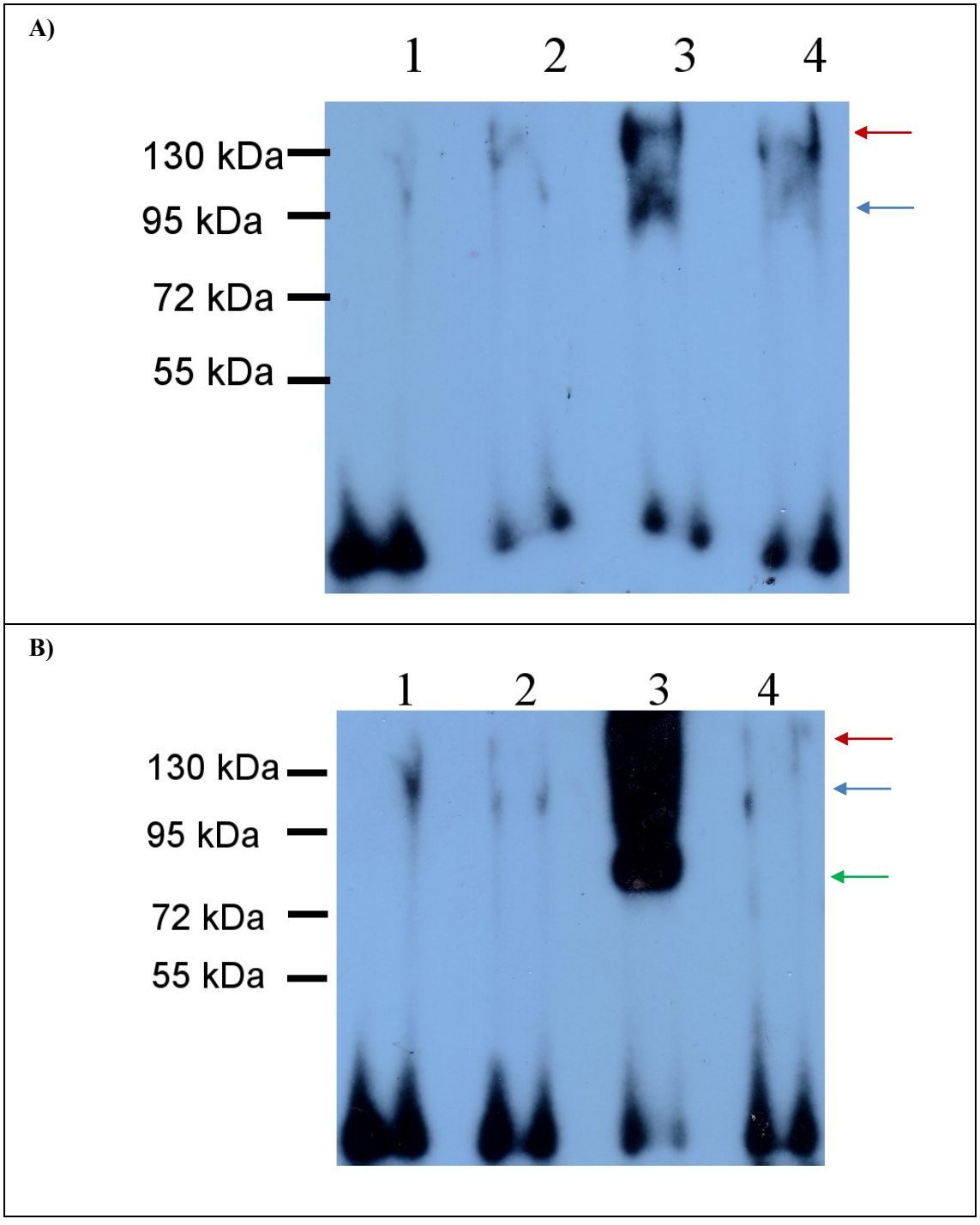

C)

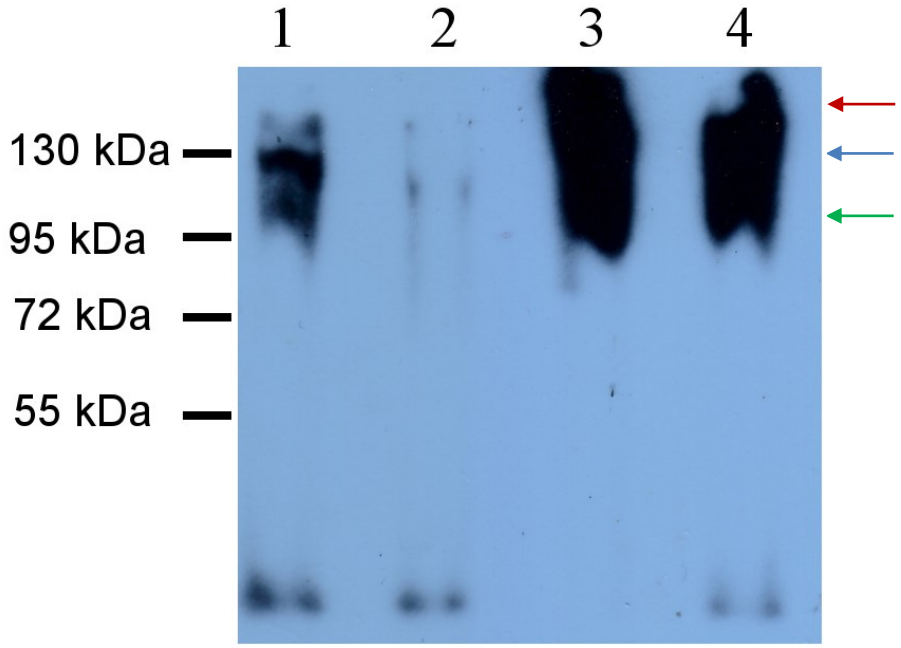
1
2
3
4
130 kDa
95 kDa
72 kDa
55 kDa

D)

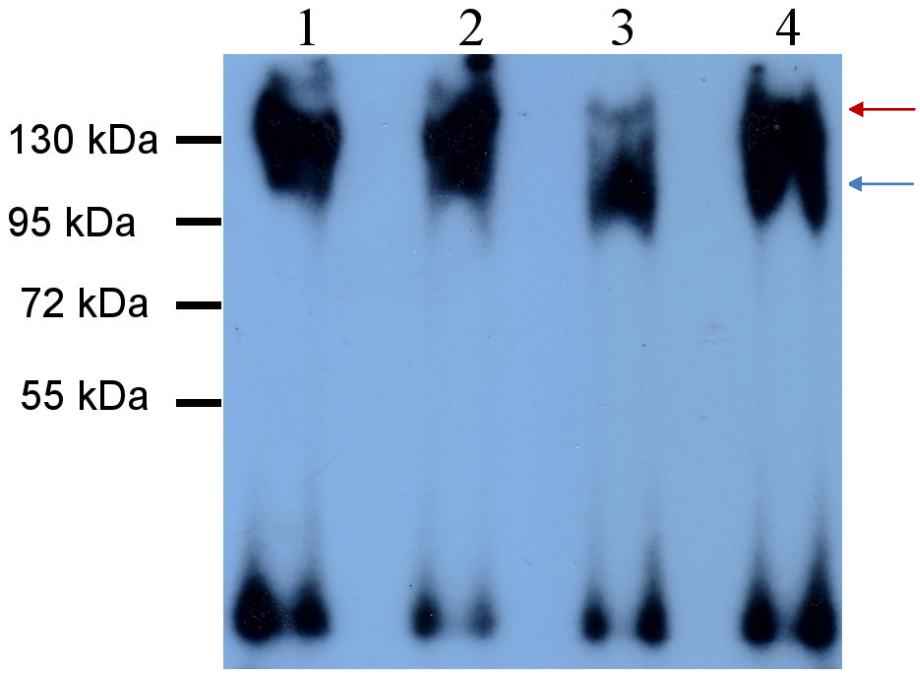
1
2
3
4
130 kDa
95 kDa
72 kDa
55 kDa

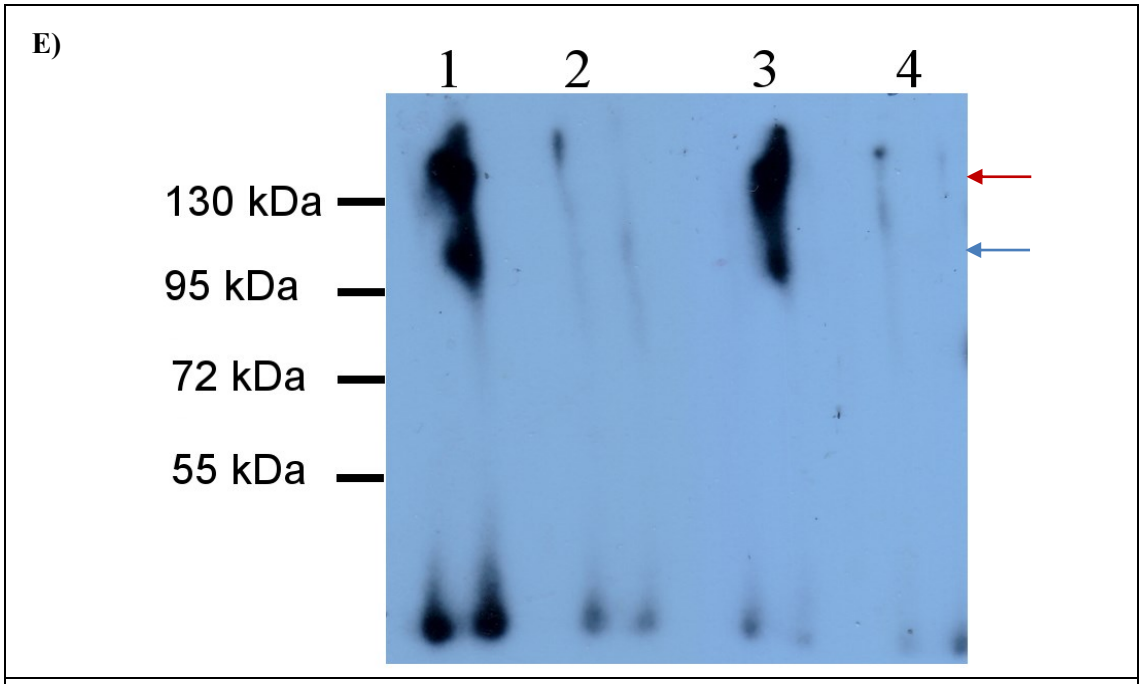

A) Band shift analysis without ALC

B) Band shift analysis with 20 µM ALC

C) Band shift analysis with 40 µM ALC

D) Band shift analysis with 80 µM ALC

E) Band shift analysis with 120 µM ALC

Lanes:

1: DMEM + 10% FCS

2: DMEM + 10% dialysed FCS (dialFCS)

3: dialFCS + 40 µM L-carnitine

4: dialFCS + 80 µM L-carnitine

Figure 45: Band shift analysis of the putative HNF4 binding site with different concentrations of added acetyl-L-carnitine (ALC).

The results of the RARRXR band shift analysis presented in fig. 45 are:

A) In the experiment presented in panel A, unlabelled acetyl-L-carnitine (ALC) was omitted from the reaction mix. The band shift assay resulted in a possible faint band at the size range of 130 kDa when using the normal extract (lane 1) and a faint but noticeable band of the same size when loading the dialFCS extract (lane 2). In the lane where extracts from cells cultivated with 40 µM L-carnitine were analysed, two bands

could be observed. An upper shift band migrating with a size of about 150 kDa and a lower shift band at the 95 kDa marker (lane 3). Analysis of the extracts from cells cultivated with 80 µM L-carnitine resulted in similar bands as those in lane 3, but with a fainter appearance (lane 4).

B) Addition of 20 µM unlabelled ALC to the reaction mix resulted in a strengthening of the signal in the lane with the normal extract, but still did not result in a clear band (lane 1), while the original 130 kDa band in the lane with the dialFCS extract disappeared (lane 2). A strong band shift signal was obtained in lane 3 with the 40 µM L-carnitine extract, giving one band above 130 kDa, one band between 95 kDa and 130 kDa and one band between 72 kDa and 95 kDa (lane 3). Appending of 20 µM unlabelled ALC led to the disappearance of both bands in the lane with the 80 µM L-carnitine extract.

C) Addition of 40 µM unlabelled ALC to the reaction mix resulted in a distinct shift band at the 95 kDa and 130 kDa markers in the lane with the normal extract (lane 1) and had no effect in the lane with the dialFCS extract (lane 2). The signal was intensified in the lane with the 40 µM L-carnitine extract, showing two bands, one at the 95 kDa marker and one at the 130 kDa marker, and a possible band above the 130 kDa marker, but which cannot be clearly determined due to signal strength (lane 3). Appending of 20 µM unlabelled ALC to the 80 µM L-carnitine extract resulted to similar bands than in the lane 40 µM L-carnitine lane (lane 4).

D) Appending of 80 µM unlabelled ALC to the reaction mix resulted in the appearance of a distinct shift band at the 130 kDa marker in the lane with the normal extract (lane 1) compared to previous analyses without unlabelled ALC. A similar effect could be observed in lane 2 where the dialFCS extract was loaded, with the appearance of a band shift at the 130 kDa marker. In the lane with the 40 µM L-carnitine extract, the original upper shift band weakened, while the 95 kDa band increased in signal strength (lane 3). Addition of 80 µM unlabelled ALC to the 80 µM L-carnitine extract resulted in an augmentation of the signal, with an intensification of the 130 kDa band (lane 4).

E) Appending of 120 µM unlabelled ALC to the reaction mix resulted in the upshift of the 130 kDa band and the appearance of a second band between the 95 kDa and 130 kDa markers in the lane with the normal extract (lane 1). In contrast, no bands were visible in the lane where the extract from cells grown with dialFCS was separated (lane 2). The lane with the 40 µM L-carnitine extract (lane 3) produced a result as in lane 1, whereas the shift bands in the lane with the 80 µM L-carnitine extract completely disappeared after the addition of 120 µM unlabelled ALC (lane 4).

A compilation of all observed effects in the band shift analyses of HNF4 is given in table 8.

Table 8: Signal intensities and migration patterns of the mobility shift bands for HNF4

HNF4							
		Band size [kDa]					
Appended ALC	**Nuclear Extract**	~150	130	~110	95	~80	72
No ALC	N						
	Dial		*				
	40		*		**		
	80		*		*		
20 µM	N		*				
	Dial						
	40	****		****		****	
	80						
40 µM	N		***		*		
	Dial						
	40	****		****	****		
	80	**		****	****		
80 µM	N	***					
	Dial	***					
	40	**		**			
	80	***		**			
120 µM	N	**		**			
	Dial						
	40	**		*			
	80						

Legend to table 8: N – protein extract from cells grown in normal cell culture medium (DMEM and 10% FCS); D – protein extract from cells kept in dialysed medium (DMEM and 10% dialysed FCS); 40 – protein extract from cells grown in medium with 10% dialysed FCS and supplemented with 40 µM L-carnitine; 80 – protein extract from cells cultivated in medium with 10% dialysed FCS and supplemented with 80 µM L-carnitine; * - very weak band; ** - weak band; *** - strong band; **** - very strong band.

3.5. Analysis of the effect of varying concentrations of SDS on the binding of the oligonucleotides to the CrAT promoter

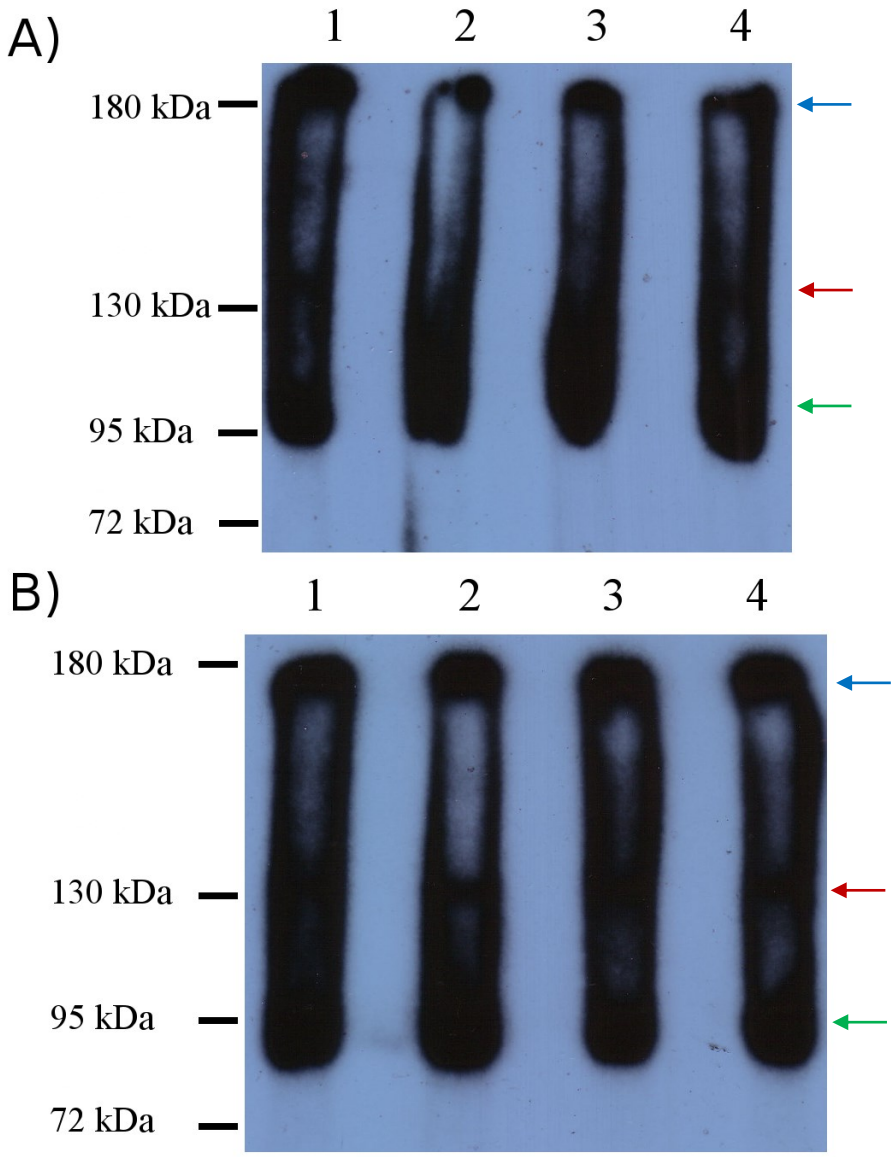

Figure 46: Effect of varying SDS concentrations on the binding of the ^{32}P-labelled RARRXR oligonucleotides to the nuclear extracts in the presence of acetyl-L-carnitine. A) Lane 1: no SDS; lane 2: 0.2% SDS; lane 3: 0.1% SDS; lane 4: 0.05% SDS. B) Lane 1: 0.001% SDS; lane 2: 0.005% SDS; lane 3: 0.01% SDS; lane 4: 0.02% SDS.

To better observe the interaction of acetyl-L-carnitine with the CRAT promoter and the oligonucleotides, increasing concentrations of SDS were added to the reaction mix (hRARRXR oligonucleotide, nuclear proteins from cells supplemented with 40 μM L-

carnitine and the addition of 80 µM acetyl-L-carnitine) before running the EMSA, while one reaction mix was loaded without SDS as control (see fig. 46).

In the test lane where no SDS was added to the slot, three distinct shift bands could be observed after running the gel: an upper shift band with a weight of about 260 kDa, a middle band with a weight of 180 kDa and a lower shift band with a weight of 130 kDa. In the lane where a high concentration of SDS (0.2%) was appended to the mix (lane A2), the middle band disappeared and the upper shift band was weakened, while the lower shift band remained unchanged. The middle band did not reappear in the lane with 0.1% SDS (lane A3), but could be observed in the lane with 0.05% SDS (lane A4), although it was still very faint. A stronger signal was achieved again in the lane with 0.02% SDS (lane B4), after which there was minimal or no change in the strength of this band when lowering the concentrations. These results indicate that the binding of the oligonucleotide in the presence of acetyl-L-carnitine may be non-covalent in nature.

3.6. Supershift assay

After the electrophoretic mobility shift assays, the putative RARRXR and PPAR binding sites were analysed by additional supershift assays. Before starting the assays, probe assays were performed to determine which extract to use and if antibodies should be added to the reaction mix before or after incubation (Materials and methods: Electrophoretic mobility shift assay and supershift assay). By subsequent electrophoretic super shift assays it was determined that the extracts should be obtained from WRL68 cells cultivated in DMEM with 10% dialysed FCS and supplemented with 40 µM L-carnitine before extraction and that the antibodies better ought to be added prior the incubation.

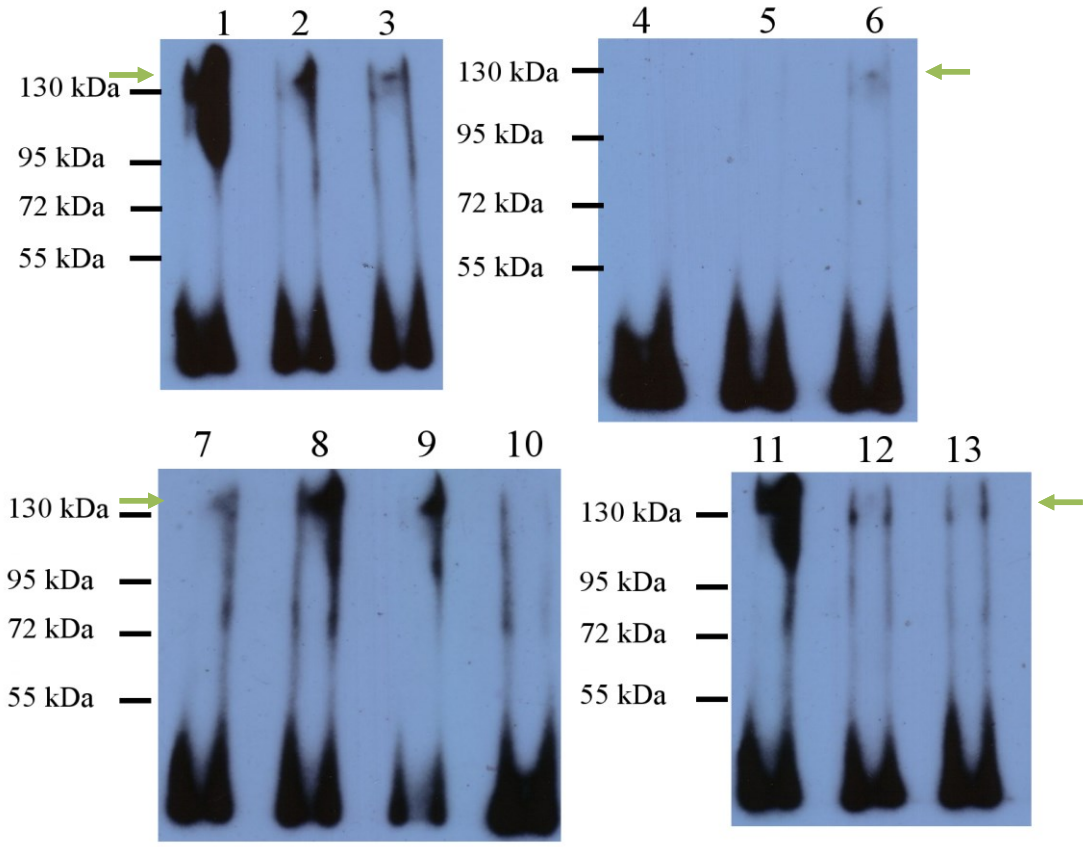

Figure 47: Supershift analysis using the hRARRXR oligonucleotide. Legend: lane 1: no antibody; lane 2: RXRα/β/γ (sc-46659); lane 3: PPARα (sc-398394); lane 4: RXRβ_1 (sc-376301); lane 5: RXRβ_2 (sc-56869); lane 6: RARγ (sc-398065); lane 7: no antibody; lane 8: PPARγ (sc-7273); lane 9: LXRα/β (sc-377260); lane 10: RXRγ (sc-365252); lane 11: FXR (sc-25309); lane 12: FXR1 (sc-374148); lane 13: FXR2 (sc-32266).

The original band shift assay for hRARRXR with the nuclear extract from 40 µM L-carnitine-supplemented cells resulted in a band near the 130 kDa marker, which could also be seen in the supershift assay in the lane where antibodies were omitted (fig. 47, lane 1). The addition of the RXRα/β/γ (fig. 47, lane 2) and PPARα monoclonal antibody (fig. 47, lane 3) resulted in the weakening of the band. In the lanes with the added RXRβ_1, RXRβ_2 and RARγ antibodies (fig. 47, lanes 4-6), no bands could be resolved. The repetition of the mobility shift assay omitting the antibodies resulted in a weaker band than the first one (fig. 47, lane 7), which could probably be the result of degraded proteins. Compared to lane 1, the addition of PPARγ (fig. 47, lane 8) and LXRα/β antibody (fig. 47, lane 9) resulted in the weakening of the band, while the band fig. disappeared after the addition of RXRγ (fig. 47, lane 10). While FXR (fig. 47, lane 11) had no effect on the complex in our experiment, the addition of either FXR1 (fig. 47, lane 12) or FXR2 (fig. 47, lane 13) resulted in the complete disappearance of the shift complex band.

4. Discussion

The goals of our work positioned in two major directions: the first aim was analysing the time-dependent effect of L-carnitine supplementation on the gene expression of key-members of signalling pathways. The first, the mTOR pathway, is one of the major amino acid sensing pathways in the body, and we wanted to analyse if carnitine is acting on the transcript levels of the Rheb, SREBP-1, PGC-1α and GCN2 genes. The other genes we tested were Rac1, which is involved in the release of insulin through GLUT4 translocation [39] into the bloodstream upon elevated blood glucose levels, and two members of the SLC superfamily, SLC22A4 (OCTN1) and SLC35F2. We measured how L-carnitine affects these genes under hyperglycaemic, hyperglycaemic + hyperlipidaemic and normoglycaemic conditions. The second aim was the analysis of the human CRAT promoter. We wanted to verify the presence of transcription factor binding sites, predicted by theoretical promoter analysis, which could influence the transcriptional activity of the gene. We also wanted to see if and how acetyl-L-carnitine, one of the most obvious biological esters of L-carnitine, can interact with the transcription factor complexes on the CRAT promoter.

OCTN1 responded positively to L-carnitine supplementation. The first expression level peak was reached in cells that were supplemented with 40 μM L-carnitine for 4 hours. Supplementation with 80 μM was also successful, but induction was significantly less effective at shorter supplementation times and took at least 24 hours to exceed levels reached with 40 μM L-carnitine supplementation. These findings confirm that OCTN1 responds to L-carnitine and can almost immediately act as its membrane transporter, which corresponds with previous studies [100] and suggests that it responds most effectively to short-term supplementation of physiological L-carnitine levels (40 μM) or long-term supplementation of higher amounts. In cells that were treated with cholesterol, L-carnitine supplementation led to only small changes in gene expression in cells that were treated with 0.65 mM and 1.3 mM cholesterol, but was able to significantly lower OCTN1 steady state mRNA in cells treated with 2.6 mM of cholesterol (from 3.5×10^9 down to 130-fold relative transcript amount). It has to be stated that the measured OCTN1 steady state mRNA level of OCTN1 (supported by three independent measurements) in these cells gains levels that are artificially high, propelled to supra-physiological levels by high cholesterol amounts. But the results definitely point towards a very important metabolic fact: cholesterol itself can exert a heavy impact on the transcriptome, in addition L-carnitine is able to palliate the OCTN1 transcripts almost back to normal levels. Based on these results it is very tempting to conclude that L-

carnitine is important in lowering lipids, which by the way was documented by Seccombe *et al.* [101].

L-carnitine was also able to increase steady state mRNA levels of SLC35F2. Although the reduction of transcript amounts in dialysed FCS medium was minimal, supplementation of 40 µM L-carnitine doubled mRNA-expression compared to normal values. Supplementation of 80 µM L-carnitine, while also raising levels above normal, was less effective than 40 µM, with the peak effect measured after 24 hours. In cholesterol-treated cells, carnitine was only able to lower expression in case of treatment with 0.65 mM cholesterol and even raised them in cells that were exposed to 1.30 mM cholesterol, while the values for 2.6 mM cholesterol could not be evaluated because no specific transcripts could be measured by real-time RT-PCR in the sample without L-carnitine. Therefore, one can conclude that in the experiment with 2.6 mM cholesterol SLC35F2 specific transcripts are not produced anymore, due to the high cholesterol levels, but they can be re-induced by L-carnitine. This is another proof for its biological importance and demonstrates that even brief exposure to physiological concentrations of L-carnitine is sufficient to convert metabolic tilts. As SLC35F2 has not been studied as much as some other genes, these results could offer a basis for further research, while once again confirming the ability of L-carnitine to lower the effect of elevated cholesterol levels [101].

Rac1 in liver cells did not respond to the supplementation of L-carnitine under hyperglycaemic conditions, with all measured transcript levels being lower than normal values and even lower than in cells kept in dialysed FCS. The response was stronger under normoglycaemic conditions, where 15 hours of supplementation of L-carnitine could raise steady state mRNA levels above those in unsupplemented cells, reaching close to normal levels. Interestingly, addition of 0.65 mM and 1.30 mM cholesterol lowered Rac1 steady state mRNA levels below normal levels and was even further lowered by L-carnitine. In contrast to this, there was an extreme increase in gene expression after 24 hours of treatment with 2.6 mM cholesterol, which could be brought down to almost normal levels with the supplementation of 80 µM L-carnitine. This relationship opens another interesting topic for future research and it would be worth evaluating the influence of L-carnitine on Rac1 in muscles cells, where it has been shown to possess an important role in preventing insulin intolerance [39].

Steady state mRNA levels of Rheb could not be induced with supplementation of 40 µM L-carnitine for 4 hours, but increased after 4 hours of supplementation of 80 µM and reached their peak levels after 48 hours. L-carnitine was able to lower Rheb levels in

cells that were treated with lower amounts of cholesterol (0.65 and 1.30 mM), but the strongest effect could be observed in cells that were treated with 2.6 mM cholesterol. While Rheb that is already present in cells cannot be induced by short-term supplementation of physiological concentrations of L-carnitine, it responds well to supra-physiological concentrations, indicating that high levels of L-carnitine could act as a transcriptional activator of this gene and can indirectly upregulate mTORC1 activation. Rheb also responds markedly to elevated lipid concentrations, which again offers an interesting point for forthcoming research.

GCN2 exhibits a weaker response to L-carnitine addition, but not to deprivation. GCN2 transcript levels rose in cells kept in medium with dialysed FCS, they decreased subsequently with supplementation of 40 µM L-carnitine and short-term supplementation of 80 µM L-carnitine (4 hours and 15 hours). Interestingly the transcript levels increased again with longer L-carnitine exposure after 24 hours and peaked after 48 hours. In cholesterol-treated cells, supplementation of 80 µM L-carnitine caused minimal changes when 0.65 mM cholesterol was added, while it lowered steady state mRNA levels in cells supplemented with 1.30 mM cholesterol. The strongest effect could once again be observed in cells that were exposed to 2.6 mM cholesterol for 24 hours, where supplementation of L-carnitine reduced GCN2 mRNA levels 8-fold. The increase of these transcripts in cells cultivated in dialysed FCS medium corresponds with the fact that GCN2 is activated in the absence of amino acids [20, 23]. The initial lowering of its mRNA levels after carnitine supplementation indicates that L-carnitine is able to modulate members of the mTOR1 pathway differently. Thus, regulating mTORC1 through the activation of one of its members, while also preventing activation of the GCN2 pathway.

PGC-1α steady state mRNA levels increased after supplementation of 40 µM L-carnitine for 4 hours and 80 µM L-carnitine for 48 hours. The results are somehow statistically hampered because of the undesired significance value of $p<0.5$. The low significance values prevailed in the cholesterol supplementation experiments. A possible reason for the high fluctuation in steady state mRNA levels measured from the same cells could be cell type specific low mRNA expression levels of the PGC-1α gene. Since fasting is known to promote PGC-1α expression [50], an increase above normal levels would have been expected in the cells kept in dialysed FCS containing medium.

Levels of SREBP-1 steady state mRNA increased in the dialysed medium compared to the levels seen in the normal medium. These transcript levels were further raised by supplementation of 40 µM L-carnitine. Supplementation of 80 µM L-carnitine lowered gene expression in the beginning, but induced it after 24 hours. SREBP-1 levels in

cholesterol-treated cells were lower than normal in the case of 0.65 mM and 1.30 mM cholesterol and were further lowered by the addition of L-carnitine. L-carnitine was also able to successfully lower the increased mRNA levels that were measured in cells that were treated with 2.6 mM cholesterol. This indicates that SREBP-1 responds to carnitine differently, depending on the amount of L-carnitine and the presence of cholesterol, probably because of the “carnitine-effect” on mTORC1, which is the positive regulator of SREBP1 [25]. The results show a decrease in SREBP-1c steady state mRNA levels after cholesterol supplementation. While this is in contrast to studies performed with animal models, where it was shown that cholesterol increases SREBP-1 mRNA in the liver of rats [102] or that the expression SREBP-1c in the intestine of hamsters was lowered upon cholesterol deficiency [103], these studies were performed on animals and used other methods to obtain their results. Another possible reason for this discrepancy could be fact that cell culture cells react differently to cells studied in *in vivo* systems [104], as growth conditions in cell cultures are optimised for better cell growth, which can result in changes in gene expression.

In contrast to the above described effects of L-carnitine on steady state mRNA levels of specific genes under hyperglycaemic conditions, the “carnitine-effect” was much weaker in cells that were grown in a normoglycaemic medium. Steady state mRNA levels of all genes alleviated when grown in the dialysed medium, and L-carnitine was only able induce gene expression for SLC35F2, PGC-1α and SREBP1. SLC35F2 expression was restored by supplementation of 80 µM for 15 hours and by supplementation for 48 hours with raised glucose levels, while SREBP1 responded positively to supplementation of 40 µM L-carnitine for 4 hours, both under normoglycaemic and in hyperglycaemic conditions. An interesting effect could be observed when glucose levels were artificially raised to hyperglycaemic conditions. While SLC35F2 responded positively to the additional glucose and expression levels were slightly higher than in cells that were only supplemented with L-carnitine, for SREBP1 glucose slightly lowered gene expression in most treatments. In the case of PGC-1α, the steady state mRNA levels slowly increased with the time of the supplementation of 80 µM L-carnitine, with the effect being strengthened by increasing the glucose levels in the medium. The markedly increased steady state transcript levels, measured after 15 hours, could indicate that the carnitine-effect is most pronounced at this point. But when carnitine gets metabolised with time, a return to standard low expression values after 24 hours of treatment takes place. For all other genes, supplementation of L-carnitine was unable to effectively reinduce gene expression, with one exception in the case of Rac1. Here, supplementation of 80 µM L-carnitine for 15 hours almost restored gene expression to normal values. These results

show that the studied genes exhibit weaker expression levels under normoglycaemic conditions *in vitro*, and supplementation of L-carnitine is able to exert a stronger effect under hyperglycaemic conditions.

The effect of L-carnitine on different genes on the RNA level was already tested in our lab by a Chip Screen analysis, where it was shown that L-carnitine as a nutrigenomic metabolite is also able to influence various signalling pathways [105]. Therefore, it was a logical decision to measure the impact of L-carnitine on nuclear receptors by a Cignal receptor pathway array, carrying a test format for 10 specific nuclear receptor pathways [106]. For us it was important to see how L-carnitine affects gene expression on protein level measured by a completely different analytical approach. Out of the 10 pathways, the oestrogen, retinoic acid, vitamin D, retinoid X and HNF4 pathways were stimulated by L-carnitine supplementation, while it had little or no effect on the androgen, PPAR, glucocorticoid, progesterone and liver X pathways. The upregulation of the HNF4 pathway shown in the assay implies an interaction between L-carnitine and HNF4, which would correspond with the function of HNF4 as a regulator of lipid metabolism [77]. The best results were achieved with supra-physiological concentrations at 80 µM L-carnitine, but unphysiologically high L-carnitine concentrations had a weaker effect, possibly resulting in inhibition. Retinoid X and retinoic acid receptors play an important role in the regulation of genes by forming heterodimers with other nuclear receptors [81], indicating that L-carnitine is able to influence the expression levels of other genes besides contributing to beta-oxidation. While the highest measured retinoid X signalling levels occurred in cells grown in dialysed FCS, supplementation of L-carnitine lowered these values, although they were still higher as in unsupplemented cells in “normal” medium. These results also indicate that L-carnitine did not increase the activity of the progesterone pathway, but even lowered it under normal values when supplemented with concentrations below 120 µM. This outcome is in accordance with another study, which provided proof that L-carnitine has no effect on the secretion of progesterone in cultured follicles [107]. L-carnitine was shown to upregulate the oestrogen pathway, implying that supra-physiological concentrations of L-carnitine could affect female sexual development, which heavily argues for additional research. While L-carnitine did not have an effect on the androgen pathway in our study, another study did show that long-term supplementation of L-carnitine increase androgen receptor levels in muscle cells [108]. This suggests that the short supplemental regimens, used in our experimental setup, should be expanded more than 48 hours [109]. Previously, it was also shown that in other cases cells respond differently to L-carnitine supplementation regimens. The lack of effect on the androgen pathway also corresponds with the research of Fenkci *et*

al. [110], who did show that serum levels of L-carnitine may drop during hyperandrogenism [110]. We expected that the PPAR and glucocorticoid pathways would respond more pronounced to supplementation, as PPARα was shown to be upregulated by carnitine [66] and it was confirmed that PPARα has a major role in regulating carnitine homeostasis [111], while it was also shown that high concentrations of L-carnitine can activate glucocorticoid receptors [85].

The electrophoretic mobility shift assays confirmed the presence of the RARβ/RARα/RXR, PPARα, GRα and HNF4α binding sites, despite the inherent instability of the protein extracts, where proteins get degraded during incubation. This we could observe even in those assays that were performed under similar conditions. Results could slightly differ especially when extracts were thawed repeatedly. Altogether, they clearly showed that acetyl-L-carnitine is able to bind to the different protein complexes, indicating a role in their regulation. Some of the bands generated by shift complexes in many experiments had a distinct “U” shape, which could have been caused by biochemical instability or probably by a technical background: prolonged loading times, increased diffusion during electrophoresis, spaces between the gel and the glass plates during the polymerisation of the stacking gel. There are several reasons that could have enabled the samples to diffuse and migrate out of the gel.

The most obvious effect occurred when the RARβ/RARα/RXR binding site was investigated. A new protein complex band appeared after the addition of 20 µM acyl-L-carnitine, resulting in finally three shifted bands. This new band slightly diminished and migrated faster at concentrations of 80 µM acetyl-L-carnitine and higher, indicating that supra-physiological acetyl-L-carnitine concentrations act repressive on distinct transcription factor complexes on the CRAT promoter. Another interesting aspect to note is that this band was strongest when the used nuclear extracts were isolated from cells, grown already with 40 µM and 80 µM L-carnitine, showing that L-carnitine supplementation is capable of restoring gene expression of this factor, or somehow pre-establishing it. The correlation of the intensity of this signal in cells supplemented with L-carnitine could be a possible consequence of the upregulation of other factors, needed for carnitine homeostasis, such as PPAR, which forms heterodimers with RXR [84].

Analysis of the GRα binding site revealed that increasing concentrations of acetyl-L-carnitine may have a negative impact on the binding of proteins to this oligonucleotide. There was a noticeable supershift in the gel where no acetyl-L-carnitine was added to the samples, while addition of 20 µM and 40 µM acetyl-L-carnitine resulted in the downshift of the bands, indicating that it could have blocked another factor to be part of

the whole complex, resulting in faster migrating bands. The upper shift band was the strongest in the sample supplemented with 40 µM L-carnitine, which could imply a role in the control of GRα expression. Increasing the acetyl-L-carnitine concentration further weakened this interaction, resulting in only one band under all conditions. It is also noticeable that while acetyl-L-carnitine weakened the signals in the dialFCS and carnitine-supplemented samples, it generally strengthened the signals in the normal sample.

The analysis of the PPARα was less conclusive. There were two possible bands in the mobility shift assay without appended acetyl-L-carnitine, an upper shift band at 130 kDa and a lower shift band between 95 kDa and 72 kDa. These two bands can also be resolved on the gel where 20 µM ALC was appended to the reaction mix. Especially in this case the lanes with the normal and 40 µM L-carnitine extracts were empty. The presence of two bands could be resolved in both samples where either 40 µM or 80 µM acetyl-L-carnitine was added to the reaction mix. In the analysis where 120 µM ALC was appended to the extracts, no bands were detectable in the lanes where normal or dialysed samples were loaded. The bands in the lanes where the 40 µM and 80 µM extracts were analysed a downwards shift of the promoter factor complex occurred, with the upper shift band between the 130 kDa and 95 kDa markers and the lower shift band closer to the 72 kDa marker. These bands migrated faster compared to the other analyses for PPAR, where the upper shift bands had a weight of 130 kDa and the lower band a weight of 95 kDa. Interestingly, in both the 40 µM and 80 µM acetyl-L-carnitine-appended cases the most pronounced band shifts emerged in the extract from cells grown in dialFCS. These results indicate that the PPARα binding site in the CRAT promoter is present and is influenced by high concentrations of acetyl-L-carnitine, which seems to interfere with the binding of some factor to the complex, rendering it smaller. The relationship between acetyl-L-carnitine and PPARα would require further analysis, probably with the optimization of the methods and preparations of the nuclear extracts especially for this transcription factor.

In the analysis of HNF4α there was a noticeable change between the gel without acetyl-L-carnitine and the gel where 20 µM acetyl-L-carnitine was added to the reaction mix. While in the band shift with the 40 µM L-carnitine-supplemented sample only two bands could be resolved, after the addition of 20 µM acetyl-L-carnitine the bands shifted downwards, and there appeared a possible supershift at the top, which cannot be resolved easily because of the signal intensity. These bands were also present after the addition of 40 µM acetyl-L-carnitine, but started to weaken with the addition of 80 µM acetyl-L-carnitine, with the possible supershift band completely vanishing. Bands in the

lane with the normal sample could be seen only from 40 µM acetyl-L-carnitine upwards, whereas the sample from cells in dialFCS produced two bands when appended with 80 µM acetyl-L-carnitine. Appending 120 µM ALC to the reaction mix resulted in weaker signals, indicating that high concentrations of it are able to interfere with the promoter or one of the factors, hindering the binding of the factors. The lanes with the dialysed (fig. 45E, lane 2) and the 80 µM L-carnitine sample (fig. 45E, lane 4) show a weak signal, possibly as a result of protein degradation. We were able to verify the presence of the HNF4α binding site on the CRAT promoter and it can be influenced by acetyl-L-carnitine.

While the presence of all four binding sites was verified on the CRAT promoter, there were some differences and similarities observable between the four translation factor complexes and in their response to the supplementation of acetyl-L-carnitine. First of all, our mobility shift assays did show that the size of the complexes on the RARRXR, PPAR and HNF4 binding sites is similar with a size of around 130 kDa, indicating that these binding sites bind protein factors with a comparable size. With ~150 kDa, the complex reacting with the glucocorticoid binding site was the heaviest one. ALC had the most visible effect on the protein complex on the RARRXR binding site: while ALC could weaken the complex, leading to the appearance of new bands, it did not completely destroy the 130 kDa band. In the case of GRα, the original upper band had a weight of ~150 kDa, with a lower band at 130 kDa, making it the largest shift complex. While concentrations of up to 40 µM ALC strengthened the upper band, it also lightened the 130 kDa band, leading to a downshift to about 100 kDa, indicating that ALC can dissociate some of the proteins from the complex. Addition of 80 µM or 120 µM ALC resulted in the complete disappearance of the 100 kDa band, while making the upper band lighter, resulting in a downshift to 130 kDa. Addition of up to 80 µM ALC to the samples with the PPAR oligonucleotide resulted in the alternated weakening and strengthening of an upper 130 kDa band and a lower 95 kDa band, while 120 µM ALC led to a downshift from 130 kDa and 95 kDa to ~100 kDa and ~80 kDa, respectively. All this indicates that larger concentrations of ALC (>80 µM) can inhibit the protein complex binding on the PPAR site, similarly to GRα, either by associating directly with the proteins or by preventing their binding through association with the promoter. In the case of PPAR, the nuclear extracts responded strongly to supplementation of ALC, with the strongest response observed in extracts originating from cells cultivated in medium with dialyzed FCS. The result of appending 20 µM and 40 µM ALC to the shift experiments with the HNF4 oligonucleotide was an intensification of the signal height in the bands and the appearance of a new band with an approximate size of 150 kDa in the samples from 40 µM and 80 µM L-carnitine-supplemented cells. The addition of 80 µM and 120

μM ALC to the reaction mixes resulted in the upshift of the original bands from 130 kDa and 95 kDa to approximately 150 kDa and 110 kDa, respectively. These results indicate that while ALC is able to interact with the protein complex on the HNF4 binding site, making it heavier, it probably has no negative effect on the complex, as opposed to the other three factors, where ALC caused a downshift or the weakening of the bands. A compendium of all observed interactions of ALC with the investigated promoter factors GRα, HNF4α, PPARα and RARRXR is presented in fig. 48. This figure basically points out the major effects and changes upon ALC interplay. More details of specific alterations related to molecular weight shifts or promoter factor complex influences that finally occurred are summarised in Table 5 for RARRXR, Table 6 for GRα, Table 7 for PPAR and Table 8 for HNF4.

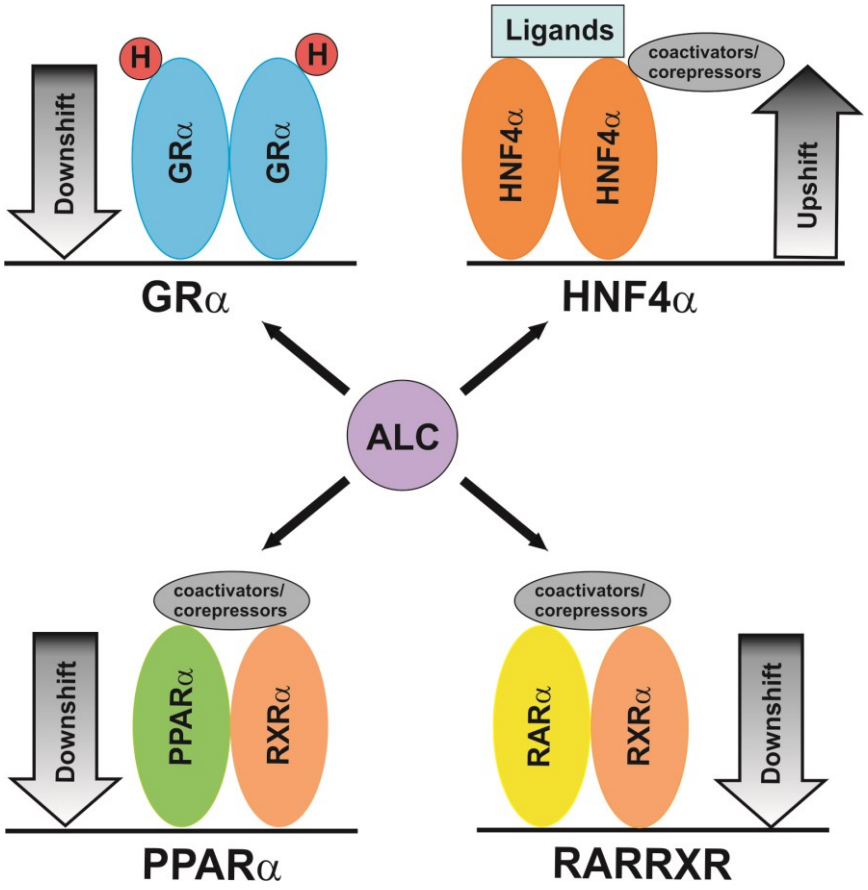

Figure 48: A synopsis of the influence of acetyl-L-carnitine (ALC) upon the four analysed transcription factor binding sites: glucocorticoid α, HNF4α, PPARα and RARRXR**.** The arrows indicate changes in the migration behaviour of the bands: the darker part denotes higher molecular weight shifts, whereas the white part displays shifts to lower molecular weights. Complexes modified after: Glucocorticoid α – Mikuni *et al.* [112]; HNF4α – Chiang, J. Y. [113]; PPARα – Ruan *et al.* [114]; RARRXR – Sigma-Aldrich [115]. Legend: H – hormone.

The experiment where varying concentrations of SDS were added to the nuclear extracts before performing the band shift assay showed that acyl-L-carnitine can interact with the transcription complex on the human CRAT promoter, but the binding is not covalent in nature. This is an important additional proof of the fact that the addition of acetyl-L-carnitine to the band shift cocktail is able to interact and bind to the promoter complex altogether, or to one of the promoter factors.

In the supershift assay, most of the antibodies weakened the band shift signal of RARXR, resulting in a weakening or the disappearance of the 130 kDa band, seen on the electrophoretic mobility shift assay and in the lane without added antibodies. The antibody that had no effect was FXR, which contrasts the study by Forman *et al.,* which shows that RXR and FXR can form heterodimers [116]. Interestingly, both FXR1 and FXR2 prevented the binding of the DNA probe, resulting in the disappearance of the band. RXR can also form homodimers with itself or heterodimers with RAR [83], and the use of antibodies against RXRα/β/γ resulted in a weakening of the signal, while antibodies against RARγ, RXRβ_1 and RXRβ_2 led to the complete disappearance of the band. Other common dimerization partners for RXR are PPAR's [70] and LXR's [117], and antibodies against PPAR, PPAR and LXR all led to the weakening of a band.

In conclusion, the results show that OCTN1 and SLC35F2 respond to supplementation of L-carnitine, similarly to OCTN2, which was already determined in our lab by Sabrina Demuth [118]. We could also clearly show that L-carnitine had an effect on key members of the mTOR pathway, which play an important role in the sensing of nutrients and cell growth. This indicates that L-carnitine can induce cell growth, either through induction of mTORC1 or even as a possible substrate in the pathway. On the other hand, L-carnitine did not affect Rac1 expression in liver cells. As this gene has a more pronounced expression in muscle cells [39], it would be an interesting possibility for a future research to study the interaction between Rac1 and L-carnitine in these cells. Our findings also show that L-carnitine is able to counteract the negative effects of elevated lipid concentrations, opening the possibilities for further research, such as studies to fight hypercholesterolaemia or other diseases with elevated cholesterol levels. The studied genes were shown to respond to L-carnitine supplementation better under hyperglycaemic than under normoglycaemic conditions. Interestingly, the Cignal assays showed that L-carnitine participates and interferes with different pathways. This is of importance in particular because these protein based reporter gene assays affirm previous results obtained by chip screen analyses [105]. Since some results were contradictory to previously published ones, more detailed experimental efforts will be necessary to clarify these questions [66, 108]. The electrophoretic mobility shift assays

have confirmed the presence of the RARβ/RARα/RXR, PPARα, GRα and HNF4α binding sites from the theoretical promoter analysis, and we have shown that acetyl-L-carnitine is able to interact with the transcription complex on the CRAT promoter. Further studies to research this relationship could be conducted by performing simultaneous band shift assays, where matching band shifts should be performed with radioactively labelled oligonucleotides, in parallel to labelled ^{14}C-acetyl-L-carnitine and to align them afterwards.

Zusammenfassung

Der Metabolit und nutrigenomische Faktor L-Carnitin ist ein Aminosäurederivat, das eine wichtige Funktion im Energiemetabolismus hat, wo es lang- und mittelkettige Fettsäuremoleküle als Ester durch die innere Mitochondrienmembran transportiert. Im Matrixraum der Mitochondrien wird aus ihnen durch β-Oxidation Acetyl-Coenzym A synthetisiert wird, das dann in anderen Prozessen verbraucht wird. Im menschlichen Organismus wird ein kleiner Teil des gesamten Carnitins aus den Aminosäuren Lysin und Methionin synthetisiert, während der Großteil durch die Nahrung aufgenommen wird.

Wegen der aminosäureähnlichen chemischen Struktur von L-Carnitin war es einer unser Ziele, dass wir uns neben Genen des Lipid- und Glukosemetabolismus den mTOR-Signalweg analytisch zuwenden. mTOR ist eine Serin/Threonin-Kinase, die einen Teil des mTORC1 Proteinkomplexes bildet. Dieser Signalweg ist verantwortlich für das Messen und Registrieren von Aminosäuren, Wachstumsfaktoren, zellulärem Stress, O_2-Gehalt der Zelle und des Energiestatus, und sorgt für die Hochregulierung der Proteinsynthese und somit des Zellwachstums, wenn alle Gegebenheiten ausreichend vorhanden sind.

Der konzentrationsabhängige nutrigenomische Effekt von L-Carnitin auf die Genexpression von einer Vielzahl verschiedenen Genen, wie jüngst zum Beispiel Membran-Shuttleproteine, wurde bereits in einer Reihe von Arbeiten dokumentiert. Die vorliegende Arbeit hatte mehrere Ziele: erstens, hat L-Carnitin einen zeit- und konzentrationsabhängigen Effekt auf die Genexpression von wichtigen Vertretern des mTOR Signalweges? Wenn das der Fall wäre dann übt dieser Metabolit somit einen wichtigen Einfluss auf die biologische Aktivität dieser zentralen Zellwachstum- und Zellzyklussteuerung aus? Und wie wirkt sich ein erhöhter Cholesterinspiegel auf die Expression von ausgewählten Stoffwechselgenen aus und welche günstige Wirkung vermag L-Carnitin auf deren Expressionsspiegel auszuüben. Zu diesem Zweck wurden die steady state mRNA Spiegel mittels real-time RT-PCR (qPCR) von folgenden Genen untersucht: SLC22A4, SLC35F2, Rac1, PGC-1α, Rheb, SREBP1 und GCN2. Da für die vorhin beschriebenen metabolischen Prozesse die Leber als Zielorgan sehr wichtig ist, wurden WRL68 Zellen (Leberkarzinomzelllinie) ausgewählt, die zuerst auf Carnitinmangelmedium gehalten wurden und anschließend für 4, 15, 24 oder 48 Stunden mit 80 µM L-Carnitin supplementiert wurden. Ein weiteres wichtiges Ziel bildete der humane CRAT Promotor und die Untersuchung der Interaktion von L-Carnitin mit den daran bindenden Proteinfaktoren. Als Basis diente zuerst eine theoretische Promotoranalyse, um anschließend die tatsächliche Präsenz von den in der Analyse

vorhergesagten RARRXR, PPAR, GRα und HNF4 Bindungsstellen zu verifizieren. Mit Hilfe von Electrophoretic Mobility Shift (EMSA) und Supershift Assays mit spezifischen Antikörpern wurden diese in weiterer Folge bestätigt. Mithilfe dieser Analysetechnik wurde in einem weiteren Ansatz untersucht, ob L-Carnitin konzentrationsabhängig als Acetylester direkt mit Promoter-bindenden Faktoren wechselwirken und auf diese Weise die Genexpression direkt beeinflussen kann.

Die Ergebnisse bestätigten eindeutig, dass L-Carnitin die steady state mRNA Spiegel der Membrantransporter SLC22A4 (OCTN1) und SLC35F2 steigern kann, ähnlich wie für OCTN2. Auch bei Genen aus dem mTOR Signalweg PGC-1α, GCN2, SREBP-1 und Rheb, wurde eine Steigerung der Genexpression beobachtet, dass darauf hindeutet, dass L-Carnitin ein wichtiger Cofaktor oder Aktivator des mTOR Signalweges sein kann. L-Carnitin war auch fähig in den meisten Fällen die zum Teil enorm gesteigerte Genexpression in Lipid-supplementierten Zellen zu normalisieren. Der Effekt auf Rac1 war unter hyperglykämischen Bedingungen sehr gering, während man unter normoglykämischen Bedingungen ein stärkerer Effekt zu beobachten konnte. Mit den EMSA und Supershift Assays wurde erfolgreich die Anwesenheit von allen vier Transkriptionsfaktoren am CRAT-Promoter verifiziert, sowie die Fähigkeit, dass Acetyl-L-Carnitin als Molekül mit dem Transkriptionsfaktorkomplex interagiert oder nichtkovalent bindet und so die Aktivität modifiziert. Dabei werden neue Proteinshiftkomplexe gebildet und die Bandenmuster durch zugesetztes Acetylcarnitin konzentrationsabhängig verändert.

Abstract

The metabolite and nutrigenomic factor L-carnitine is a “conditionally-essential” amino acid derivative that has an important function in energy metabolism, where it helps to transport long- and medium chain fatty acid molecules in the form of esters through the inner mitochondrial membrane into the mitochondrial matrix, where they are used in β-oxidation for the synthesis of acetyl-coenzyme A, which is then used in other processes. A small amount of total L-carnitine in the human body is synthesized from the amino acids lysine and methionine, while most of it is taken up through nutrition.

Because of the amino acid-like structure of L-carnitine, one of our goals besides studying genes, involved in the lipid- and glucose metabolism, was to analyse the mTOR signalling pathway. mTOR is a serine/threonine kinase and is a part of the mTORC1 protein complex. This pathway is responsible for the sensing of amino acids, growth factors, cellular stress, O_2 content of the cell and the energy status, and under favourable conditions upregulates protein synthesis and consequently cell growth.

The concentration-dependent nutrigenomic effect of L-carnitine on the expression of different genes, such as membrane shuttle proteins most recently, was already documented in a series of researches. Our study had various goals: first, does L-carnitine have a time-dependent effect on the expression of important members of the mTOR signalling pathway, thereby having an important influence on the biological activity of this central and decisive cell growth and cell cycle regulating pathway? And how do elevated cholesterol levels affect the expression of selected genes, and can L-carnitine influence and maybe even positively impact this change. To achieve this, real-time RT-PCR was used to study the steady state mRNA levels of the following genes: SLC22A4, SLC35F2, Rac1, PGC-1α, Rheb, SREBP1 and GCN2. As the liver is an important target organ for the previously described metabolic processes, we used WRL68 cells (hepatic cancer cell line), which were grown in a carnitine-depleted medium and subsequently supplemented with 80 µM L-carnitine for 4, 15, 24 or 48 hours. Another important aim was the human CRAT promoter and the study of the interaction between L-carnitine and protein factors binding to this promoter. The basis for this built a theoretical promoter analysis, followed by a verification of the presence of RARRXR, PPAR, GRα and HNF4 binding sites. These promoter elements were subsequently verified with the help of electrophoretic mobility shift (EMSA) and supershift assays performed with specific antibodies. As an attachment, this analytic technique was used to study if L-carnitine as acetyl ester can directly interact with the promoter-binding factors in a concentration-dependent manner and directly influence gene expression in this way.

Our results confirm that L-carnitine can directly increase the steady state mRNA levels of the membrane transporters SLC22A4 (OCTN1) and SLC35F2, similar to OCTN2. An increase in gene expression could also be observed with the mTOR pathway-genes PGC-1α, GCN2, SREBP-1 and Rheb, which indicates that L-carnitine can act as an activator or cofactor in the mTOR signalling pathway. L-carnitine was in most cases also able to normalise the enormously increased gene expression in lipid-supplemented cells. It could not affect the expression of Rac1 under hyperglycaemic conditions, while it slightly increased steady state mRNA levels under normoglycaemic conditions. With the help of EMSA and supershift assays we successfully confirmed the presence of all four transcription factors on the CRAT promoter, as well as the ability of acetyl-L-carnitine to directly influence the activity of the transcription factor complex by interacting with it or binding in a non-covalent manner and thus modifying their activity. In direct consequence of this interaction, new protein shift complexes of different sizes are formed and the banding pattern is altered dependent on the ALC concentration.

Appendix

RevertAid Reverse Transcriptase and Fermentas M-MuLV Reverse Transcriptase 5x Reaction Buffer were exchanged for GoScript Reverse Transcriptase and GoScript 5x Reaction Buffer, respectively, when RevertAid Reverse Transcriptase ran out. The rest of the cDNA synthesis was carried out the same way.

Buffers and solutions:

10x TAE (1000ml)

Tris base	48.4 g
0.5 M EDTA pH 8.0	20 ml
Glacial acetic acid	11.44 g
dH_2O	

10x PBS (1000 ml)

NaCl	80 g/l
KCl	2 g/l
Na_2HPO_4	14.4 g/l
KH_2PO_4	2 g/l
Adjust pH to:	7.4

10x TEN

Tris-Cl (pH 8.0)	0.1 M
EDTA (pH 8.0)	0.01 M
SDS	0.1% (w/v)

5x Binding Buffer

Glycerol	20%
Tris-HCl pH 8.0	100 mM
KCl	300 mM
$MgCl_2$	25 mM
Bovine serum albumin	500 µg/ml

30% Acrylamide-Bisacrylamide (100 ml)

Acrylamide	38 g
Bisacrylamide	2 g
BioRAD Resin	1 spoon
ddH_2O	100 ml

10x TBE (1000 ml)

Tris base	108 g
Boric acid	55 g
0.5 M EDTA (pH 8.0)	40 ml
dH_2O	

List of abbreviations:

µl	microlitre
µM	micromolar
ALC	acyl-L-carnitine
AMPK	5' AMP-activated protein kinase
CACT	acylcarnitine-carnitine translocase
CoA	coenzyme A
CPT-I	carnitine palmitoyltransferase I
CPT-II	carnitine palmitoyltransferase II
dialFCS	dialysed foetal calf serum
DMEM	Dulbecco's Modified Eagle Medium
DNA	deoxyribonucleic acid
EDTA	ethylenediaminetetraacetic acid
EMSA	electrophoretic mobility shift assay
FCS	foetal calf serum
FKBP12	FK506 binding protein 12
GLUT4	glucose transporter type 4
GR	glucocorticoid receptor
hCRAT	human carnitine acetyltransferase
HNF4	hepatocyte nuclear factor 4
Hyperglycaemic medium	DMEM (4500 mg/l glucose) + P/S + Qmax

LDL	low-density lipoprotein
mg	milligram
ml	millilitre
mLST8	mammalian lethal with SEC13 protein 8
mm	millimetre
mM	millimolar
mTOR	mechanistic target of rapamycin
Normoglycaemic medium	DMEM (1000 mg/l glucose) + P/S + Qmax
OCTN2	organic cation/carnitine transporter 2
P/S	penicillin/streptomycin
PBS	phosphate-buffered saline
PCR	polymerase chain reaction
PPAR	peroxisome proliferator-activated receptor
PPRE	PPAR response element
RAP	receptor-associated proteins
RAR	retinoic acid receptor
rcf	relative centrifugal force
RNA	ribonucleic acid
rpm	round per minute
RT-PCR	reverse transcription polymerase chain reaction
RXR	retinoid X receptor
TAE	tris-acetate-EDTA

5. References

1. Vaz, F.M. and R.J. Wanders, *Carnitine biosynthesis in mammals.* Biochem J, 2002. **361**(Pt 3): p. 417-29.
2. Harmeyer, J., *The physiological role of L-Carnitine.* Lohmann Information, 2002. **27**: p. 15-21.
3. MacArthur, I. *Reconsidering L-Carnitine*. 2013 [cited 2017 8.11.2017]; Available from: https://columbiasciencereview.com/2013/04/10/reconsidering-l-carnitine/.
4. Tein, I., S.W. Bukovac, and Z.W. Xie, *Characterization of the human plasmalemmal carnitine transporter in cultured skin fibroblasts.* Arch Biochem Biophys, 1996. **329**(2): p. 145-55.
5. Bremer, J., *Carnitine--metabolism and functions.* Physiol Rev, 1983. **63**(4): p. 1420-80.
6. Strijbis, K., F.M. Vaz, and B. Distel, *Enzymology of the carnitine biosynthesis pathway.* IUBMB Life, 2010. **62**(5): p. 357-62.
7. Rebouche, C.J., *Kinetics, pharmacokinetics, and regulation of L-carnitine and acetyl-L-carnitine metabolism.* Ann N Y Acad Sci, 2004. **1033**: p. 30-41.
8. Rebouche, C.J. and H. Seim, *Carnitine metabolism and its regulation in microorganisms and mammals.* Annu Rev Nutr, 1998. **18**: p. 39-61.
9. Kepka, A., et al., *The role of carnitine in the perinatal period.* Dev Period Med, 2014. **18**(4): p. 417-25.
10. Steiber, A., J. Kerner, and C.L. Hoppel, *Carnitine: a nutritional, biosynthetic, and functional perspective.* Mol Aspects Med, 2004. **25**(5-6): p. 455-73.
11. Rebouche, C.J. and D.J. Paulson, *Carnitine metabolism and function in humans.* Annu Rev Nutr, 1986. **6**: p. 41-66.
12. Stephens, F., *Skeletal muscle carnitine transport*, in *Carnitine Metabolism and Human Nutrition*, B. Wall, Porter, C Editor. 2014, CRC/Taylor & Francis Group, Boca Raton. p. 51-62.
13. Tamai, I., et al., *Molecular and functional identification of sodium ion-dependent, high affinity human carnitine transporter OCTN2.* J Biol Chem, 1998. **273**(32): p. 20378-82.
14. Borum, P., *Carnitine homeostasis in humans*, in *Carnitine Metabolism and Human Nutrition*, B. Wall, Porter, C Editor. 2014, CRC/Taylor & Francis Group, Boca Raton. p. 3-10.
15. Porter, C., *The role of carnitine in the integration of skeletal muscle fuel metabolism*, in *Carnitine Metabolism and Human Nutrition*, B. Wall, Porter, C, Editor. 2014, CRC/Taylor & Francis Group, Boca Raton. p. 37-50.
16. Flanagan, J.L., et al., *Role of carnitine in disease.* Nutr Metab (Lond), 2010. **7**: p. 30.
17. Famularo G, M.F., Nucera E, Santini G, De Simone C, *Carnitine Deficiency: Primary and Secondary Syndromes*, in *Carnitine Today*, D.F.G. Simone C, Editor. 1997, Chapman & Hall, Austin, Texas. p. 119-162.
18. Sigauke, E., et al., *Carnitine palmitoyltransferase II deficiency: a clinical, biochemical, and molecular review.* Lab Invest, 2003. **83**(11): p. 1543-54.
19. Erguven, M., et al., *A case of early diagnosed carnitine deficiency presenting with respiratory symptoms.* Ann Nutr Metab, 2007. **51**(4): p. 331-4.
20. Avruch, J., et al., *Amino acid regulation of TOR complex 1.* Am J Physiol Endocrinol Metab, 2009. **296**(4): p. E592-602.
21. Wullschleger, S., R. Loewith, and M.N. Hall, *TOR signaling in growth and metabolism.* Cell, 2006. **124**(3): p. 471-84.
22. Sarbassov, D.D., et al., *Prolonged rapamycin treatment inhibits mTORC2 assembly and Akt/PKB.* Mol Cell, 2006. **22**(2): p. 159-68.
23. Taylor, P.M., *Role of amino acid transporters in amino acid sensing.* Am J Clin Nutr, 2014. **99**(1): p. 223S-230S.

24. Kim, S.G., G.R. Buel, and J. Blenis, *Nutrient regulation of the mTOR complex 1 signaling pathway.* Mol Cells, 2013. **35**(6): p. 463-73.
25. Yuan, H.X., Y. Xiong, and K.L. Guan, *Nutrient sensing, metabolism, and cell growth control.* Mol Cell, 2013. **49**(3): p. 379-87.
26. Durrington, P., *Dyslipidaemia.* Lancet, 2003. **362**(9385): p. 717-31.
27. He, L., K. Vasiliou, and D.W. Nebert, *Analysis and update of the human solute carrier (SLC) gene superfamily.* Hum Genomics, 2009. **3**(2): p. 195-206.
28. Tamai, I., *Pharmacological and pathophysiological roles of carnitine/organic cation transporters (OCTNs: SLC22A4, SLC22A5 and Slc22a21).* Biopharm Drug Dispos, 2013. **34**(1): p. 29-44.
29. Koepsell, H. and H. Endou, *The SLC22 drug transporter family.* Pflugers Arch, 2004. **447**(5): p. 666-76.
30. Tokuhiro, S., et al., *An intronic SNP in a RUNX1 binding site of SLC22A4, encoding an organic cation transporter, is associated with rheumatoid arthritis.* Nat Genet, 2003. **35**(4): p. 341-8.
31. Tamai, I., et al., *Cloning and characterization of a novel human pH-dependent organic cation transporter, OCTN1.* FEBS Lett, 1997. **419**(1): p. 107-11.
32. Ingoglia, F., et al., *Functional activity of L-carnitine transporters in human airway epithelial cells.* Biochim Biophys Acta, 2016. **1858**(2): p. 210-9.
33. Grundemann, D., et al., *Discovery of the ergothioneine transporter.* Proc Natl Acad Sci U S A, 2005. **102**(14): p. 5256-61.
34. Hou, X., et al., *Association of single nucleotide polymorphism rs3792876 in SLC22A4 gene with autoimmune thyroid disease in a Chinese Han population.* BMC Med Genet, 2015. **16**: p. 76.
35. Ishida, N. and M. Kawakita, *Molecular physiology and pathology of the nucleotide sugar transporter family (SLC35).* Pflugers Arch, 2004. **447**(5): p. 768-75.
36. Li, X., et al., *Influence on the behavior of lung cancer H1299 cells by silencing SLC35F2 expression.* Cancer Cell Int, 2013. **13**(1): p. 73.
37. Bu, L., et al., *Highly expressed SLC35F2 in non-small cell lung cancer is associated with pathological staging.* Mol Med Rep, 2011. **4**(6): p. 1289-93.
38. Winter, G.E., et al., *The solute carrier SLC35F2 enables YM155-mediated DNA damage toxicity.* Nat Chem Biol, 2014. **10**(9): p. 768-73.
39. Sylow, L., et al., *Rac1 signaling is required for insulin-stimulated glucose uptake and is dysregulated in insulin-resistant murine and human skeletal muscle.* Diabetes, 2013. **62**(6): p. 1865-75.
40. Sylow, L., et al., *Rac1 is a novel regulator of contraction-stimulated glucose uptake in skeletal muscle.* Diabetes, 2013. **62**(4): p. 1139-51.
41. Wang, Z., et al., *Rac1 is crucial for Ras-dependent skin tumor formation by controlling Pak1-Mek-Erk hyperactivation and hyperproliferation in vivo.* Oncogene, 2010. **29**(23): p. 3362-73.
42. Asahara, S., et al., *Ras-related C3 botulinum toxin substrate 1 (RAC1) regulates glucose-stimulated insulin secretion via modulation of F-actin.* Diabetologia, 2013. **56**(5): p. 1088-97.
43. Unger, R.H. and S. Grundy, *Hyperglycaemia as an inducer as well as a consequence of impaired islet cell function and insulin resistance: implications for the management of diabetes.* Diabetologia, 1985. **28**(3): p. 119-21.
44. Mingrone, G., *Carnitine in type 2 diabetes.* Ann N Y Acad Sci, 2004. **1033**: p. 99-107.
45. Tan, V.P. and S. Miyamoto, *Nutrient-sensing mTORC1: Integration of metabolic and autophagic signals.* J Mol Cell Cardiol, 2016. **95**: p. 31-41.
46. Sancak, Y., et al., *Ragulator-Rag complex targets mTORC1 to the lysosomal surface and is necessary for its activation by amino acids.* Cell, 2010. **141**(2): p. 290-303.

47. Laplante, M. and D.M. Sabatini, *mTOR signaling at a glance.* J Cell Sci, 2009. **122**(Pt 20): p. 3589-94.
48. Lu, Z.H., et al., *Mammalian target of rapamycin activator RHEB is frequently overexpressed in human carcinomas and is critical and sufficient for skin epithelial carcinogenesis.* Cancer Res, 2010. **70**(8): p. 3287-98.
49. Zhang, Y., et al., *Peroxisomal proliferator-activated receptor-gamma coactivator-1 alpha (PGC-1 alpha) enhances the thyroid hormone induction of carnitine palmitoyltransferase I (CPT-I alpha).* J Biol Chem, 2004. **279**(52): p. 53963-71.
50. Yoon, J.C., et al., *Control of hepatic gluconeogenesis through the transcriptional coactivator PGC-1.* Nature, 2001. **413**(6852): p. 131-8.
51. Louet, J.F., et al., *The coactivator PGC-1 is involved in the regulation of the liver carnitine palmitoyltransferase I gene expression by cAMP in combination with HNF4 alpha and cAMP-response element-binding protein (CREB).* J Biol Chem, 2002. **277**(41): p. 37991-8000.
52. Deng, Q., et al., *SREBP-1c gene silencing can decrease lipid deposits in bovine hepatocytes cultured in vitro.* Cell Physiol Biochem, 2014. **33**(5): p. 1568-78.
53. Pettinelli, P., et al., *Enhancement in liver SREBP-1c/PPAR-alpha ratio and steatosis in obese patients: correlations with insulin resistance and n-3 long-chain polyunsaturated fatty acid depletion.* Biochim Biophys Acta, 2009. **1792**(11): p. 1080-6.
54. Zammit, V.A., *Carnitine acyltransferases: functional significance of subcellular distribution and membrane topology.* Prog Lipid Res, 1999. **38**(3): p. 199-224.
55. Ramsay, R.R. and J.H. Naismith, *A snapshot of carnitine acetyltransferase.* Trends Biochem Sci, 2003. **28**(7): p. 343-6.
56. van der Leij, F.R., et al., *Genomics of the human carnitine acyltransferase genes.* Mol Genet Metab, 2000. **71**(1-2): p. 139-53.
57. Hsiao, Y.S., G. Jogl, and L. Tong, *Structural and biochemical studies of the substrate selectivity of carnitine acetyltransferase.* J Biol Chem, 2004. **279**(30): p. 31584-9.
58. Seiler, S.E., et al., *Obesity and lipid stress inhibit carnitine acetyltransferase activity.* J Lipid Res, 2014. **55**(4): p. 635-44.
59. Jogl, G. and L. Tong, *Crystal structure of carnitine acetyltransferase and implications for the catalytic mechanism and fatty acid transport.* Cell, 2003. **112**(1): p. 113-22.
60. Brunner, S., et al., *Cloning and characterization of murine carnitine acetyltransferase: evidence for a requirement during cell cycle progression.* Biochem J, 1997. **322 (Pt 2)**: p. 403-10.
61. Messeguer, X., et al., *PROMO: detection of known transcription regulatory elements using species-tailored searches.* Bioinformatics, 2002. **18**(2): p. 333-4.
62. Farre, D., et al., *Identification of patterns in biological sequences at the ALGGEN server: PROMO and MALGEN.* Nucleic Acids Res, 2003. **31**(13): p. 3651-3.
63. Rebouche, C.J., D.D. Panagides, and S.E. Nelson, *Role of carnitine in utilization of dietary medium-chain triglycerides by term infants.* Am J Clin Nutr, 1990. **52**(5): p. 820-4.
64. Dreos, R., et al., *The eukaryotic promoter database in its 30th year: focus on non-vertebrate organisms.* Nucleic Acids Res, 2017. **45**(D1): p. D51-D55.
65. Dreos, R., et al., *The Eukaryotic Promoter Database: expansion of EPDnew and new promoter analysis tools.* Nucleic Acids Res, 2015. **43**(Database issue): p. D92-6.
66. Kienesberger, K., *L-Carnitine and its transcriptional modulation*. 2012, University of Vienna.
67. Schoonjans, K., B. Staels, and J. Auwerx, *Role of the peroxisome proliferator-activated receptor (PPAR) in mediating the effects of fibrates and fatty acids on gene expression.* J Lipid Res, 1996. **37**(5): p. 907-25.
68. Grygiel-Gorniak, B., *Peroxisome proliferator-activated receptors and their ligands: nutritional and clinical implications--a review.* Nutr J, 2014. **13**: p. 17.

69. Kliewer, S.A., et al., *Fatty acids and eicosanoids regulate gene expression through direct interactions with peroxisome proliferator-activated receptors alpha and gamma.* Proc Natl Acad Sci U S A, 1997. **94**(9): p. 4318-23.
70. Berger, J. and D.E. Moller, *The mechanisms of action of PPARs.* Annu Rev Med, 2002. **53**: p. 409-35.
71. Bensinger, S.J. and P. Tontonoz, *Integration of metabolism and inflammation by lipid-activated nuclear receptors.* Nature, 2008. **454**(7203): p. 470-7.
72. Li, J.L., et al., *Effects of L-carnitine against oxidative stress in human hepatocytes: involvement of peroxisome proliferator-activated receptor alpha.* J Biomed Sci, 2012. **19**: p. 32.
73. Forman, B.M., J. Chen, and R.M. Evans, *Hypolipidemic drugs, polyunsaturated fatty acids, and eicosanoids are ligands for peroxisome proliferator-activated receptors alpha and delta.* Proc Natl Acad Sci U S A, 1997. **94**(9): p. 4312-7.
74. Watt, A.J., W.D. Garrison, and S.A. Duncan, *HNF4: a central regulator of hepatocyte differentiation and function.* Hepatology, 2003. **37**(6): p. 1249-53.
75. Lu, H., *Crosstalk of HNF4alpha with extracellular and intracellular signaling pathways in the regulation of hepatic metabolism of drugs and lipids.* Acta Pharm Sin B, 2016. **6**(5): p. 393-408.
76. Wisely, G.B., et al., *Hepatocyte nuclear factor 4 is a transcription factor that constitutively binds fatty acids.* Structure, 2002. **10**(9): p. 1225-34.
77. Sladek, F.M., et al., *Liver-enriched transcription factor HNF-4 is a novel member of the steroid hormone receptor superfamily.* Genes Dev, 1990. **4**(12B): p. 2353-65.
78. Hertz, R., et al., *Thioesterase activity and acyl-CoA/fatty acid cross-talk of hepatocyte nuclear factor-4{alpha}.* J Biol Chem, 2005. **280**(26): p. 24451-61.
79. Hertz, R., et al., *Fatty acyl-CoA thioesters are ligands of hepatic nuclear factor-4alpha.* Nature, 1998. **392**(6675): p. 512-6.
80. Bogan, A.A., et al., *Analysis of protein dimerization and ligand binding of orphan receptor HNF4alpha.* J Mol Biol, 2000. **302**(4): p. 831-51.
81. Allenby, G., et al., *Retinoic acid receptors and retinoid X receptors: interactions with endogenous retinoic acids.* Proc Natl Acad Sci U S A, 1993. **90**(1): p. 30-4.
82. Pogenberg, V., et al., *Characterization of the interaction between retinoic acid receptor/retinoid X receptor (RAR/RXR) heterodimers and transcriptional coactivators through structural and fluorescence anisotropy studies.* J Biol Chem, 2005. **280**(2): p. 1625-33.
83. Mader, S., et al., *The patterns of binding of RAR, RXR and TR homo- and heterodimers to direct repeats are dictated by the binding specificites of the DNA binding domains.* EMBO J, 1993. **12**(13): p. 5029-41.
84. Keller, H., et al., *Fatty acids and retinoids control lipid metabolism through activation of peroxisome proliferator-activated receptor-retinoid X receptor heterodimers.* Proc Natl Acad Sci U S A, 1993. **90**(6): p. 2160-4.
85. Bamberger, C.M., et al., *Glucocorticoid Receptor-Beta, a Potential Endogenous Inhibitor of Glucocorticoid Action in Humans.* Journal of Clinical Investigation, 1995. **95**(6): p. 2435-2441.
86. Manoli, I., et al., *Modulatory effects of L-carnitine on glucocorticoid receptor activity.* Carnitine: The Science Behind a Conditionally Essential Nutrient, 2004. **1033**: p. 147-157.
87. Macfarlane, D.P., S. Forbes, and B.R. Walker, *Glucocorticoids and fatty acid metabolism in humans: fuelling fat redistribution in the metabolic syndrome.* Journal of Endocrinology, 2008. **197**(2): p. 189-204.
88. Koba, K.Y., T., *Beneficial Effects of Conjugated Linoleic Acid*, in *Nutrigenomics and Proteomics in Health and Disease: Food Factors and Gene Interactions*, Y.M. Y. Mine, K.; Shahidi, F., Editor. 2009, Wiley-Blackwell. p. 85-96.

89. Honda, S.T., Y.; Yokota, S., *Licorice flavonoids*, in *Nutrigenomics and Proteomics in Health and Disease: Food Factors and Gene Interactions*, Y.M. Mine, K.; Shahidi, F., Editor. 2009, Wiley-Blackwell. p. 291-300.
90. Miyashita, K.H., M., *Antiobesity Effect of Allenic Carotenoid, Fucoxanthin*, in *Nutrigenomics and Proteomics in Health and Disease: Food Factors and Gene Interactions*, Y.M. Mine, K.; Shahidi, F., Editor. 2009, Wiley-Blackwell. p. 145-160.
91. Goto, T.T., N.; Hirai, S.; Kawada, T., *Isoprenols*, in *Nutrigenomics and Proteomics in Health and Disease: Food Factors and Gene Interactions*, Y.M. Mine, K.; Shahidi, F., Editor. 2009, Wiley-Blackwell. p. 301-310.
92. Chin, S.F.L., W.; Storkson, J.M.; Ha, Y.L.; Pariza, M.W., *Dietary Sources of Conjugated Dienoic Isomers of Linoleic Acid, a Newly Recognized Class of Anticarcinogens.* Journal of Food Composition and Analysis, 1992: p. 185–197.
93. Moya-Camarena, S.Y., et al., *Conjugated linoleic acid is a potent naturally occurring ligand and activator of PPAR alpha.* Journal of Lipid Research, 1999. **40**(8): p. 1426-1433.
94. Rahman, S.M., et al., *Effects of conjugated linoleic acid on serum leptin concentration, body-fat accumulation, and beta-oxidation of fatty acid in OLETF rats.* Nutrition, 2001. **17**(5): p. 385-390.
95. Brown, P.J., et al., *Diet and Refsums Disease - the Determination of Phytanic Acid and Phytol in Certain Foods and the Application of This Knowledge to the Choice of Suitable Convenience Foods for Patients with Refsums Disease.* Journal of Human Nutrition and Dietetics, 1993. **6**(4): p. 295-305.
96. Ellinghaus, P., et al., *Phytanic acid activates the peroxisome proliferator-activated receptor alpha (PPAR alpha) in sterol carrier protein 2- sterol carrier protein x-deficient mice.* Journal of Biological Chemistry, 1999. **274**(5): p. 2766-2772.
97. Goto, T., et al., *Phytol directly activates peroxisome proliferator-activated receptor alpha (PPAR alpha) and regulates gene expression involved in lipid metabolism in PPAR alpha-expressing HepG2 hepatocytes.* Biochemical and Biophysical Research Communications, 2005. **337**(2): p. 440-445.
98. Aoki, F., et al., *Suppression by licorice flavonoids of abdominal fat accumulation and body weight gain in high-fat diet-induced obese C57BL/6J mice.* Bioscience Biotechnology and Biochemistry, 2007. **71**(1): p. 206-214.
99. Siu, F.K.Y., L.T.O. Lee, and B.K.C. Chow, *Southwestern blotting in investigating transcriptional regulation.* Nature Protocols, 2008. **3**(1): p. 51-58.
100. Yabuuchi, H., et al., *Novel membrane transporter OCTN1 mediates multispecific, bidirectional, and pH-dependent transport of organic cations.* J Pharmacol Exp Ther, 1999. **289**(2): p. 768-73.
101. Seccombe, D.W., et al., *L-carnitine treatment in the hyperlipidemic rabbit.* Metabolism, 1987. **36**(12): p. 1192-6.
102. Fushimi, T., et al., *Dietary acetic acid reduces serum cholesterol and triacylglycerols in rats fed a cholesterol-rich diet.* Br J Nutr, 2006. **95**(5): p. 916-24.
103. Field, F.J., et al., *Regulation of sterol regulatory element-binding proteins in hamster intestine by changes in cholesterol flux.* J Biol Chem, 2001. **276**(20): p. 17576-83.
104. Shimomura, I., et al., *Differential expression of exons 1a and 1c in mRNAs for sterol regulatory element binding protein-1 in human and mouse organs and cultured cells.* J Clin Invest, 1997. **99**(5): p. 838-45.
105. Hofer-Litzlbauer, E., *Biochemical and genetical consequences of carnitinedeficiency caused by downregulation of the carnitine acyltransferasegenes*. 2005, University of Vienna.
106. Quiagen. Available from: https://www.qiagen.com/us/shop/protein-and-cell-assays/cignal-finder-reporter-arrays/?catno=CCA-005L#orderinginformation.

107. Dunning, K.R., et al., *Increased beta-oxidation and improved oocyte developmental competence in response to l-carnitine during ovarian in vitro follicle development in mice.* Biol Reprod, 2011. **85**(3): p. 548-55.
108. Kraemer, W.J., et al., *Androgenic responses to resistance exercise: effects of feeding and L-carnitine.* Med Sci Sports Exerc, 2006. **38**(7): p. 1288-96.
109. Godarova, A., Litzlbauer, E., Brunner, S., Agu A.C., Lohninger A., Hofbauer, R., *L-Carnitine regulates mRNA expression levels of the carnitine acyltransferases CPT I, CPT II and CRAT.* Chemical Monthly, 2005. **136** p. 1349-1363.
110. Fenkci, S.M., et al., *Serum total L-carnitine levels in non-obese women with polycystic ovary syndrome.* Human Reproduction, 2008. **23**(7): p. 1602-1606.
111. Wen, G., et al., *Mouse gamma-butyrobetaine dioxygenase is regulated by peroxisome proliferator-activated receptor alpha through a PPRE located in the proximal promoter.* Biochem Pharmacol, 2011. **82**(2): p. 175-83.
112. Mikuni, S., et al., *Negative Correlation between the Diffusion Coefficient and Transcriptional Activity of the Glucocorticoid Receptor.* Int J Mol Sci, 2017. **18**(9).
113. Chiang, J.Y., *Hepatocyte nuclear factor 4alpha regulation of bile acid and drug metabolism.* Expert Opin Drug Metab Toxicol, 2009. **5**(2): p. 137-47.
114. Ruan, X., F. Zheng, and Y. Guan, *PPARs and the kidney in metabolic syndrome.* Am J Physiol Renal Physiol, 2008. **294**(5): p. F1032-47.
115. Sigma-Aldrich. [cited 2017 26.10.2017]; Available from: http://www.sigmaaldrich.com/technical-documents/articles/biofiles/retinoic-acid-and.html.
116. Forman, B.M., *Identification of a nuclear receptor that is activated by farnesol metabolites.* Cell, 1995. **81**: p. 687-693.
117. Hong, C. and P. Tontonoz, *Liver X receptors in lipid metabolism: opportunities for drug discovery.* Nature Reviews Drug Discovery, 2014. **13**(6): p. 433-444.
118. Demuth, S., *Short time reaction at mRNA levels of solute carrier member's (SLC) on different steady state L-carnitine and PPARα-agonist fenofibrate concentrations*. 2016, University of Vienna.